

CHEMICALLY REACTING FLOWS IN POROUS MEDIA

A THESIS

Presented to

The Faculty of the

Division of Graduate Studies

by

Allen Charles Merritt

In Partial Fulfillment

of the Requirements for the Degree

Doctor of Philosophy

in the School of Chemical Engineering

Georgia Institute of Technology

May, 1976

CHEMICALLY REACTING FLOWS IN POROUS MEDIA

Approved:

Dr. C. W. Gorton, Chairman

Dr. W. Z. Black

Dr. H. C. Ward

Date Approved by Chairman: June 4, 1976

ACKNOWLEDGMENTS

The author wishes to thank his thesis advisor, Dr. C. W. Gorton, for his guidance and suggestions which were invaluable to the completion of this work.

In addition, Dr. W. Z. Black and Dr. H. C. Ward served on the thesis reading committee. Their constructive comments have certainly improved the quality of this work.

Thanks are also due to Continental Oil Company for a fellowship received during the early part of this study. The Georgia Institute of Technology Engineering Experiment Station also provided laboratory space for preliminary experiments.

Numerous people contributed to the conduct of this investigation and the author is grateful to them. The staff of the Rich Electronic Computer Center provided frequent assistance. Mr. Tomas F. Camacho provided many helpful suggestions. The clerical staff of the Gold Kist Engineering Department, especially Ms. Patty Woodall, Ms. Eva Rodum, and Ms. Elizabeth Farrow, typed the many drafts of this text.

TABLE OF CONTENTS

	Page
ACKNOWLEDGMENTS.	ii
LIST OF TABLES	v
LIST OF ILLUSTRATIONS.	vi
SUMMARY.	vii
NOMENCLATURE	ix
Chapter	
I. INTRODUCTION.	1
II. TRANSPORT PHENOMENA IN POROUS MEDIA	6
Equation of Motion	
Equation of Continuity	
Equation of Continuity Species i	
III. ANALYSIS OF PACK CEMENTATION	23
Porous Media Description	
Transport Equations	
Auxiliary Equations and Further Assumptions	
Finite Difference Equations	
Stability and Convergence	
Boundary and Initial Conditions	
Computer Program	
IV. IMPLEMENTATION OF THE NUMERICAL SOLUTION AND RESULTS	39
Thermodynamic and Transport Properties of the Gas Species	
Thermodynamic and Transport Properties of the Solid	
Further Modification of the Momentum Equation	
Input Data	
Results	
Accuracy of Results	

TABLE OF CONTENTS (CONTINUED)

Chapter	Page
V. CONCLUSIONS AND RECOMMENDATIONS	81
APPENDIX.	82
I. CONTINUITY EQUATION FOR POROUS MATERIAL	82
II. BINARY DIFFUSION COEFFICIENT FOR POROUS MEDIA	85
III. COMPARISON OF VARIOUS FORMS FOR THE BINARY DIFFUSION EQUATION IN POROUS MEDIA.	88
IV. MULTICOMPONENT DIFFUSION EQUATION FOR POROUS MEDIA.	90
V. MULTICOMPONENT ENERGY CONSERVATION EQUATION FOR POROUS MEDIA.	93
VI. CALCULATION OF THE SUBSURFACE TEMPERATURE	97
VII. INTERFACE CONTINUITY EQUATION AND THICKNESS CALCULATION	99
VIII. CALCULATION OF INTERFACE MASS FRACTIONS BOUNDARY CONDITIONS	104
IX. CALCULATION OF INTERFACE TEMPERATURE BOUNDARY CONDITIONS	107
X. CALCULATION OF THE OVERALL DIFFUSIVITY AND OVERALL THERMAL CONDUCTIVITY FOR THE CORE INTERFACE.	113
XI. COMPUTER PROGRAM.	117
XII. PROPERTIES FOR GAS PHASE SPECIES.	162
XIII. PROPERTIES FOR SOLID SPECIES.	163
XIV. CALCULATION OF THE AVERAGE PRESSURE	164
LITERATURE CITED.	166
VITA.	172

LIST OF TABLES

Table		Page
1	Input Data.	48
2	Results of the Solution for the Multicomponent Case after 100 Seconds.	50
3	Results of the Solution for the Multicomponent Case after 1,000 Seconds.	52
4	Results of the Solution for the Multicomponent Case after 1,900 Seconds.	54
5	Results of the Solution for the Multicomponent Case after 2,000 Seconds.	56
6	Results of the Solution for the Case Where All Binary Diffusivities are Equal with No Knudsen Diffusion after 100 Seconds	60
7	Results of the Solution for the Case Where All Binary Diffusivities are Equal with no Knudsen Diffusion after 1,000 Seconds	62
8	Results of the Solution for the Case Where All Binary Diffusivities are Equal with no Knudsen Diffusion after 1,900 Seconds	64
9	Results of the Solution for the Case Where All Binary Diffusivities are Equal with no Knudsen Diffusion after 2,000 Seconds	66

LIST OF ILLUSTRATIONS

Figure	Page
1. Schematic Representation of a Volume Element of Coated Porous Media	11
2. Mole Fraction of HCl versus Station at Times Shown for the Multicomponent Case.	59
3. Comparison of Diffusivity for the Multicomponent Case and the Case of Equal Binary Diffusivities After 300 Seconds.	68
4. Diffusivity versus Station After 1,900 Seconds.	69
5. Comparison of Coating Deposited versus Time for Diffusion Cases with No Knudsen Diffusion.	70
6. Mole Fraction of HCl versus Station for Times and Pore Radii Shown for the Multicomponent Case	72
7. Mole Fraction of HCl versus Station for Times and Pore Radii Shown for the Equal Binary Diffusivities Case	73
8. Diffusivity versus Station for Pore Radii Shown at 1,900 Seconds	74
9. Coating Thickness versus Time for Pore Radii Shown for the Multicomponent Case.	75
10. Coating Thickness versus Time for Pore Radii Shown for the Equal Binary Diffusivities Case.	76
11. Arnold Solution versus the Multicomponent Solution at Early Times.	78
12. Steady State Solution versus the Multicomponent Solution at 1,900 Seconds.	79
13. Schematic Representation of the Porous Media--Core Gap	100

SUMMARY

In order to study the domains of Chemical Vapor Deposition in the industrial process of pack cementation, a comprehensive analytical model describing simultaneous transport phenomena in porous media is developed. Distinction is made between consolidated and unconsolidated media. Particular attention was paid to the models in the literature which described specific aspects of transport phenomena in porous media. In this work a novel approach to the equation of continuity is developed by using a single representation for effects in the solid and gas phases. Since no work previously discussed multicomponent diffusion in porous media, a model extending the "dusty gas theory" of Evans et al. is derived.

The specific problem in pack cementation chosen for study is the hydrogen reduction of HSiCl_3 to produce a silicon coating on an inert substrate. In this study, the substrate is also the wall of the pack cementation container. One of the objectives of this study is to show that coatings can be deposited on inert substrates due to the inherent advantages of the transient heat transfer, which exists early in the pack process. The generalized porous media transport equations are tailored to meet the constraints of the specific pack process chosen. These equations are then solved as an initial value problem through standard numerical techniques on a CDC digital computer. Due to depletion and deposition of a solid phase by chemical reaction at the walls and throughout the porous media, special boundary conditions and transport properties in the vicinity of the wall are developed.

Results are presented which show the effects of Knudsen diffusion on the amount of coating deposited and composition profiles. The effects of multicomponent diffusion are compared with those for equal binary diffusivities. Since actual experimental results are not available, accuracy of the numerical results is difficult to project. However, stability and convergence tests are used. In addition, results of the numerical mole flux calculations are compared to those from the Stephan-Maxwell equation. Early time results are compared to an analytical solution derived by Arnold.

The most important conclusion reached from the results of this thesis is that the model chosen for multicomponent diffusion will provide a successful solution for initial value problems in multicomponent mass transfer. The second important conclusion is that the assumption of equal binary diffusivities will provide a reasonable solution, thus greatly simplifying calculations. And finally, Knudsen diffusion can be a significant contribution to mass transfer in porous medium.

Several areas of further work and development in this area are evident from the results of this thesis. A nested iterative scheme to better calculate the molar concentrations in the porous media when deposition occurs should be developed. Laboratory experiments should be conducted to provide actual data for comparison with the model. And finally, experimental work to better relate porous media properties to transport properties should be conducted.

NOMENCLATURE

α_i	fraction of gas molecules diffusely reflected from capillary walls (dimensionless)
c	molar density (lb-mole/ft ³)
c'	number of molecules per unit volume (molecules/ft ³)
c_i	number of molecules of gas species i per unit volume (molecules/ft ³)
c_p	number of molecules of solid species p per unit volume (molecules/ft ³)
\tilde{C}_{p_i}	molar heat capacity of the gas species (BTU/lb-mole °F)
\hat{C}_p	heat capacity (BTU/lb-°F)
\hat{C}_{pp}	of solid substrate p
\hat{C}_{pc}	of coating c
\hat{C}_{p_i}	of gas species i
D_{ij}	binary diffusivity for species pair ij (ft ² /hr)
D_{ij}	effective binary diffusivity for dusty gas theory (ft ² /hr)
D_{ij}	binary diffusion coefficient for dusty gas theory (ft ² /hr)
\bar{D}_{im}^e	effective multicomponent diffusion coefficient in porous media for gas species i (ft ² /hr)
\bar{D}_{im}^e	overall diffusivity for the core interface (ft ² /hr)
DI	deposition index defined by equation 3-5 (dimensionless)
D_{xi}	Knudsen diffusivity for gas species i (ft ² /hr)
\bar{D}_p	average particle diameter (μ)
\bar{g}	acceleration due to body force on fluid (ft/sec ²)
H	constant defined by equation 2-20 (b)

\hat{H}	enthalpy (BTU/lb)
\hat{H}_i	of the gas species i
\hat{H}_p	of the solid substrate p
\hat{H}_c	of the coating c
\bar{J}_i^*	molar flux with respect to molar average velocity (lb-mole/hr-ft ²)
\bar{J}_i^{*e}	effective molar flux with respect to molar average velocity (lb-mole/hr-ft ²)
\bar{J}_i^c	effective mass flux with respect to mass average velocity (lb-mole/hr-ft ²)
K_p	equilibrium constant (dimensionless)
\bar{K}_o	porous media shape factor (dimensionless)
\bar{R}	tortuosity factor (dimensionless)
k	Boltzmann Constant
k_e	static effective thermal conductivity of the porous media (BTU/hr-ft-°F)
\bar{k}_e	overall thermal conductivity for the core interface (BTU/hr-ft-°F)
k_r	apparent thermal conductivity of the porous media due to radiation (BTU/hr-ft-°F)
k_r^o	radiation contribution to k_p defined by equation 2-21b
k_p	thermal conductivity of the solid substrate material (BTU/hr-ft-°F)
k_i	of the gas species i
k_f	of the fluid
k_s	of the shell or core material in a pack concentration model
L	actual length of a pore channel along a tortuous path (ft)
$LPWPI$	integer signifying the node point nearest the core-porous medium interface
L_e	linear depth of a porous substrate (ft)

L_0	length of the cylinder containing the pack (ft)
M_w	molecular weight of a gas mixture (lb-mole)
M_i	of gas species i
\bar{M}_i	of element i
m_i	molecular mass of species i (lb/molecule)
\bar{m}	reduced molecular mass (dimensionless)
m_p	mass of the solid substrate and coating at time t (lb)
m_{p_0}	of the solid substrate at initial time
m_c	of coating c
\bar{N}_i	molar flux of species i in a capillary (lb-mole/hr-ft ²)
\bar{N}_i^e	effective molar flux of gas species i (lb-mole/hr-ft ²)
\bar{N}_p^e	effective molar flux of solid species p (lb-mole/hr-ft ²)
\bar{n}_i^e	effective mass flux of species i (lb/hr-ft ²)
\bar{n}_t	total mass flux in the porous medium for dusty gas theory (lb/hr-ft ²)
\bar{n}^e	total effective mass flux (lb/hr-ft ²)
n_i	number of molecules of the gas species i per unit volume (molecule/cu ft)
n_p	number of molecules of the solid species i per unit volume (molecule/cu ft)
n	sum of gas species molecules
n'	sum of gas and solid molecules
P	pressure (psf)
P°	reference pressure (psf)
\bar{P}	average pressure in a porous medium (psf)
p	represents solid species p
\bar{q}	total energy flux (BTU/hr-ft ²)

r_i	generation term of species i (lb/hr-ft ³)
R_c	radius of the core material (ft)
R_p	radius of the porous material (ft)
\bar{R}_p	average radius of a particle (μ)
\bar{R}	average radius of the pore (\AA)
R	universal gas constant (cal/gm-mole-°K)
r	distance variable (ft)
S_o	specific surface of the particles of porous media (ft ²)- ⁻¹
T	temperature (°R)
T_{ci}	critical temperature of species i (°K)
t	time variable (hr)
\tilde{V}_{ci}	critical volume of species i (cm ³ /gm-mole)
V_p	volume of solid substrate (ft ³)
V_t	total unit volume of porous medium (ft ³)
\bar{V}_e	superficial velocity through porous media (ft/hr)
\bar{V}	actual velocity within a pore (ft/hr)
X	total amount of elemental hydrogen (lb)
x_i	mole fraction of species i (dimensionless)
Δr_p	incremental distance between the core and porous medium interface (ft)
Δr_s	incremental distance between the shell and porous medium interface (ft)
Δr	incremental radius (ft)
Δt	incremental time (hr)
α	thermal diffusivity (ft ² /hr)
ϵ	porosity or void volume of the porous medium (dimensionless)

ϵ_p	volume fraction of solid substrate and coating in a porous medium (dimensionless)
ϵ_p	of solid substrate only
ϵ	emissivity (dimensionless)
ϕ	term defined by equation 4-5b
κ	permeability of porous media (ft^2)
K	permeability coefficient of porous media ($\text{ft}^4/\text{lb}_f\text{-sec}$)
\bar{K}_0	shape factor representative of a specific porous medium (dimensionless)
λ_0	mean free path at reference pressure P_0 (ft)
λ_i	mean free path of a gas species i (ft)
μ	viscosity of the fluid ($\text{lb}/\text{ft}\text{-hr}$)
μ_i	of the gas species i ($\text{lb}/\text{ft}\text{-hr}$)
ρ	density of the fluid (lb/ft^3)
ρ_c	of the coating c
ρ_i	of the gas species i
ρ_p	of the solid substrate p
ρ_{p_0}	of the solid substrate at initial time
ρ_s	of the core or shell material
σ_i	collision diameter for the species i (ft)
σ_{ij}	collision diameter for the pair ij (ft)
τ	tortuosity of the porous medium (dimensionless)
δ_i	term defined by equation 2-9c
Ω_{ij}	diffusion collision integral for the pair ij (dimensionless)
$\Omega_{\mu i}$	collision integral for viscosity of the gas species i (dimensionless)

- ω_i mass fraction of gas species i (dimensionless)
- ω_{ci} of coating species i
- ν number of gas phase species (dimensionless)

CHAPTER I

INTRODUCTION

In the early stages of the multi-year program, "A Study of Interfacial Phenomena," sponsored at the Georgia Institute of Technology by the United States Air Force as part of the Project Themis, a search of the technical literature and a survey of the defense and space-oriented industry was conducted in the specific area of high temperature, oxidation resistant surface and diffusion coatings.¹ This study was undertaken to identify technology gaps and to determine research needs in this special coatings field. One of the recommendations resulting from this study was to investigate the domains of chemical vapor deposition as a coating mechanism. Chemical vapor deposition (CVD) is a basic coating process which may include both homogeneous gas phase and heterogeneous chemical reactions to produce a coating on a heated substrate material. In response to this particular recommendation, an experimental and analytical investigation of the CVD process was undertaken. The chemical system chosen for this research was the hydrogen reduction of silicon tetrachloride to elemental silicon and hydrogen chloride. At the time of this study, silicide coatings were of considerable interest to the aerospace industry for protection of refractory metals in severe thermal environments under oxidizing conditions.^{1,2} One technique used for the deposition of these coatings is CVD.^{3,4} Coincidentally, considerable effort had also been spent during this period by the semi-conductor industry in the production of single crystals and epitaxial thin-films of pure silicon on suitable

substrates by CVD for use in electronic components manufacturing.⁵ In both of these coatings-oriented industries, analysis and improvement of the CVD coating process were approached with experiment techniques. Many associated technical papers dealt with metallurgical implications.^{6,7,8} In most of the thin-film and single crystal work, theoretical considerations were limited to thermodynamic predictions.^{9,10} Only a few papers concerned with coating or thin-film characterizations and performance analysis considered the aspects of transport phenomena in the production of the coating.^{11,12,13} This omission was also particularly evident in the analysis of the production of diffusion coatings by CVD. While the solid-solid diffusion of the coating material into the substrate to produce an alloy is an essential part of the overall deposition process, in many cases this phenomena may not be the controlling mechanism.

Specifically, the research program mentioned above was a parametric study of the deposition rate of silicon on a tungsten wire. The important parameters, besides deposition rate, were wire temperature, gas phase flow rate, gas phase composition, and wire diameter. This first CVD study was conducted in a simple glassware system composed of a drying tube, two condensers, a bubbler flask, and a deposition tube. The substrate was electrically heated. Enough data were obtained from this preliminary experimental work to design and build a more substantial CVD apparatus. The construction of this system allowed for operation under partial vacuum or in positive pressures. This equipment was also constructed so that either a gas-liquid, a gas-gas, a gas-solid, or a solid-solid feed system could be utilized. The solid-solid feed system required that one of the components decompose into gaseous products which would react with the other solids to

give the desired reaction gases. In this apparatus, CVD coatings could be deposited on inert oxide substrates. Several experiments were conducted with this experiment. Coatings were obtained on tungsten wires and on inert alumina substrates.

Because of production related problems, the pure CVD process was found to be used in limited, often laboratory, situations. In more common industrial coating operations, other techniques incorporating CVD concepts were prevalent. One such technique in wide use is termed "pack cementation."¹⁴ This name described a process that has changed considerably in basic concept since its inception. Originally, "pack cementation" implied that coatings were produced by diffusion from metal powders in physical contact with the substrate surface at elevated temperatures.¹⁵ Examples of this process are the early cementation coatings of aluminum, zinc, or chromium on iron in the steel industry. In the chromizing process, pieces of iron or steel were packed in a retort surrounded by chromium powders.¹⁶ The pack was heated in a furnace at a temperature of 1300° C for four hours. To avoid excessive sintering of the coating material, inert refractory powders were mixed with the finely divided chromium. In 1927, Marshall modified the pack design in the chromizing process to include carrier gases which combined with chromium in the solid phase to form a gas phase species.¹⁷ This gas then reacted with the iron surface to produce a coating. The reaction of a carrier gas with the substrate is almost universal in modern pack cementation processes, thus chemical vapor deposition has become the basic coating mechanism in this operation. Several descriptions of the pack process for uses other than chromium coatings on iron may be found in references

18 through 22. In addition, workers have more recently used pack cementation successfully to produce complex coatings containing several elements which are deposited simultaneously.^{23,24}

The pack cementation process has been generally limited to diffusion coatings produced by solid-solid reactions or substitution reactions between the coating element and substrate, where the entire bulk of the material within the retort is maintained at constant temperature. Although very desirable, no results have been found in the literature which indicate pack cementation coatings can be produced on inert substrates. In pure CVD processes, however, inert substrates may be coated by surface reaction if the substrate temperature is sufficiently high. This phenomena may occur in a pack process during the transient period when the mass is heated from ambient to furnace temperatures.

In this thesis, the possibility of the production of a coating on an inert substrate is analyzed. In the past, only a few researchers have considered aspects of depletion, heat transfer, or flow within the pack.^{24,25} Any attempt to analyze this process will require an understanding of transport phenomena in porous media. A search of the literature did not reveal any considerations of pack cementation or other porous media related processes that incorporated flow, heat transfer, and mass transfer simultaneously. Several researchers have discussed separate aspects of transport phenomena in porous media, particularly the development of diffusivity and thermal conductivity. These discussions have been included in a general set of equations describing transport phenomena for porous media. These equations are presented in detail in the next chapter. The nature of this development is not limited just to the analysis of pack

cementation. Application can be found for these theories in several seemingly diverse fields including grain drying or aeration, shale oil recovery, and catalyst performance prediction.

In Chapter III, the general transport equations for porous media presented in Chapter II are applied to the specific problem in pack cementation mentioned above. Results of a digital computer solution to this problem based on finite difference equations are discussed in Chapter IV. Recommendations and conclusions follow in Chapter V.

CHAPTER II

TRANSPORT PHENOMENA IN POROUS MEDIA

Analytical analysis of simultaneous heat, mass, and momentum transport in porous media is relatively undeveloped. As was mentioned in the Introduction, certain aspects of the individual conservation equations have been studied by researchers of different disciplines. For example, hydrologists have investigated flow through sand beds and have proposed empirical relations for the steady state equation of motion. Chemical engineers have experimented with diffusion in catalyst pellets and have proposed semi-empirical relations for the diffusion coefficient. Because most of the reported work is experimental in nature, the resulting relationships are practically oriented and not readily suited to theoretical application. A good example of this deficiency concerns studies of heat transfer with flow through a porous medium in which the convective effect and the Knudsen effect are treated as conduction and included in the apparent thermal conductivity.

Comparison of the various relations describing transport phenomena in porous media is further complicated because substantially different models were chosen to characterize the media. In many flow and heat transfer studies, media structures have been classified as either "consolidated" or "unconsolidated." Unconsolidated media are formed from randomly oriented particles. Consolidated media are those media which may have closed ended or completed closed pores. These media could have originated from

an unconsolidated structure which could have sintered or undergone some other process to close the pores. Much of the literature involved with flow and heat transfer studies concerns the porous media characterizations with different models for the pore size distribution within a given structure. In diffusion studies, especially where catalyst pellets have been formed from porous particles, the structure has not been classified. However, different models are used to describe the pore size.

In the discussions of this chapter, a comprehensive analytical model describing simultaneous transport phenomena in porous media will be developed. Because results of the present study might be applied to either of the two general classifications of porous structure, the following discussions will include consolidated and unconsolidated media. Effects of the various pore size models will also be discussed where appropriate. The development of each transport equation will be separately shown. The particular transport properties associated with porous media will also be discussed in each appropriate section. Equations for calculation of the properties not influenced by porous media effects, such as gas density and gas heat capacity, will be presented later.

Equation of Motion

The equation of motion for flow through porous media is an expression of the experimental results of several workers. Notable among them is Darcy. His work has been formulated into an equation which bears his name and is given below as equation 2-1. This relation and its historical development are well documented.^{26,27,28}

$$\bar{v}_e = -\frac{K}{\mu} (\nabla P - \rho \bar{g}) \quad (2-1)$$

where \bar{v}_e is the superficial velocity of the fluid flowing in the porous medium
 K is the permeability
 μ is the fluid viscosity
 ∇P is the pressure gradient
 ρ is the fluid density
 \bar{g} is the body force on the fluid.

Darcy's Law differs considerably from the classical equation of motion (as it appears in Bird et al.²⁹ for example); however, this relation applies to macroscopic rather than microscopic observations of a fluid passing through fine channels in porous media. Although no transient terms appear in Darcy's Law, this equation is used in the solution of time dependent problems.²⁹ To better describe certain specific problems such as in flow through a porous mass and an adjoining empty space, Brinkmann has proposed a modification to equation 2-1 which reduces to Darcy's Law for low values of the permeability.³⁰ This relation was more rigorously derived by Slattery.³¹

Since Darcy's Law was determined experimentally for flow through unconsolidated porous media with a uniform pore size, a correction must be made for application to consolidated porous media. The accounting for the different types of porous media is incorporated in the value used for the permeability. Carman has discussed methods for the determination of this property and other problems encountered in the characterization of porous media for flow in detail. Results of his efforts and others

are presented briefly below for both consolidated and unconsolidated media.

Carman based his work on the earlier studies of Blake³² and Kozeny.³³ These independent efforts were among the first to apply the concept of a hydraulic radius to the viscous flow of fluids through unconsolidated porous media with uniform pore size. Carman chose to describe flow through the porous medium in terms of the superficial velocity \bar{V}_e and the bed depth L_e instead of the actual quantities, \bar{V} and L , for the individual capillaries of the medium. In doing so, he defined a new variable, τ , called the tortuosity, to represent the ratio $\frac{L}{L_e}$. Then he modified the results of Dupuit³⁴, which relate actual velocity, \bar{V} , to the apparent velocity, \bar{V}_e , to include the tortuosity. These modifications have been included in the definition of the permeability which is given below:

$$K = \frac{\epsilon^3}{\bar{K} S_o^2 (1-\epsilon)^2} \quad (2-2)$$

where ϵ is the porosity or the void fraction
 S_o is the specific surface of the particles
 \bar{K} is the tortuosity factor which is a function of τ^2 and a shape factor \bar{K}_o .

All of the quantities in equation 2-2 may be determined experimentally with relative ease with the exception of the tortuosity factor, \bar{K} . Carman has reported results of many experiments to evaluate this quantity. Carman has also stated that for most unconsolidated media, the value of K is approximately 5.0 inches².

Evaluation of the quantities in equation 2-2 for consolidated

porous media is more difficult. Usual experimental procedures to determine the value of S_0 (e.g., nitrogen absorption) are not applicable since these procedures include closed ended pores where flow does not occur. Wyllie and Rose have proposed a relation to calculate the tortuosity factor of consolidated media.³⁵ The result of their work as reported by Carman is given below:

$$\bar{k} = 2.5 \tau^2 \quad (2-3)$$

Experimental values reported in Carman indicate that this relation is adequate for the porosities expected for consolidated media. As with the definition for the permeability for unconsolidated media, experiments are required to arrive at a value for τ . Carman also mentions the problem of a nonuniform pore size and provides, as a solution, an integral technique for the range of particle sizes under consideration.

Recent results of diffusion studies in catalyst pellets imply that the tortuosity can be simply related to porosity for specific types of porous media. These results will be discussed in detail in a following section of this chapter.

Equation of Continuity

In general, the equation of continuity for flow through porous media has been written in two parts, one for the gas phase and one for the solid phase.³⁶ In the present study, the porosity will be allowed to change, so, for convenience, a single continuity equation for both phases will be derived.

A volume element composed of solid particles and gas is shown in Figure 1. The solid particles are assumed to be composed of a substrate

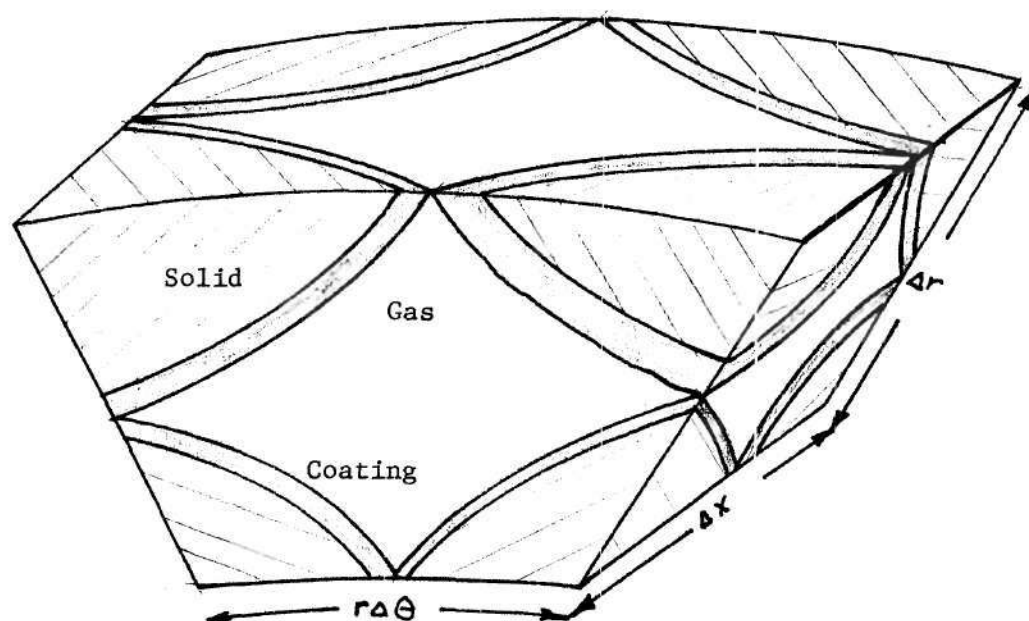


Figure 1. Schematic Representation of a Volume Element of Coated Porous Media.

with constant density ρ_{p_0} and a film of coating with constant density ρ_c . After suitable mathematical manipulation (see Appendix I for details), the density of the solid particle composed of the original substrate plus the coating may be determined as follows:

$$\rho_p = \rho_c + (\rho_{p_0} - \rho_c) \frac{\epsilon_{p_0}}{\epsilon_p} \quad (2-4)$$

where ϵ_p is the volume fraction of solid per unit volume of solid and gas for any time.

ϵ_{p_0} is the initial volume fraction of solid per unit volume of solid and gas.

The equation of continuity for a volume composed of both solid particles and gases where the mass velocity of the solid is zero is also derived in Appendix I. The result of this development is given below:

$$\frac{\partial}{\partial t}(\epsilon \rho) + \frac{\partial}{\partial t}(\epsilon_p \rho_p) + \nabla \cdot \rho \vec{v}_e = 0 \quad (2-5)$$

where t is time.

Substitution of equation 2-4, the expression for the density of the solid particles, into equation 2-5 yields:

$$\frac{\partial}{\partial t}(\epsilon \rho) + \frac{\partial}{\partial t}(\rho_c (\epsilon_p - \epsilon_{p_0})) + \nabla \cdot \rho \vec{v}_e = 0 \quad (2-6)$$

Noting that the change in the initial porosity with time is zero, equation 2-6 may be reduced to the continuity equation used in this work which is presented below:

$$\frac{\partial}{\partial t}(\epsilon \rho) + \rho_c \frac{\partial \epsilon_p}{\partial t} + \nabla \cdot \rho \bar{v}_e = 0 \quad (2-7)$$

Equation of Continuity Species i

The equation of continuity for species i is derived in a manner similar to that for the overall continuity equation and is given below:

$$\frac{\partial}{\partial t}(\epsilon \rho \omega_i) + \rho_c \frac{\partial}{\partial t}(\epsilon_p \omega_{ci}) + \nabla \cdot \bar{n}_i^e = r_i \quad (2-8)$$

where ω_i is the mass fraction of the species i in the gas phase
 r_i is the generation term for species i
 \bar{n}_i^e is the effective mass flux of species i based on a unit area of both solid and gas
 ω_{ci} is the mass fraction of the species i in the coating.

Over the last several years, many papers have been published on methods used to determine values for the diffusion coefficient for use in the mass or mole flux relationship. Much of this work was generated by the increased interest in catalyst pellets formed by pressing together small porous particles. At low pressures, the usual pore size distribution was such that both normal diffusion and Knudsen diffusion occurred. As previously mentioned, all of the publications reviewed involved only binary diffusion. However, Evan, Watson and Mason proposed a diffusion model for constant pressure and temperature based on a "dusty gas" theory that offered promise for adaptation to a multi-component system.³⁷ In this model, the Stefan-Maxwell equations were written to include the solid as a giant molecule with zero mass velocity. This approach resulted in an equation which conformed to the accepted relations describing the

transition region between normal diffusion and free molecular flow.³⁸

This equation also reduced to the proper form for conditions at either limiting case. The results of the work by Evans et al. are given below as equation 2-9a. A brief summary of the derivation of these equations is presented in Appendix II.

$$\bar{N}_i^e = -D_i^e \frac{\partial n_i}{\partial z} + \frac{n_i}{n} \bar{N} \delta_i \quad (2-9a)$$

where $D_i^e = \frac{n_i}{n} \delta_i D_{ij}^{e'}$ (2-9b)

$$\delta_i = \left(1 + \frac{n_d}{n} \frac{D_{ij}^{e'}}{D_{ip}^{e'}} \right)^{-1} \quad (2-9c)$$

- and
- \bar{N}_i^e is the molecular flux of species i based on a cross-sectional area of both solid and gas
 - n_i is the number of molecules of the gas phase species i per unit total volume
 - n is the total number of gas phase molecules per unit total volume
 - n_p is the number of molecules of the solid per unit total volume
 - n' is the sum of n and n_p
 - $D_{ij}^{e'}$ is the effective diffusion coefficient for a porous medium
 - $D_{ip}^{e'}$ is the effective Knudsen diffusivity for a porous medium.

The effective diffusion coefficients are related to the normal diffusivities by the generally accepted relationship given in equation 2-10.³⁷

Through the definition of τ , specific contributions to the diffusion by consolidated or unconsolidated media can be made.

$$D_{ij}^{e'} = \frac{\varepsilon}{\tau} \phi_{ij}' \quad (2-10)$$

where ε is the porosity
 τ is the tortuosity
 ϕ_{ij}' is the binary diffusivity for the dusty gas theory.

The binary diffusivity for the gas phase species can be obtained from the following equation:²⁹

$$\phi_{ij}' = \left(\frac{16}{3} n' \left(\frac{\bar{m}}{2\pi kT} \right)^{\frac{1}{2}} (\pi \sigma_{ij}^2 \Omega_{ij}) \right)^{-1} \quad (2-11a)$$

$$\text{where} \quad \bar{m} = \frac{m_i m_j}{m_i + m_j} \quad (2-11b)$$

and m_i is the molecular mass of species i
 k is the Boltzmann constant
 T is the absolute temperature
 σ_{ij} is the collision diameter
 Ω_{ij} is the collision integral.

The diffusivity, $D_{ip}^{e'}$, representing the interaction between the solid and gas species is equivalent to a Knudsen diffusivity.³⁷ Based on assumptions provided by Evans et al., this diffusivity is calculated by assuming the reduced mass, \bar{m} , becomes m_i , and the collision diameter, σ_{ij} , becomes \bar{R}_p , the radius of the solid particles. According to Epstein, as reported by Evans et al., the collision integral, Ω_{ip} , reduces to $(1 + \frac{\alpha_i \pi}{8})$.³⁹ The equation for D_{ip} thus becomes:

$$D_{ip}^{e'} = \frac{\varepsilon}{\tau} \left(\frac{16}{3} n' \left(\frac{m_i}{2\pi kT} \right)^{\frac{1}{2}} (\pi \bar{R}_p^2) \left(1 + \frac{\alpha_i \pi}{8} \right) \right)^{-1} \quad (2-12)$$

where \bar{R}_p is the radius of the solid particles
 a_i is the fraction of species i diffusely scattered by the wall.

According to Schmitt, again as reported in Evans et al., a_i is usually equal to unity.⁴⁰ Independently, Rothfield derived a similar expression for equation 2-9a based on momentum balances.⁴¹ In this model, a special definition for the Knudsen diffusivity was used which contained a bulk flow term. Scott and Dullien, in their analysis of mixed mode diffusion in porous media, first derived a diffusion equation for a single circular capillary where both normal and Knudsen diffusion applied.⁴² To extend their model to porous media, they also used a value determined by the ratio $\frac{E}{\epsilon}$ to express the effects of porous media on the binary diffusivity. Integrated forms of the equation of Evans et al., Scott and Dullien, and Rothfield have all been shown to be equal.⁴³ These equations are discussed further in Appendix III.

From first appearances, the definition for the effective Knudsen diffusivity derived by Evans et al., as shown in equation 2-12, will allow for direct calculation from basic porous media property data. With the more common definition (see for example Pollard and Present⁴⁴), diffusion studies are required to evaluate a constant in the Knudsen diffusivity equation, K_0 , which accounts for the porous media effects. In comparing their equation to these earlier works, Evans et al. state that the collection of terms $\frac{\pi}{\epsilon} n' \bar{R}_p^2 (1 + \frac{a_i \pi}{8})$ must be evaluated from diffusion experiments rather than calculated directly. In effect, Evans et al. have simply expanded the definition for the experimental constant K_0 .

Most of the later papers on diffusion in porous media have been concerned with modifications of the early work to better account for the

effect of actual porous structures on the diffusivities. These models have utilized either experimental diffusion data or porous media characterization data to predict results for new diffusion conditions. For example, several papers published by J. M. Smith and his co-workers were based on diffusion in catalyst pellets assumed to have a bi-disperse, randomly oriented, non-continuous pore structure.^{45,46,47} Johnson and Stewart developed a different model to show the effect of pore geometry on the effective diffusivity.⁴⁸ This modification also assumed randomly oriented circular pores but considered the distribution to be continuous rather than bi-disperse and non-continuous. The results of Johnson and Stewart and Smith and co-workers are consistent. Brown et al. compared the two techniques with experimental data and reached a similar conclusion.⁴⁹ The results of Smith and co-workers are particularly important to the present study. According to these workers, if the porous media has a single mode pore size distribution with a single radius, $\frac{\epsilon}{\tau}$ would be equal to ϵ^2 in the local diffusion equation. Thus the need for experimental determination of τ is eliminated. For a bimodal distribution, the definition of the ratio $\frac{\epsilon}{\tau}$ would be more complex. Considerable data are presented in Carman which can be used to show that $\frac{\epsilon}{\tau}$ is approximated by ϵ^2 .²⁶ In addition, Smith and coworkers show that pore size distribution data can be used to calculate the Knudsen diffusivity without results from prior diffusion studies.⁴⁵

Smith and co-workers have also extended their work on pure diffusion processes in porous media to include the effects of chemical reaction and of absorption on the diffusion phenomena.⁵⁰⁻⁵⁴ Wakao and Smith proposed a modification for the effective diffusion coefficient in which reaction

or absorption is occurring.⁵³ Scott has proposed a similar model to account for the effect of reaction during diffusion in porous media.⁵⁵

As was previously mentioned, no work has yet been presented for multi-component diffusion in porous media. The approach used in this work to analyze such a problem is based on an extension of the method given by Evans et al. In addition, the benefit of the later work by Smith and co-workers and Johnson and Stewart which provides better definitions for the term $\frac{\bar{E}}{\bar{c}}$ and the Knudsen diffusivity will be utilized. The results of the derivation of the multi-component mass flux term \bar{n}_i^e is presented below.

By rearranging the basic diffusion equation proposed by Evans et al. in terms of concentrations based on a unit volume of both solid and gas molecules, the following equation results:

$$\nabla x_i = \sum_{j=1}^N ((c'D_{ij}^e)') (x_i \bar{N}_j^e - x_j \bar{N}_i^e) + (c'D_{ip}^e)' (\frac{c_i}{\bar{c}} \bar{N}_p^e - \frac{c_p}{\bar{c}} \bar{N}_i^e) \quad (2-13)$$

where c' is the molar concentration of the gas and solid
 c_p is the number of solid molecules per unit volume
 x_i is the mole fraction of the gas species i
 \bar{N}_i^e is the molar flux of the gas species i
 \bar{N}_p^e is the molar flux of the solid species.

The derivation of this equation is presented in Appendix IV. The molar flux of the solid, \bar{N}_p^e , is assumed to be identically equal to zero. Further, the quantity $c'D_{ip}^e$ may be rearranged to give:

$$c'D_{ip}^e = c D_{ip}^e \quad (2-14)$$

Insertion of these results into equation 2-13 gives:

$$\nabla \kappa_i = \sum_{\substack{j=1 \\ i \neq j}}^N ((c' D_{ij}^e)^{-1} (\kappa_i \bar{N}_j^e - \kappa_j \bar{N}_i^e)) - (c D_{ip}^e)^{-1} \bar{N}_i^e \quad (2-15)$$

For the gas phase species, the term $c' D_{ij}^e$ is equal to $c D_{ij}^e$. If the molar flux of species i is defined as follows:

$$\bar{N}_i^e = J_i^{*e} + \kappa_i \bar{N}^e \quad (2-16a)$$

where $J_i^{*e} = -c \phi_{im}^e \nabla \kappa_i \quad (2-16b)$

equation 2-15 and 2-16a may be combined to give:

$$c \phi_{im}^e = \left(\frac{\sum_{j=1}^N ((c D_{ij}^e)^{-1} (\kappa_i \bar{N}_j^e - \kappa_j \bar{N}_i^e)) + (c D_{ip}^e)^{-1} \bar{N}_i^e}{\bar{N}_i^e - \kappa_i \bar{N}^e} \right)^{-1} \quad (2-17)$$

The mass flux is obtained from the following relation:

$$\bar{n}_i^e = \left(-\rho \frac{\phi_{im}^e}{M_w} \nabla \kappa_i + \kappa_i \bar{N}^e \right) M_i \quad (2-18)$$

where M_w is the molecular weight of the mixture

M_i is the molecular weight of the gas species i .

Equation of Energy

The derivation of the equation for energy conservation in porous media begins with a generalized form in which potential and kinetic terms are neglected. This relation must be modified to include the contributions

of both the solid and gas phases. Therefore the change in enthalpy within a unit volume composed of a solid and flowing gas is assumed to reflect both the change of the enthalpy of the gas and solid on an additive basis. The generalized equation is further modified by assuming that the velocity of the solid is zero and that the change in solid density with time is zero. The modified energy equation is given below as equation 2-19. This derivation is presented in detail in Appendix V.

$$\begin{aligned}
 (\epsilon_P c_P + \epsilon_P \rho_P c_{P_0} + (\epsilon_P - \epsilon_P) \rho_c c_{P_c}) \frac{\partial T}{\partial t} + \rho_c (\hat{H} - \hat{H}_c) \frac{\partial \epsilon}{\partial t} \\
 + \epsilon_P \sum_{i=1}^N (\hat{H}_i \frac{\partial w_i}{\partial t}) = -\rho c_P \bar{v}^e \cdot \nabla T - \rho \bar{v}^e \cdot \sum_{i=1}^N (\hat{H}_i \nabla w_i) \\
 - \nabla \cdot \sum_{i=1}^N (\hat{H}_i \bar{f}_i^a) + \epsilon \frac{\partial P}{\partial t} + \nabla \cdot k_e \nabla T
 \end{aligned} \quad (2-19)$$

where \hat{H}_i is the mass enthalpy of the gas species i

\hat{H}_c is the enthalpy of the coating

k_e is the effective thermal conductivity.

In a manner analogous to the previous section, the effect of the porous media on heat conduction is expressed in the thermal conductivity.

Considerable literature has been published describing various models for the thermal conductivity in porous media. A number of studies have dealt with heat transfer in a porous solid filled with a static fluid.⁵⁶⁻⁶² Studies have also been conducted for heat transfer in porous media with flowing fluids.^{63,64,65} In many of these publications, considerations have also been made for the difference between consolidated and unconsolidated materials. One paper included the effects of gas-solid

reactions on the thermal conductivity.⁶⁶ Recently, Huang proposed that for porous rock, the static thermal conductivity be given by the following equations:⁶⁷

$$k_e = \epsilon_p k_p \exp\left(-\frac{\eta}{\epsilon_p}\right) + \epsilon(k_f + k_r) \exp\left(-\frac{\eta}{\epsilon}\right) + H^2(1 - \exp\left(-\frac{\eta}{\epsilon}\right))^{-1} \quad (2-20a)$$

$$\text{where} \quad H = 1 - \epsilon \exp\left(-\frac{\eta}{\epsilon}\right) - \epsilon_p \exp\left(-\frac{\eta}{\epsilon_p}\right) \quad (2-20b)$$

and ϵ is the porosity

η is the pore geometric factor

k_p is the solid thermal conductivity

k_f is the fluid thermal conductivity

k_r is the apparent radiation thermal conductivity.

Huang based his derivation on a probability argument for a model combining three mechanisms: heat transfer by conduction through the solid, heat transfer through the solid and fluid in series by conduction and radiation, and heat transfer through the fluid phase by conduction and radiation. This relation is applicable to both consolidated and unconsolidated porous media through the value chosen for η .

Various relations have also been proposed to calculate k_r , k_p , and k_f . Schotte has proposed the following relation for k_r in packed beds:⁶⁰

$$k_r = \left(\frac{1 - \epsilon}{\frac{1}{k_p} + \frac{1}{k_r^0}} \right) + \epsilon k_r^0 \quad (2-21a)$$

$$\text{where} \quad k_r^0 = 0.692 \epsilon D_p \left(\frac{T}{100} \right)^3 \quad (2-21b)$$

and ϵ is the emissivity

D_p is the particle diameter.

Schotte compared his results with the experimental data of Yagi and Kunii⁵⁷ with good success.

The term k_p is the thermal conductivity of the solid material and can be found in specific literature related to that material. The term k_f , which is the fluid conductivity, must be corrected for pore size if the fluid is a gas with a low pressure. Huang has proposed the following relation:⁶⁷

$$k_f^* = k_f \left(1 + \frac{1}{S} \right) \quad (2-22a)$$

where
$$S = \frac{2\bar{R}_p}{\lambda_0 P^0} \quad (2-22b)$$

and k_f is the conductivity of the gas mixture

P is the pressure

P^0 is the reference pressure

λ_0 is the gas mean free path at the reference pressure

\bar{R}_p is the mean particle radius.

For a multi-component gas mixture, an averaging technique must be used to calculate the mean free path. The multi-component gas conductivity, k_f , will be calculated as described in the next chapter.

CHAPTER III

ANALYSIS OF PACK CEMENTATION

As was mentioned in the Introduction, the specific problem chosen for analysis in this thesis is the deposition of solid silicon on an inert alumina shell by the pack cementation process. In order to postulate a problem whose solution can be obtained with a realistic amount of computer time while still preserving all of the essential features, a single chemical vapor deposition reaction based on the hydrogen reduction of trichlorosilic acid to form hydrogen chloride and solid silicon is specified. In the past, workers concerned with this chemical system chose silicon tetrachloride as the predominant gas phase silicon bearing species (see for example, reference 68). Recent studies by Harper and Lewis have shown that the particular species chosen for this thesis are predominant.⁶⁹

In the proposed process, a ceramic cylinder, filled with a porous pack material with a solid silicon core at the center, all at constant temperature, is placed in a hot furnace. The porous mass is assumed to contain a mixture of hydrogen, hydrogen chloride, and trichlorosilic acid. At the start, heat is added to the outside surface of the alumina shell. As the temperature of the system rises, hydrogen chloride reacts with the silicon at the core surface to form trichlorosilic acid and hydrogen. As the species diffuse outward toward the hot alumina shell and attain a higher temperature, the equilibrium shifts so that solid silicon is deposited as a coating.⁶⁹

For this problem, all transport phenomena effects are assumed to

be symmetrical about the cylindrical axis. The analysis of this process is based on a reduced set of the generalized transport equations for consolidated porous media as presented in Chapter II. The specific equations are given below. In addition, the remaining constraints necessary for analysis of the proposed problem are presented below. Unfortunately, analytical techniques for the simultaneous solution below of these relations are not available. As is typical of many such problems, numerical solution schemes using a digital computer have been combined to provide an algorithm which may be used to predict events in pack cementation. In this chapter, details of this algorithm are also presented. Boundary and initial conditions are discussed in terms of their numerical representations.

Porous Media Description

The hypothetical porous media selected for this study is assumed to be consolidated and made from pressed alumina powder with a single pore radius. These assumptions allow for the calculation of the tortuosity from the porosity without experimental determination and thus simplify the porous media effect on both the diffusivity and permeability as previously discussed. The actual material properties selected are those used in many previous diffusion and heat conduction studies as reported in Smith et al.⁴⁵ Pertinent data are summarized as follows:

Material	$\text{Al}_2\text{O}_3 \cdot \text{H}_2\text{O}$
Particle diameter	90 μ
Macropore radius	To be determined
Particle density	2.45 gm/cc

The value for n in equation 2-20 for this material as reported by Huang is approximately 1.0.⁶⁷

Transport Equations

The general transport equations for porous media presented in the previous chapter may be simplified for the analysis of this pack coating process. Because the coating is composed of a single component, silicon, and because this species does not exist in the gas phase, the conservation of silicon represented by equation 2-8 becomes:

$$-\rho_{si} \frac{\partial \epsilon}{\partial t} = r_{si} \quad (3-1)$$

Equation 2-8 for the continuity of the gas phase species also reduces as follows:

$$\frac{\partial}{\partial t}(\epsilon \rho \omega_i) + \nabla \cdot \bar{n}_i^e = r_i \quad (3-2)$$

Application of the assumptions mentioned in the previous paragraph to equation 2-19 gives the equation for energy conservation,

$$\begin{aligned} (\epsilon \rho c_p + \epsilon_p \rho_p c_{p,p} + (\epsilon_p - \epsilon_p) \rho_{si} c_{p,si}) \frac{\partial T}{\partial t} + \rho_{si} (\hat{H} - \hat{H}_{si}) \frac{\partial \epsilon}{\partial t} + \epsilon \rho \sum_{i=1}^N (\hat{H}_i \frac{\partial \omega_i}{\partial t}) = \\ - \rho c_p \bar{v}_e \cdot \nabla T - \rho \bar{v}_e \cdot \sum_{i=1}^N (\hat{H}_i \nabla \omega_i) - \nabla \cdot \sum_{i=1}^N (\hat{H}_i \bar{n}_i^e) + \nabla \cdot k_e \nabla T + \epsilon \frac{\partial p}{\partial t} + p \frac{\partial \epsilon}{\partial t} \end{aligned} \quad (3-3)$$

For this problem, the equation of motion remains as equation 2-1. The overall equation of continuity, equation 2-7, also remains the same as previously derived.

The only transport equation needed to describe both the core material and the inert shell for the problem chosen for this work concerns

conservation of energy. Even though the shell is composed of a ceramic material, temperatures anticipated in this problem are not sufficient to cause changes in pressure with time or distance. The equation used to describe the conservation of energy for either the shell or the core is given below:

$$\rho_s c_p \frac{\partial T}{\partial t} = \nabla \cdot k_s \nabla T \quad (3-4)$$

Auxiliary Equations and Further Assumptions

One of the more interesting aspects of the present problem lies in the deposition of a condensed phase by chemical reaction. Unfortunately, experimental data of sufficient accuracy are not available to obtain a reliable empirical relationship to predict condensation rates for the chemical system considered in the present study. In addition, theories for condensation kinetics are not well developed so theoretical results are also not available. Thus, the assumption is made that the gas phase is in equilibrium with the condensed phase, should one be present. The implication in this assumption is that the condensation kinetics are infinite or at least so rapid that species transport processes are rate controlling. The extent to which assumption is valid must rest on experimental data obtained under conditions in which the diffusional and equilibrium conditions have been precisely determined. In order to determine when condensation occurs, the following procedure is followed in the present study. For convenience a deposition index, DI, is defined as:

$$DI = \frac{P X_{HCl}^3}{X_{H_2} X_{H_2SiCl_3}} \quad (3-5)$$

The numerical value of DI is compared with the numerical value of the equilibrium constant, K_p , for the specific gas phase-condensed phase equilibrium. If DI is less than K_p , the thermodynamic implication is that a condensed phase is formed. The gas phase composition is calculated accordingly. Use of the appropriate continuity equation results in a prediction of the amount of the solid phase deposited.

In addition to this major point, several other relationships must be used to analyze the pack cementation process. These equations are discussed in the following paragraphs.

The ideal gas law needed to calculate the systems pressure is presented below in equation 3-6:

$$P = \frac{\rho RT}{M_w} \quad (3-6)$$

Another set of constraints which must be satisfied concerns the conservation of the elements. Equations are given below for the specific chemical system at hand.

$$2 \frac{\bar{M}_H}{M_{H_2}} r_{H_2} + \frac{\bar{M}_H}{M_{HCl}} r_{HCl} + \frac{\bar{M}_H}{M_{HSiCl_3}} r_{HSiCl_3} = 0 \quad (3-7)$$

$$3 \frac{\bar{M}_{Cl}}{M_{HSiCl_3}} r_{HSiCl_3} + \frac{\bar{M}_{Cl}}{M_{HCl}} r_{HCl} = 0 \quad (3-8)$$

$$\frac{\bar{M}_{Si}}{M_{HSiCl_3}} r_{HSiCl_3} + r_{Si} = 0 \quad (3-9)$$

The final equation used in the mathematical description of this pack cementation problem satisfies the requirement that the sum of the mass fractions in the gas phase must equal unity. This relation is mathematically represented below:

$$\sum_{i=1}^N \omega_i = 1 \quad (3-10)$$

Finite Difference Equations

The initial step in the solution to the problem for this thesis concerns the representation of the partial differential equations and the accompanying boundary conditions as numerical relations. In the method selected, the derivative terms in the partial differential equations are replaced by finite difference ratios. Detailed discussions of this technique to solve differential equations are presented by Mickley et al.⁷⁰ The following is a brief summary of the approach used here.

Finite difference ratios are easily derived from a Taylor's series. As an example, the time derivative of temperature, $\frac{\partial T}{\partial t}$, where temperature is both a function of space and time can be considered. A Taylor's series expansion of temperature at a fixed point with time as a variable is given below:

$$T(r, t + \Delta t) = T(r, t) + \Delta t \frac{\partial T}{\partial t} + \frac{\Delta t^2}{2} \frac{\partial^2 T}{\partial t^2} + \frac{\Delta t^3}{6} \frac{\partial^3 T}{\partial t^3} + \dots \quad (3-11)$$

If time increments are sufficiently small, terms in Δt of second order or higher may be neglected. Thus the derivative of temperature with respect

to time may be approximated as:

$$T(r, t + \Delta t) = T(r, t) + \Delta t \frac{\partial T}{\partial t} \quad (3-12)$$

This equation is described as "forward marching" in time. For partial derivatives of temperature with respect to the position variable r , third order terms of Δr are neglected and two series approximations combined to give:

$$\frac{\partial T}{\partial r} = \frac{T(r + \Delta r, t) - T(r - \Delta r, t)}{2\Delta r} \quad (3-13)$$

For second derivatives with respect to r , suitable manipulation of the two series yields:

$$\frac{\partial^2 T}{\partial r^2} = \frac{T(r + \Delta r, t) - 2T(r, t) + T(r - \Delta r, t)}{\Delta r^2} \quad (3-14)$$

Equations 3-13 and 3-14 are described as "centered" difference relations. In some cases, the space variable increments may not be equal. To obtain a finite difference relation, two series equations with different incremental distances are utilized to give:

$$\frac{\partial T}{\partial r} = \frac{\frac{\Delta x}{\Delta x} (T(r + \Delta x, t) - T(r, t)) + \frac{\Delta x}{\Delta x} (T(r, t) - T(r - \Delta x, t))}{\Delta x + \Delta x} \quad (3-15)$$

Similar manipulations of the Taylor's series expansions will yield a finite difference equation for the second derivative of temperature with respect

to the space variable where the incremental space variables are not identical.

The choice of a "forward marching" difference equation for the time derivative and a "centered" difference equation for the space derivatives is typical for the solution of initial value problems. In this case, values for all variables are known at the initial time. Values at the next time may be calculated by the algebraic solution of the suitable finite temperature at time $t + \Delta t$, as for example the equation for transient heat conduction with constant properties:

$$T(r, t + \Delta t) = T(r, t) + \frac{\Delta t k}{\rho c_p} \left(\frac{T(r + \Delta r, t) - 2T(r, t) + T(r - \Delta r, t))}{\Delta r^2} \right) \quad (3-16)$$

Other, more accurate difference equations may be derived from alternate forms of the Taylor's series expansion. For example, the time derivative may be based on $t + 2\Delta t$, or higher terms may be included. However, these equations require an iterative scheme for solution. As a result, these alternatives will use greater amounts of computer time for solution for the same increment size. In any finite difference representation of a differential equation, the accuracy of the solution will be determined by the size of the increments of the numerical solution if both stable and convergent.⁷¹ These two basic criteria are discussed further below.

Stability and Convergence

If there is an exact solution for a given partial differential equation, there is an exact solution for any given finite difference equation used to represent this partial differential equation. Any difference

between these two solutions is known as the truncation error. If the exact solution to the finite difference equation approaches the solution to the partial differential equation in the limit as the incremental variable approaches to zero, the finite difference equation is said to be convergent.⁷¹

In a practical solution of a given problem utilizing finite difference equations, only a finite number of significant figures can be carried in the computations. The difference between the exact solution of the finite difference equations and this practical solution is known as the numerical error. Generally, these errors are predominantly errors of round-off. A practical solution to a difference equation in which the numerical error does not increase as the solution progresses is said to be stable.⁷¹ Unless a proposed numerical solution is both stable and convergent, or unless the instability is predictable, the accuracy of the results is unknown. Several tests have been published which may be used to determine the stability and convergence of the special class of numerical schemes which represent linear partial differential equations with constant coefficients.⁷¹ For the transient heat conduction equation with constant properties, stability is insured if a modulus, defined as $\alpha \frac{\Delta t}{\Delta r^2}$, is less than 0.5. If stability is assured, the solution will also be convergent and the accuracy will only be a function of the increment sizes chosen.⁷¹

In such cases where variable properties or nonlinear equations are involved, the modulus $\alpha \frac{\Delta t}{\Delta r^2}$ cannot be used to predict stability and convergence. However, this concept may serve as a guide to test a proposed solution. If a solution exhibits oscillation or unreasonable physical results, the modulus can be changed and the new results studied. Results

using several grid spacings can also be studied to check for convergence.

Boundary and Initial Conditions

For the solution to the problem of pack cementation, conditions at three interfaces must be specified. In the following paragraphs, boundary conditions for the shell-furnace interface and the center of the core are presented first. These discussions are followed with derivations for the relations which apply at the core-porous medium interfaces. Relationships for the second porous medium interface will be similar and will not be given here.

At the interface between the surface of the shell and furnace environment, only heat is transferred across the boundary, so only energy related conditions are required. For this boundary, the shell surface temperature is assumed to be known as a function of time. Determination of these values is readily done experimentally. A Hermite interpolation polynomial is used to generate additional values between postulated experimental data points. To improve the accuracy of the numerical solution in the vicinity of the surface, a special calculation for the temperature at the station just inside the shell surface is used. This technique ensures that the heat flux predicted by the finite difference solution at this interior station is consistent with the implied heat flux resulting from an experimental surface temperature. The development of this equation is given in Appendix VI. This procedure has been used in other work.⁷²

Assuming symmetry, the heat flux at the center of the silicon core must be zero. The value for the temperature at this location is assumed to be equal to the temperature at the station nearest the center. As with the surface of the shell and the furnace, only energy related boundary

conditions apply at this interface.

At the interface between the porous medium and the core material, or between the porous medium and the shell, unusual boundary conditions are required. In this numerical solution, an interface is treated as an increment rather than a surface of zero thickness. As a result, volume element terms must be included in the derivation of the equations which describe the boundary conditions. For the mass boundary condition between the porous medium and the core, a storage term and a generation term are required. The equation representing these considerations is presented below. A similar equation is needed for the other interface.

$$\frac{\partial}{\partial t} (2\pi R(LCW) L_0 (\Delta r_P - \Delta r_{P_0}) \rho_{wi} + 2\pi R(LCW) L_0 \Delta r_P \epsilon \rho_{wi} + 2\pi R(LCWPI) L_0 \bar{n}_i^e(LCWPI)) = 2\pi R(LCW) L_0 \Delta r_P r_i \quad (3-17)$$

where $\bar{n}_i^e(LCWPI)$ is the mass flux of species i as evaluated at the station in the porous medium nearest the interface

L_0 is the cylinder length

Δr_P is the incremental distance between the core material interface and the first node point in the porous material

Δr_{P_0} is the initial value of Δr_P .

Because chemical reactions at the interfaces may either deplete or deposit solid silicon, the incremental distance between the core interface and the first node point in the porous medium will vary with time. An equation has been developed to calculate the change in thickness and equation of continuity for this increment. Details of these derivations are given in Appendix VII. Results are given below for the thickness of the increment between the porous medium and the core. A similar equation is used

for the increment between the porous medium and the shell.

$$\Delta r_p(t+\Delta t) = \Delta r_p(t) - \frac{\Delta t}{\rho_{si}} (\Delta r_p(t) r_{si} + \rho_{si} \Delta r_p \frac{\partial \epsilon}{\partial t}) \quad (3-18a)$$

$$\Delta p_r(t+\Delta t) = \Delta p_r(t) - \frac{\Delta t (\Delta p_{r0} r_{si} + \rho_{si} \Delta p_r(t) \frac{\partial \epsilon}{\partial t})}{\rho_{si} (\epsilon - \epsilon_0 + 1)} \quad (3-18b)$$

where Δr_{p0} is the initial value for Δr_p

Δp_{r0} is the initial value for Δp_r

Because the boundary condition is most conveniently used in terms of concentration rather than as a derivative, equation 3-17 is used in the definition of a finite difference time derivative to calculate the value. This resulting relation is presented below in equation 3-19. As mentioned above, large differences in the derivatives between any two successive times are not expected to occur. However, at early times when reaction does occur, substantial inaccuracies in derivative calculations can be created because of the nature of the numerical solution. To minimize the effect, time derivatives of the species calculations are averaged.

$$\begin{aligned} w_i(LCW, t+\Delta t) = & (w_i(LCW, t) + \frac{\Delta t}{2} \frac{\partial w_i}{\partial t} \Big|_t + \frac{\Delta t}{2} \left(\frac{\Delta r_p}{\Delta r_{p0}} r_{si} \Big|_t + \right. \\ & \frac{R(LCWPI)}{R(LCW)} \rho(LCWPI, t+\Delta t) \bar{M}_i^e(LCWPI, t+\Delta t) / M_w(LCWPI, t) \left(\frac{\Delta r_p}{\Delta r} \right. \\ & (x_i(LCWPI, t+\Delta t) - x_i(LCWPI, t+\Delta t)) + \frac{\Delta r}{\Delta r_p} x_i(LCWPI, t+\Delta t)) / \\ & (\Delta r + \Delta r_p) + x_i(LCWPI, t+\Delta t) \bar{M}_i^e(LCWPI, t+\Delta t) M_i / \Delta r_{p0} \Big|_t \Big) / (\rho(LCW, \\ & t+\Delta t) (\epsilon(LCW, t) + \frac{\Delta r_p}{\Delta r_{p0}} - 1))) / (1 + \frac{\Delta t}{2} \frac{R(LCWPI)}{R(LCW)} \rho(LCWPI, t+\Delta t)) \end{aligned} \quad (3-19)$$

$$\begin{aligned} & \text{Dim}(LCWPI, t+\Delta t) / M_w(LCWPI, t) \left(\frac{\Delta r}{\Delta r_p} / (\Delta r + \Delta r_p) M_w(LCW, t) \right. \\ & \left. / \Delta r_p \right) + \left(\varepsilon(LCW, t) + \frac{\Delta r_p}{\Delta r_p} - 1 \right) \frac{\partial \rho}{\partial t} \Big|_t + \rho(LCW, t) \left(\frac{\partial \varepsilon}{\partial t} \Big|_t \right. \\ & \left. + \frac{\partial \Delta r_p}{\partial t} / \Delta r_p \right) \Big/ \left(\rho(LCW, t+\Delta t) \left(\varepsilon(LCW, t) + \frac{\Delta r_p}{\Delta r_p} - 1 \right) \right) \end{aligned} \quad \begin{array}{l} (3-19) \\ \text{Cont'd} \end{array}$$

As before, a similar equation is used for the other interface and is presented in Appendix VIII.

In addition to equation 3-17, two other constraints must be satisfied simultaneously at the boundaries between the solid layers. Equilibrium is assumed to exist at all times and the sum of the mass fractions must equal unity.

When reaction does not occur, the velocity at the wall is equal to zero. When reaction does occur, the velocity is calculated as follows:

$$\bar{v}_e = \frac{\sum_{i=1}^N \bar{n}_i^e}{\rho} \quad (3-20)$$

The calculation for the energy related boundary conditions at the two solid interfaces are performed in a manner similar to the method described above for mass considerations. This equation is presented below:

$$\begin{aligned} T(LCW, t+\Delta t) = & \left(T(LCW, t) + \Delta t \left(\frac{R(LCWPI)}{R(LCW)} \left(- \sum_{i=1}^N \bar{n}_i^e \right. \right. \right. \\ & (LCWPI, t+\Delta t) \hat{H}_i(LCWPI, t+\Delta t) + k(LCWPI, t+\Delta t) T(LCWPI, t+\Delta t) / \\ & \Delta r_p \Big) + \frac{R(LCWMI)}{R(LCW)} k(LCWMI, t+\Delta t) T(LCWMI, t+\Delta t) / \Delta cr - \text{ARGETA} \\ & \frac{\partial \varepsilon}{\partial t} \Big|_t - \text{ARGRHO} \frac{\partial \rho}{\partial t} \Big|_t - \text{ARGDRP} \frac{\partial \Delta r_p}{\partial t} \Big|_t + \text{ARGP} \frac{\partial \rho}{\partial t} \Big|_t \Big) / \text{ERC} \end{aligned} \quad (3-21)$$

$$1 / (1 + \Delta t \left(\frac{R(LCWMI)}{R(LCW)} k(LCWMI, t + \Delta t) / \Delta r + \frac{R(LCWPI)}{R(LCW)} k(LCWPI, t + \Delta t) / \Delta r_p \right) / ERC) \quad (3-21)$$

Cont'd

The equations for the other interface and the arguments are shown in Appendix IX.

Because the depletion of solid silicon at the interface between the core and the porous medium will create a gap, the thermal conductivity and the diffusivity for the increment between the interface and the first node point in the porous medium must be modified to include the contribution due to the gap. The approach used in this thesis is to calculate an overall diffusivity and an overall thermal conductivity in a similar manner as an overall heat transfer coefficient is calculated for heat conduction through composite materials. The development of these equations is given in Appendix X. Results are given below in equations 3-22 and 3-23.

$$\bar{D}_{im}^e = \frac{\Delta r_p}{R_c} \left(\frac{\ln\left(\frac{R_c + \Delta r_p}{R_c + \Delta r_p - \Delta r_p_0}\right)}{\bar{D}_{im}(LCWPI)} + \frac{\ln\left(\frac{R_c + \Delta r_p - \Delta r_p_0}{R_c}\right)}{\bar{D}_{im}(LCW)} \right)^{-1} \quad (3-22)$$

where \bar{D}_{im}^e is the overall diffusivity for the composite.

$$\bar{k}_e = \frac{\Delta r_p}{R_c} \left(\frac{\ln\left(\frac{R_c + \Delta r_p}{R_c + \Delta r_p - \Delta r_p_0}\right)}{k_e(LCWPI)} + \frac{\ln\left(\frac{R_c + \Delta r_p - \Delta r_p_0}{R_c}\right)}{k_e(LCW)} \right)^{-1} \quad (3-23)$$

where \bar{k}_e is the overall thermal conductivity for the composite.

Computer Program

The computer program for the numerical solution of the equations describing the pack cementation problem is divided into several elements. Element 1 reads input data and establishes initial conditions such as temperature and concentration profiles. The remaining elements of the program constitute a primary loop with time as the incremental stepping variable. Element 2 calculates the temperature profile in the core material. Element 3 calculates the temperature, concentration, and velocity profiles for the porous media. Element 4 calculates the boundary conditions for the interface between the core material and the porous media. Element 5 calculates the temperature profile in the shell material, and Element 6 calculates the boundary conditions for the interface between the porous media and the shell material. The remaining portion of the program calculates the pressure in the porous medium, the amount of core depleted, and the amount of coating deposited. Also calculated are normalized values of concentration and distance for comparison with the Arnold Solution as discussed later. Finally, old values of certain variables are established and output data generated.

With knowledge of all variables at the initial time, the program calculates values for all variables at the next time by starting at the center of the core and progressing outward to the surface. At the surface, the program requires the temperature to be input from experimental data or from a proposed profile. In actual practice, the pack cementation device would be placed in a furnace and the surface temperature measured as discrete points in time. The program receives these discrete points as input data and interpolates additional values as may be required. After values

for all variables have been calculated, the computer returns to Element 2 and begins computation again for a new time. A copy of the software is included as Appendix XI. For convenience, values for the diffusivity are calculated in a sub-routine to the main program. Software for this procedure is also included in Appendix XI.

In order to increase the usefulness of the results of the present study, the computer program has been written in a general way to accommodate practical dimensions and other actual physical data for a system composed of three gas phase species and a single coating species. For example, thermodynamic properties of chemical components may be easily changed as long as these data fit the polynomial equations used in the computer program. In addition, the program will process problems with radii greater than exact multiples of the selected stepping increment.

CHAPTER IV

IMPLEMENTATION OF THE NUMERICAL SOLUTION AND RESULTS

In Chapter III, the specific transport equations describing the deposition of solid silicon on an alumina substrate during pack cementation were presented. Also proposed was a digital computer program to obtain the numerical solution to the transport equations. In this chapter, the results of the numerical solution are presented. This discussion is preceded by a description of the relations for the various component and mixture physical and transport properties. Even though considerable time was spent reviewing recent developments in this area, relationships for the gas mixture properties and the individual species properties were selected to some extent on a basis of convenience in the numerical solution as increased accuracy in this area will not significantly improve the results of the primary goal of analysis of the pack cementation problem. Also presented is a discussion of the transport and thermodynamic properties of the solid materials. Other input data are shown later.

Thermodynamic and Transport Properties of the Gas Species

The equations used to calculate the heat capacity and enthalpy of the gas mixture are given below:

$$\hat{c}_p = \frac{\sum_{i=1}^N (x_i \tilde{c}_{p_i})}{M_w} \quad (4-1)$$

$$\hat{H} = \frac{\sum_{i=1}^N \int_{T_b}^T \kappa_i \tilde{c}_{p_i} dT + \kappa_i \Delta \tilde{H}_f^\circ}{M_w} \quad (4-2)$$

The generalized equation for the heat capacity of the individual gas phase species is given below in units of Kcal/mole °K. This equation represents a regression analysis of experimental data as a function of temperature in degrees Kelvin over the range 273 to 1500° K.

$$\tilde{c}_{p_i} = A + BT + CT^2 + DT^3 + \frac{E}{T^2} \quad (4-3)$$

Values for the constants in equation 4-3 are reported in Appendix XII for each of the species. Also included are values for the standard heat of formation at 298.16° K, in units of Kcal/mole, and the reference to the values for the heat capacity constants. The standard heats of formation used are those reported in reference 73.

The thermodynamic value for the equilibrium constant for the reaction proposed above is obtained from data presented in reference 73. These data have been fitted to an equation as a function of temperature as shown below.

$$\log_{10} K_p = A + \frac{B}{T} \quad (4-4)$$

Values for the constants in equation 4-4 are presented in Appendix XII.

The equation used to calculate the viscosity of the gas mixture is based on an extension of the Chapman-Enskog theory by Curtis and Hirschfelder⁷⁴ and further modified by Wilke.⁷⁵ This equation is given below:

$$\mu = \sum_{i=1}^J \left(\frac{x_i \mu_i}{\sum_{j=1}^J (x_j \phi_{ij})} \right) \quad (4-5a)$$

where $\phi_{ij} = \frac{1}{\sqrt{8}} \left(1 + \frac{M_i}{M_j} \right)^{-\frac{1}{2}} \left(1 + \left(\frac{\mu_i}{\mu_j} \right)^{\frac{1}{2}} \left(\frac{M_j}{M_i} \right)^{\frac{1}{4}} \right)^2$ (4-5b)

and μ_i is the species viscosity.

The equation used to calculate the viscosity of the individual gas species is given below in equation 4-6. This relation has been previously reported in Bird et al.²⁹ for both monatomic and polyatomic gases.

$$\mu_i = 2.6933 (10^{-5}) \frac{\sqrt{M_i T}}{\sigma_i^2 \Omega_{\mu i}} \quad (4-6)$$

where σ_i is the collision diameter

$\Omega_{\mu i}$ is the collision integral for viscosity.

The collision integral has been tabulated as a function of reduced temperature by Hirschfelder et al.⁷⁶ Values for this integral in the reduced temperature range 1.4 to 30 have been fit to the following equation:⁷⁷

$$\Omega_{\mu i} = (0.697 (1.0 + 0.323 \ln T_r))^{-1} \quad (4-7a)$$

where $T_r = \left(\frac{e}{k} \right)_i T$ (4-7b)

and $\left(\frac{e}{k} \right)_i$ is a constant unique for each species.

Several techniques have been proposed to calculate σ_i and $\left(\frac{e}{k} \right)_i$ and are

reviewed in reference 29 and 78. The method used in this work is given below:

$$\left(\frac{e}{k}\right)_i = 0.77 T_{ci} \quad (4-8a)$$

and
$$\sigma_i = 0.841 \tilde{V}_{ci}^{\frac{1}{3}} \quad (4-8b)$$

where T_{ci} is the critical temperature for species i
 \tilde{V}_{ci} is the critical molar volume for species i .

Values for T_{ci} and \tilde{V}_{ci} are given in Appendix XII.

The equation for the gas mixture thermal conductivity is based on a modification by Bird et al.,²⁹ of an equation first proposed by Mason and Saxena.⁷⁸ This equation is given below:

$$k_f = \sum_{i=1}^N \left(\frac{x_i k_i}{\sum_{j=1}^N (x_j \phi_{ij})} \right) \quad (4-9)$$

where k_i is the species thermal conductivity.

Equations to calculate the thermal conductivity of monatomic gases have been proposed which are similar to those used for the viscosity.^{29,76} Extension of these equations for use with polyatomic gases has not been as successful.²⁹ A model used in this work was proposed by Mason and Monchick and is presented below.⁷⁹

$$k_i = (\tilde{c}_{p,i} + 1.25 R) \mu_i \quad (4-10)$$

A considerable number of papers have been published on ways to calculate the binary diffusion coefficients of gas species combinations.^{29,76,80-88} Values for this property are needed for calculation of the effective diffusion coefficient discussed in the previous chapter. The method used in this work is that reported by Hirschfelder, Curtis, and Bird⁷⁶ and is given below in equation 4-11a. Even though this method is one of the earlier works, most of the newer methods do not give significantly better accuracy for a majority of combinations. In addition, this method is consistent with those used to calculate μ_i and k_i . A comparison of the several methods is given in reference 88 along with experimental data.

$$D_{ij} = 1.8583 (10^{-3}) \frac{\sqrt{\bar{M} T^3}}{P \sigma_{ij} \Omega_{ij}} \quad (4-11a)$$

where
$$\bar{M} = \left(\frac{1}{M_i} + \frac{1}{M_j} \right) \quad (4-11b)$$

and σ_{ij} is the collision diameter for the pair ij
 Ω_{ij} is the collision integral for the pair ij .

The collision integral for diffusion is calculated by a similar method to that for viscosity based on specific table values for diffusion reported by Hirschfelder et al.⁷⁶ The equation for the diffusion collision integral is given below for the reduced temperature in the range 1.4 to 30.

$$\Omega_{ij} = (0.7549 (1.0 + 0.3476 \ln T_r))^{-1} \quad (4-12)$$

For these calculations $\left(\frac{e}{k}\right)_{ij}$ and σ_{ij} are calculated as suggested in reference

29 as follows:

$$\left(\frac{e}{k}\right)_{ij} = \left(\left(\frac{e}{k}\right)_i \left(\frac{e}{k}\right)_j\right)^{\frac{1}{2}} \quad (4-13)$$

$$\sigma_{ij} = \frac{1}{2} \sigma_i \sigma_j \quad (4-14)$$

The value for the Knudsen diffusivity for the gas phase species is calculated from an equation reported by Youngquist.⁴³ This relation may be modified to include the results of Smith and coworkers to calculate a value for the pore radius.⁴⁵

$$D_{ip}^e = \frac{2}{3} \bar{R} \left(\frac{8RT}{\pi M_i} \right)^{1/2} \left(\frac{2-a_i}{a_i} \right) \quad (4-15)$$

where \bar{R} is the average pore radius.

As mentioned in Chapter II, a_i is probably equal to unity so the last term in equation 4-15 is also equal to unity.

Thermodynamic and Transport Properties of the Solid

The equation for the heat capacity of solid silicon is given below in equation 4-16. This relation is reported to represent experimental values in units of cal/mole °K for the temperature range 273.16° to 1173°K.⁸⁹

$$\tilde{C}_p = 5.74 + 0.614(10^{-3})T - 1.01(10^{-5})/T^2 \quad (4-16)$$

The equation for the heat capacity of alumina, which comprises both the porous media substrate and the outer shell, is given in equation 4-17.

This relation is reported to represent experimental values in units of BTU/lb°-F for temperature in degrees Fahrenheit over the range 325° F to 2930° F.⁹⁰ Similar values were reported in three other independent observations and compiled in reference 91.

$$\hat{c}_p = 0.239 + 0.0402 (10^{-3}) T \quad (4-17)$$

Jakob has shown that the thermal conductivity of non-metallic crystalline materials is inversely proportional to the temperature and would fit an equation of the following form:⁹²

$$k_s = A + \frac{B}{T} \quad (4-18)$$

Values of the constants for the solid materials used in this work are presented in Appendix XIII.

Further Modification of the Momentum Equation

Early runs with the computer program resulted in unstable solutions. Even though the stability moduli for the heat and mass transfer equations were maintained at very low values, the instability persisted. Finally, the problem was identified in the use of the momentum equation. Even though the momentum equation, given as equation 2-1, does not contain a second derivative or a time derivative term, values for the pressure are calculated from values of the mixture density which is calculated from the continuity equation. Thus, a third stability modulus must be considered. The time increment to produce a stable solution from the momentum equation based on the third stability modulus was estimated to be less than 10^{-4} seconds. In comparison, the value for the increment which will satisfy the other moduli

is only less than 10^{-2} seconds. As a result, the pressure can be assumed to be independent of position. If this assumption is used, the momentum equation is not needed. In addition this assumption implies that a change in pressure at any point, as a result of other transport or reaction phenomena, very quickly changes the pressure throughout the porous media. This assumption changes the initial algorithm. The velocity at any point is now calculated as follows:

$$\bar{v}_e = \frac{\sum_{i=1}^v \bar{n}_i^e}{\rho} \quad (4-19)$$

The density is calculated from the ideal gas law. The pressure is allowed to vary with time, but its value is the same at all node points at any instant. Values for the instantaneous pressure are calculated from the equation below. This equation is based on the assumption that the total amount of elemental hydrogen throughout the entire porous media does not change.

$$\bar{P} = \frac{\chi}{L_0} \frac{R}{2\pi} \left(\int_{R_c}^{R_p} \frac{\epsilon M_w}{T} \left(\frac{\omega_{HCl}}{M_{HCl}} + \frac{2\omega_{H_2}}{M_{H_2}} + \frac{\omega_{HS,Cl_2}}{M_{HS,Cl_2}} \right) r dr \right) \quad (4-20)$$

where $\frac{\chi}{L_0}$ is a constant.

The derivation of equation 4-20 is given in Appendix XIV. In order to estimate the reliability of the assumption that the gradient of pressure is small, the gradient is calculated in the computer solution from the

momentum equation. Results of the calculation, as well as other results of the numerical solution are discussed in a following section.

Input Data

Because many iterations are required to reach a solution to the problem at hand, considerable computer time is used for each run. In order to conserve computer time, the decision was made after observing results from early runs to set the initial temperature of the system at 300° F, rather than ambient, as would occur in actual practice. In addition, the surface temperature of the shell was input at 1000° F for all time. Input values which determine the properties of the shell were set so that the properties were also held constant. Constants which determine the thermal conductivity of the porous substrate were arbitrarily multiplied by ten. These constraints allowed the temperature of the porous medium to rise faster than would normally occur, thus causing interface reaction at an earlier time. Since the performance of the shell heat transfer relations were shown to be successful in another work,⁷² these constraints were not thought to compromise the study of important phenomena of diffusion and reaction in the porous medium.

One other constraint has been placed on the solutions presented herein. In actual practice for pack cementation, only hydrogen chloride would probably be injected into the pack at time zero. This case cannot be studied in this work due to limitations of the computer program. Values for all species must be greater than zero or indefinite numbers occur. In addition, early runs using small values of H_2 and $HSiCl_3$ resulted in dramatic changes in mixture molecular weight at the core interface producing an instability similar to that encountered with the continuity equation as discussed in

the previous section. To overcome this problem, excess hydrogen is used for all runs. Initial composition and other input data are summarized in Table 1.

Table 1. Input Data

Item	Value
Initial temperature	300° F.
Base temperature	70° F.
Surface temperature	1000° F.
Total pack radius	12.60 in.
Core radius	4.75 in.
Porous medium radius	10.70 in.
Pore radius	Variable
Particle diameter	90.00 μ
Space increment	0.50 in.
Emissivity	0.50
Initial porosity	0.51
Time increment	Variable
Initial species mass concentration:	
H_2	0.618
HCl	0.001
$HSiCl_3$	0.381

Results

The primary objective of this work is to show that the relations proposed in previous chapters do indeed provide a solution to the problem of pack cementation. Since no experiments were performed with an actual system, no true conclusion as to the results of the solution can be presented. Considerable experimental results have already been presented for the heat transfer and binary diffusion aspects of the porous material selected. In this light, the important considerations of this thesis thus become the performance of the relations regarding multicomponent diffusion and Knudsen diffusion. In the following paragraphs, results are presented which show that a solution to the multicomponent diffusion problem does exist. These results are then compared to the special case of equal binary diffusivity. And finally, results are presented which show the effects of Knudsen diffusion on pack cementation.

In the following Tables 2 through 5, results of the solution for the multicomponent case are presented after 100 seconds, 1,000 seconds, 1,900 seconds, and 2,000 seconds in the furnace. The pore radius specified is $90,000 \text{ \AA}$ and is not sufficient to produce a significant contribution due to Knudsen diffusion. While the program ran for 3,600 seconds, which was designated as the end of the run, data after 1,900 seconds are not valid. At approximately 1,920 seconds, temperatures and concentrations in the porous medium were sufficient to cause deposition of silicon in the pores. Apparently this phenomena could not be adequately accounted for in the algorithm proposed for the step size used, and the solution became unstable. Attempts to promote a more stable solution by reduction of the diffusion modulus were unsuccessful. More will be said about this problem in the next section.

Table 2. Results of the Solution for the Multicomponent Case After 100 Seconds

STATION	RADIUS (IN)	TEMPERATURE (DEG F)	K (BTU/FT-HR)	RFC (LB/CUFT)	CP (BTU/LB-F)	V (FT/SEC)	ETA	DELP (ATM/FT)
1	0.0000	300.00018	8.461E+01	145.4000	.2146			
2	.5000	300.00018	8.461E+01	145.4000	.2146			
3	1.0000	300.00019	8.461E+01	145.4000	.2146			
4	1.5000	300.00020	8.461E+01	145.4000	.2146			
5	2.0000	300.00023	8.461E+01	145.4000	.2146			
6	2.5000	300.00025	8.461E+01	145.4000	.2146			
7	3.0000	300.00029	8.461E+01	145.4000	.2146			
8	3.5000	300.00033	8.461E+01	145.4000	.2146			
9	4.0000	300.00038	8.461E+01	145.4000	.2146			
10	4.5000	300.00043	8.461E+01	145.4000	.2146			
11	4.7500	300.00046	9.359E-01	.0060	2.4740	-4.54E-07	5.10E-01	.0000
12	5.0000	300.00057	9.359E-01	.0060	2.4739	-5.21E-07	5.10E-01	.0000
13	5.5000	300.00040	9.359E-01	.0060	2.4738	-4.76E-07	5.10E-01	.0000
14	6.0000	300.00098	9.359E-01	.0060	2.4736	-4.40E-07	5.10E-01	.0000
15	6.5000	300.00051	9.359E-01	.0060	2.4735	-4.22E-07	5.10E-01	.0000
16	7.0000	300.00050	9.359E-01	.0060	2.4734	-4.10E-07	5.10E-01	.0000
17	7.5000	300.00073	9.359E-01	.0060	2.4733	-0.86E-07	5.10E-01	.0000
18	8.0000	300.00000	9.359E-01	.0060	2.4732	-4.94E-07	5.10E-01	.0000
19	8.5000	300.00034	9.359E-01	.0060	2.4733	-4.23E-07	5.10E-01	.0000
20	9.0000	304.00070	9.359E-01	.0060	2.4744	-6.71E-07	5.10E-01	.0000
21	9.5000	317.37031	9.359E-01	.0059	2.4799	-7.17E-07	5.10E-01	.0000
22	10.0000	364.19013	8.646E-01	.0355	2.4983	-1.43E-06	5.10E-01	.0000
23	10.5000	508.57772	7.401E-01	.0047	2.5585	-2.20E-06	5.10E-01	.0000
24	10.7000	644.44820	6.544E-01	.0041	2.6178	-2.82E-06	5.10E-01	.0000
25	11.0000	669.20666	3.000E+01	248.3000	.3017			
26	11.5000	744.81870	3.000E+01	248.3000	.3017			
27	12.0000	852.10074	3.000E+01	248.3000	.3017			
28	12.5000	975.49333	3.000E+01	248.3000	.3017			
29	12.6000	1000.00000	3.000E+01	248.3000	.3017			

Table 2 (Continued). Results of the Solution for the Multicomponent Case After 100 Seconds

STATION	DIM	DCM	DCM	MOFLX1 (MOLE/FT2/HR)	MOFLX2 (MOLE/FT2/HR)	MOFLX3 (MOLE/FT2/HR)	TOTNOF (MOLE/FT2/HR)
11	1.180E+00	1.011E+00	3.473E-01	1.820E-06	-5.568E-07	5.075E-08	1.314E-06
12	1.152E+00	9.852E-01	3.407E-01	1.093E-06	-5.275E-07	4.308E-08	6.088E-07
13	1.157E+00	9.852E-01	3.461E-01	8.918E-07	-4.768E-07	3.948E-08	4.547E-07
14	1.153E+00	9.852E-01	3.411E-01	7.505E-07	-4.262E-07	3.352E-08	3.579E-07
15	1.150E+00	9.852E-01	3.378E-01	5.635E-07	-3.842E-07	2.847E-08	2.657E-07
16	1.135E+00	9.852E-01	3.150E-01	5.070E-07	-3.524E-07	2.202E-08	1.767E-07
17	1.122E+00	9.852E-01	2.844E-01	-2.619E-06	-3.393E-07	-1.123E-08	-2.970E-06
18	1.097E+00	9.856E-01	2.169E-01	3.806E-07	-3.516E-07	1.004E-08	3.907E-08
19	1.085E+00	9.871E-01	1.531E-01	1.681E-06	-4.116E-07	1.822E-08	1.288E-06
20	1.032E+00	9.944E-01	1.335E-01	1.537E-06	-5.429E-07	1.642E-08	1.011E-06
21	1.138E+00	1.024E+00	2.210E-01	3.350E-06	-7.680E-07	4.428E-08	2.628E-06
22	1.285E+00	1.135E+00	3.251E-01	2.178E-06	-1.132E-06	6.118E-08	1.107E-06
23	1.740E+00	1.495E+00	5.154E-01	2.180E-06	-1.572E-06	1.144E-07	7.238E-07
24	2.198E+00	1.872E+00	6.734E-01	1.892E-06	-1.767E-06	1.374E-07	2.617E-07

STATION	X1	X2	X3	TEST1	TEST2	TEST3	KEO	CINDEX
11	.9909750554	.000005462	.0090243983	9.746E-01	9.746E-01	9.746E-01	1.890E-17	1.759E-17
12	.9909751691	.0000066802	.0090243507	1.000E+00	1.000E+00	1.000E+00	1.890E-17	3.219E-14
13	.9909812754	.0000179439	.0090247807	1.000E+00	1.000E+00	9.999E-01	1.890E-17	6.240E-13
14	.9909831583	.0000282471	.0090185946	1.001E+00	1.000E+00	9.998E-01	1.891E-17	2.433E-12
15	.9909859935	.0000372330	.0090168134	1.001E+00	1.000E+00	9.996E-01	1.891E-17	5.576E-12
16	.9909881509	.000047347	.0090150744	1.001E+00	1.000E+00	9.990E-01	1.891E-17	1.033E-11
17	.9909888762	.000052002	.0090139230	1.003E+00	1.000E+00	9.984E-01	1.894E-17	1.623E-11
18	.9909882438	.000061199	.0090126363	1.001E+00	1.000E+00	9.983E-01	1.894E-17	2.461E-11
19	.990988951	.0000691775	.0090119274	1.000E+00	1.000E+00	9.961E-01	2.005E-17	3.563E-11
20	.990994771	.0000798428	.0090106851	1.000E+00	1.000E+00	1.002E+00	2.524E-17	5.469E-11
21	.9909967319	.0000938091	.0090094590	9.990E-01	1.000E+00	1.002E+00	3.364E-17	8.853E-11
22	.9909974451	.0001141590	.0090080999	1.000E+00	1.000E+00	1.001E+00	1.200E-15	1.593E-10
23	.9909986220	.0001423823	.0090061957	1.003E+00	1.000E+00	1.003E+00	2.273E-12	3.093E-10
24	.99099861525	.0001546610	.00899591865	1.001E+00	1.000E+00	1.000E+00	4.301E-10	3.961E-10

Table 3. Results of the Solution for the Multicomponent Case After 1000 Seconds

STATION	RADIUS (IN)	TEMPERATURE (DEG F)	K (BTU/FT/HR)	R/G (LE/CFRT)	CP (BTU/LB/F)	V (FT/SEC)	ETA	DELP (ATM/FT)
1	0.0000	302.73195	8.461E+01	145.4000	.2147			
2	.5000	302.73195	8.461E+01	145.4000	.2147			
3	1.0000	302.74502	8.461E+01	145.4000	.2147			
4	1.5000	302.77581	8.461E+01	145.4000	.2147			
5	2.0000	302.82297	8.461E+01	145.4000	.2147			
6	2.5000	302.88150	8.461E+01	145.4000	.2147			
7	3.0000	302.95256	8.461E+01	145.4000	.2147			
8	3.5000	303.03738	8.461E+01	145.4000	.2147			
9	4.0000	303.12627	8.461E+01	145.4000	.2147			
10	4.5000	303.24558	8.461E+01	145.4000	.2147			
11	4.7500	303.31160	9.580E-01	.0075	2.4536	-1.30E-05	5.10E-01	.0000
12	5.0000	305.25854	9.246E-01	.0074	2.4535	-1.25E-05	5.10E-01	.0000
13	5.5000	321.97728	9.058E-01	.0073	2.4540	-1.16E-05	5.10E-01	.0000
14	6.0000	337.20788	8.928E-01	.0072	2.4558	-1.10E-05	5.10E-01	.0000
15	6.5000	356.81175	8.718E-01	.0070	2.4598	-1.04E-05	5.10E-01	.0000
16	7.0000	382.76291	8.456E-01	.0068	2.4666	-1.00E-05	5.10E-01	.0000
17	7.5000	417.24298	8.173E-01	.0065	2.4771	-9.81E-06	5.10E-01	.0000
18	8.0000	462.69415	7.746E-01	.0062	2.4926	-9.68E-06	5.10E-01	.0000
19	8.5000	521.80069	7.300E-01	.0058	2.5141	-9.59E-06	5.10E-01	.0000
20	9.0000	597.30887	6.809E-01	.0054	2.5432	-9.76E-06	5.10E-01	.0000
21	9.5000	691.51024	6.263E-01	.0050	2.5810	-9.95E-06	5.10E-01	.0000
22	10.0000	805.19231	5.784E-01	.0045	2.6287	-1.04E-05	5.10E-01	.0000
23	10.5000	935.96577	5.315E-01	.0041	2.6852	-1.06E-05	5.10E-01	.0000
24	10.7500	991.00549	5.146E-01	.0040	2.7096	-1.11E-05	5.10E-01	.0000
25	11.0000	992.45161	3.000E+01	248.3000	.3017			
26	11.5000	994.85693	3.000E+01	248.3000	.3017			
27	12.0000	997.23090	3.000E+01	248.3000	.3017			
28	12.5000	999.54693	3.000E+01	248.3000	.3017			
29	12.6000	1000.80000	3.000E+01	248.3000	.3017			

Table 3 (Continued). Results of the Solution for the Multicomponent Case After 1000 Seconds

STATION	DIM (SCFT/HR)	D2X (SQFT/HR)	D3M (SQFT/HR)	MOFLX1 (MOLE/FT ² /HR)	MOFLX2 (MOLE/FT ² /HR)	MOFLX3 (MOLE/FT ² /HR)	TOTNOF (MOLE/FT ² /HR)
11	9.592E-01	8.216E-01	2.758E-01	5.036E-05	-1.805E-05	1.535E-06	3.385E-05
12	9.467E-01	8.117E-01	2.719E-01	4.788E-05	-1.715E-05	1.449E-06	3.217E-05
13	9.723E-01	8.354E-01	2.703E-01	4.370E-05	-1.550E-05	1.296E-06	2.942E-05
14	1.003E+00	8.641E-01	2.862E-01	4.052E-05	-1.434E-05	1.174E-06	2.737E-05
15	1.044E+00	9.014E-01	2.962E-01	3.779E-05	-1.322E-05	1.064E-06	2.564E-05
16	1.100E+00	9.517E-01	3.103E-01	3.583E-05	-1.222E-05	9.765E-07	2.448E-05
17	1.175E+00	1.020E+00	3.293E-01	3.369E-05	-1.148E-05	8.901E-07	2.310E-05
18	1.279E+00	1.113E+00	3.561E-01	3.298E-05	-1.081E-05	8.305E-07	2.301E-05
19	1.419E+00	1.238E+00	3.917E-01	3.206E-05	-1.014E-05	7.674E-07	2.269E-05
20	1.606E+00	1.406E+00	4.405E-01	3.144E-05	-9.624E-06	7.203E-07	2.254E-05
21	1.853E+00	1.628E+00	5.032E-01	3.081E-05	-9.072E-06	6.695E-07	2.241E-05
22	2.170E+00	1.912E+00	5.855E-01	3.020E-05	-8.670E-06	6.355E-07	2.225E-05
23	2.558E+00	2.260E+00	6.827E-01	2.945E-05	-8.207E-06	5.896E-07	2.183E-05
24	2.725E+00	2.414E+00	7.260E-01	2.917E-05	-8.063E-06	5.761E-07	2.168E-05

STATION	X1	X2	X3	TEST1	TEST2	TEST3	KEQ	DINDEX
11	.3936505132	.0006005571	.0053499297	9.747E-01	9.746E-01	9.746E-01	2.292E-17	1.457E-17
12	.9904916076	.0001994895	.0053089059	1.000E+00	1.000E+00	1.000E+00	3.634E-17	6.719E-10
13	.9902008732	.0005615812	.0052375855	1.000E+00	1.000E+00	1.000E+00	8.700E-17	1.511E-08
14	.9899353949	.0008925380	.0051723671	1.000E+00	1.000E+00	1.000E+00	2.386E-16	6.111E-08
15	.9836941345	.0011903837	.0051154888	1.000E+00	1.000E+00	1.000E+00	8.288E-16	1.459E-07
16	.9854740469	.0014622200	.0050637335	1.000E+00	1.000E+00	1.000E+00	3.921E-15	2.720E-07
17	.9892720382	.0017098377	.0050181620	1.000E+00	1.000E+00	1.000E+00	2.629E-14	4.373E-07
18	.9890961803	.0019322816	.0049775381	1.000E+00	1.000E+00	1.000E+00	2.731E-13	6.341E-07
19	.9899213347	.0021269381	.0049414272	1.000E+00	1.000E+00	1.000E+00	4.036E-12	8.612E-07
20	.9807748859	.0023155558	.0049103664	1.000E+00	1.000E+00	1.000E+00	8.127E-11	1.100E-06
21	.9896325469	.0024822150	.0048662382	1.000E+00	1.000E+00	1.000E+00	1.581E-09	1.359E-06
22	.9885187171	.0026220582	.0048592247	1.000E+00	1.000E+00	1.000E+00	4.561E-08	1.606E-06
23	.9834060733	.0027568576	.0048374652	1.000E+00	1.000E+00	1.000E+00	1.054E-06	1.871E-06
24	.9883670052	.0028042650	.0048030168	1.000E+00	1.000E+00	1.000E+00	3.233E-06	1.969E-06

Table 4 (Continued). Results of the Solution for the Multicomponent Case After 1900 Seconds

STATION	D1M (SQFT/HR)	D2M (SQFT/HR)	D3M (SQFT/HR)	MOFLX1 (MOLE/FT ² /HR)	MOFLX2 (MOLE/FT ² /HR)	MOFLX3 (MOLE/FT ² /HR)	TOTMOF (MOLE/FT ² /HR)
11	9.134E-01	7.898E-01	2.587E-01	6.413E-05	-1.914E-05	1.664E-06	4.665E-05
12	9.242E-01	7.955E-01	2.602E-01	6.111E-05	-1.820E-05	1.573E-06	4.448E-05
13	9.857E-01	8.502E-01	2.789E-01	5.586E-05	-1.652E-05	1.405E-06	4.069E-05
14	1.053E+00	9.095E-01	2.951E-01	5.163E-05	-1.520E-05	1.281E-06	3.772E-05
15	1.128E+00	9.771E-01	3.149E-01	4.788E-05	-1.399E-05	1.162E-06	3.505E-05
16	1.215E+00	1.055E+00	3.381E-01	4.497E-05	-1.334E-05	1.065E-06	3.299E-05
17	1.316E+00	1.146E+00	3.644E-01	4.212E-05	-1.212E-05	9.772E-07	3.097E-05
18	1.437E+00	1.254E+00	3.962E-01	4.064E-05	-1.142E-05	9.086E-07	2.953E-05
19	1.580E+00	1.382E+00	4.326E-01	3.784E-05	-1.069E-05	8.354E-07	2.798E-05
20	1.750E+00	1.532E+00	4.767E-01	3.621E-05	-1.016E-05	7.826E-07	2.693E-05
21	1.948E+00	1.710E+00	5.258E-01	3.434E-05	-9.557E-06	7.219E-07	2.551E-05
22	2.172E+00	1.912E+00	5.838E-01	3.303E-05	-9.147E-06	6.812E-07	2.457E-05
23	2.420E+00	2.136E+00	6.441E-01	3.135E-05	-8.638E-06	6.295E-07	2.339E-05
24	2.525E+00	2.230E+00	6.701E-01	3.089E-05	-8.488E-06	6.145E-07	2.302E-05

STATION	X1	X2	X3	TEST1	TEST2	TEST3	KEQ	CINDEX
11	.9905410945	.000018537	.0094571818	9.746E-01	9.746E-01	9.746E-01	9.240E-17	4.773E-17
12	.9903750220	.0002082274	.0094167506	1.000E+00	1.000E+00	1.000E+00	2.487E-16	6.558E-16
13	.9902773735	.0005761244	.0093465051	1.000E+00	1.000E+00	1.000E+00	1.742E-15	1.485E-08
14	.9898045658	.0009123582	.0092820754	1.000E+00	1.000E+00	1.000E+00	1.176E-14	5.961E-08
15	.9895654337	.0012069034	.0092276629	1.000E+00	1.000E+00	1.000E+00	8.124E-14	1.384E-07
16	.9893451534	.0014773151	.0091775344	1.000E+00	1.000E+00	1.000E+00	5.923E-13	2.552E-07
17	.9891489400	.0017164355	.0091346204	1.000E+00	1.000E+00	1.000E+00	4.670E-12	4.023E-07
18	.9889694479	.0019350878	.0090954643	1.000E+00	1.000E+00	1.000E+00	3.984E-11	5.796E-07
19	.9888066849	.0021320079	.0090613072	1.000E+00	1.000E+00	1.000E+00	3.554E-10	7.774E-07
20	.9886603235	.0023088216	.0090308549	1.000E+00	1.000E+00	1.000E+00	3.247E-09	9.508E-07
21	.9885262543	.0024722559	.0090034498	1.000E+00	1.000E+00	1.000E+00	2.893E-08	1.220E-06
22	.9884051150	.0026149450	.0089799189	1.000E+00	1.000E+00	1.000E+00	2.354E-07	1.448E-06
23	.9882902396	.0027521417	.0089576127	1.000E+00	1.000E+00	1.000E+00	1.669E-06	1.692E-06
24	.9882492146	.0028009207	.0089498648	1.000E+00	1.000E+00	1.000E+00	3.457E-06	1.786E-06

Table 5. Results of the Solution for the Multicomponent Case After 2000 Seconds

STATION	RADIUS (IN)	TEMPERATURE (DEG F)	K (BTU/FT-HR)	RPC (LB/CUFT)	CP (BTU/LB-F)	V (FT/SEC)	ETA	DELP (ATM/FT)
1	0.0000	324.30216	8.461E+01	145.4000	.2155	-1.51E-05	5.10E-01	.0000
2	.5000	324.30216	8.461E+01	145.4000	.2155	-1.20E-05	5.10E-01	.0000
3	1.0000	324.34745	8.461E+01	145.4000	.2155	-1.94E-05	5.10E-01	.0000
4	1.5000	324.42500	8.461E+01	145.4000	.2155	-5.77E-06	5.10E-01	.0000
5	2.0000	324.54558	8.461E+01	145.4000	.2155	-1.93E-05	5.10E-01	.0000
6	2.5000	324.69682	8.461E+01	145.4000	.2156	1.78E-06	5.10E-01	.0000
7	3.0000	324.88263	8.461E+01	145.4000	.2156	-2.08E-05	5.10E-01	.0000
8	3.5000	325.10201	8.461E+01	145.4000	.2156	1.07E-05	5.10E-01	.0000
9	4.0000	325.35804	8.461E+01	145.4000	.2156	2.35E-05	5.10E-01	.0000
10	4.5000	325.64783	8.461E+01	145.4000	.2156	1.96E-05	5.10E-01	.0000
11	4.7500	325.80583	9.289E-01	.0000	.2156	-2.73E-05	5.10E-01	.0000
12	5.0000	341.42157	8.881E-01	.0078	2.4573	-2.91E-05	5.10E-01	.0000
13	5.5000	373.92491	8.543E-01	.0075	2.4604	-7.53E-05	5.10E-01	.0000
14	6.0000	408.22721	8.214E-01	.0072	2.4715	-1.07E-05	5.10E-01	.0000
15	6.5000	445.54801	7.888E-01	.0069	2.4722	1.93E-05	5.10E-01	.0000
16	7.0000	487.07336	7.554E-01	.0067	2.4970	1.78E-06	5.10E-01	.0000
17	7.5000	533.93181	7.217E-01	.0063	2.4915	-2.08E-05	5.10E-01	.0000
18	8.0000	587.12482	6.869E-01	.0060	2.5357	1.07E-05	5.10E-01	.0000
19	8.5000	647.45337	6.525E-01	.0056	2.5212	2.35E-05	5.10E-01	.0000
20	9.0000	715.34663	6.175E-01	.0054	2.5911	1.96E-05	5.10E-01	.0000
21	9.5000	790.72020	5.849E-01	.0049	2.5641	-2.73E-05	5.10E-01	.0000
22	10.0000	872.60108	5.526E-01	.0048	2.6643	3.60E-05	5.10E-01	.0000
23	10.5000	959.41668	5.250E-01	.0043	2.6205	-2.91E-05	5.10E-01	.0000
24	10.7000	994.62002	5.143E-01	.0042	2.7523	-7.53E-05	5.10E-01	.0000
25	11.0000	995.51296	3.000E+01	248.3000	2.7488		5.10E-01	.0000
26	11.5000	996.36885	3.000E+01	248.3000	.3017		5.10E-01	.0000
27	12.0000	998.37499	3.000E+01	248.3000	.3017		5.10E-01	.0000
28	12.5000	999.73435	3.000E+01	248.3000	.3017		5.10E-01	.0000
29	12.6000	1000.00000	3.000E+01	248.3000	.3017		5.10E-01	.0000

Table 5 (Continued). Results of the Solution for the Multicomponent Case After 2000 Seconds

STATION	C1M (SQFT/HR)	C2M (SQFT/HR)	D3M (SQFT/HR)	MOFLX1 (INOLE/FT2/HR)	MOFLX2 (INOLE/FT2/HR)	MOFLX3 (INOLE/FT2/HR)	TOTMOF (INOLE/FT2/HR)
11	9.019E-01	7.900E-01	2.292E-01	6.796E-05	-2.105E-05	1.472E-06	4.839E-05
12	9.278E-01	7.967E-01	2.643E-01	6.215E-05	-1.877E-05	1.653E-06	4.504E-05
13	9.609E-01	8.535E-01	2.170E-01	6.477E-05	-2.249E-05	1.226E-06	4.351E-05
14	1.145E+00	9.147E-01	3.714E-01	4.838E-05	-1.459E-05	2.105E-06	3.590E-05
15	1.122E+00	9.854E-01	2.942E-01	5.745E-05	-2.154E-05	1.409E-06	3.732E-05
16	1.606E+00	1.061E+00	4.855E-01	3.629E-05	-1.119E-05	2.792E-06	2.789E-05
17	1.338E+00	1.158E+00	3.861E-01	5.385E-05	-2.210E-05	1.689E-06	3.344E-05
18	4.858E+00	1.253E+00	6.257E-01	1.994E-05	-8.058E-06	3.604E-06	1.545E-05
19	1.631E+00	1.396E+00	4.957E-01	5.266E-05	-2.322E-05	1.996E-06	3.144E-05
20	-4.255E-01	1.504E+00	7.939E-01	-5.392E-06	-5.218E-06	4.282E-06	-6.328E-06
21	2.620E+00	1.722E+00	6.392E-01	5.289E-05	-2.425E-05	2.200E-06	3.084E-05
22	6.908E-01	1.781E+00	1.006E+00	1.006E-05	-2.492E-06	5.066E-06	1.263E-05
23	2.504E+00	2.141E+00	8.041E-01	6.873E-05	-2.479E-05	2.368E-06	4.630E-05
24	2.234E+00	2.239E+00	2.235E+00	1.148E-03	-9.778E-05	9.942E-07	1.051E-03

STATION	X1	X2	X3	TEST1	TEST2	TEST3	KEQ	DINDEX
11	.9905554353	.9906009090	.0094236557	9.747E-01	9.746E-01	9.743E-01	1.125E-16	5.739E-17
12	.9903758194	.9902283115	.0093586951	1.000E+00	1.000E+00	1.000E+00	3.132E-16	9.129E-10
13	.9901467296	.0005453277	.0093039428	1.000E+00	1.000E+00	9.997E-01	2.333E-15	1.285E-08
14	.9895575476	.0011826882	.0092597712	9.999E-01	1.000E+00	1.000E+00	1.649E-14	1.291E-07
15	.9897236150	.0011524736	.0091239114	1.000E+00	1.000E+00	1.000E+00	1.170E-13	1.211E-07
16	.9883297205	.0020454482	.0091158313	9.998E-01	1.000E+00	1.000E+00	8.638E-13	6.773E-07
17	.9895928071	.0015466652	.0089105328	1.000E+00	1.000E+00	1.000E+00	6.743E-12	3.248E-07
18	.9891625414	.0028712320	.0089022365	9.975E-01	1.000E+00	1.000E+00	5.560E-11	1.908E-06
19	.9894572026	.0018842228	.0086585746	1.000E+00	1.000E+00	1.000E+00	4.760E-10	5.577E-07
20	.9875328800	.0036730008	.0087943152	1.001E+00	1.000E+00	1.000E+00	4.098E-09	4.072E-06
21	.9895598115	.0020605231	.0083796854	1.000E+00	1.000E+00	1.000E+00	3.401E-08	7.535E-07
22	.9869311591	.0044355588	.0086292821	1.002E+00	1.000E+00	1.000E+00	2.588E-07	7.335E-06
23	.9897620700	.0021424019	.0080945272	1.000E+00	1.000E+00	1.000E+00	1.717E-06	8.777E-07
24	.9891912592	.0027114247	.0081373161	9.978E-01	1.000E+00	1.000E+00	3.470E-06	1.769E-06

In order to show that the multicomponent solution is successful, concentration profiles are presented in Figure 2 for the species HCL at several times. The results are considered stable because the profiles do not oscillate. Profiles for the other species are not plotted because they do not exhibit significant change. As was previously mentioned, concentrations for these species were set in excess initially.

In many engineering applications, the use of a single binary diffusivity in a multicomponent diffusion problem is expedient, provided errors are small. For this reason, a solution was obtained for the hypothetical case where the binary diffusivities for each specie pair were set equal to the value for $D_{1,2}$ and any effects due to Knudsen diffusion were not allowed through an option in the software. Results of this solution are presented in Tables 6 through 9 at 100 seconds, 1,000 seconds, 1,900 seconds and 2,000 seconds. Concentration profiles of the species HCL were nearly identical to those for the multicomponent case and thus are not plotted. Comparison of the effective diffusivities for the multicomponent and the equal binary diffusion cases is presented in Figure 3 at 100 seconds and in Figure 4 at 1,900 seconds. As can be easily seen, there is significant difference between the values for the multicomponent case and those for the special case. As another comparison, the amount of coating deposited is plotted for each case as a function of time in Figure 5. There is some difference in the coating deposition rates.

In order to determine the effect of Knudsen diffusion on the algorithm several runs were made with different pore radii for the multicomponent case and the case where all binary diffusivities are equal to $D_{1,2}$. As in discussions above, results are presented below in terms of

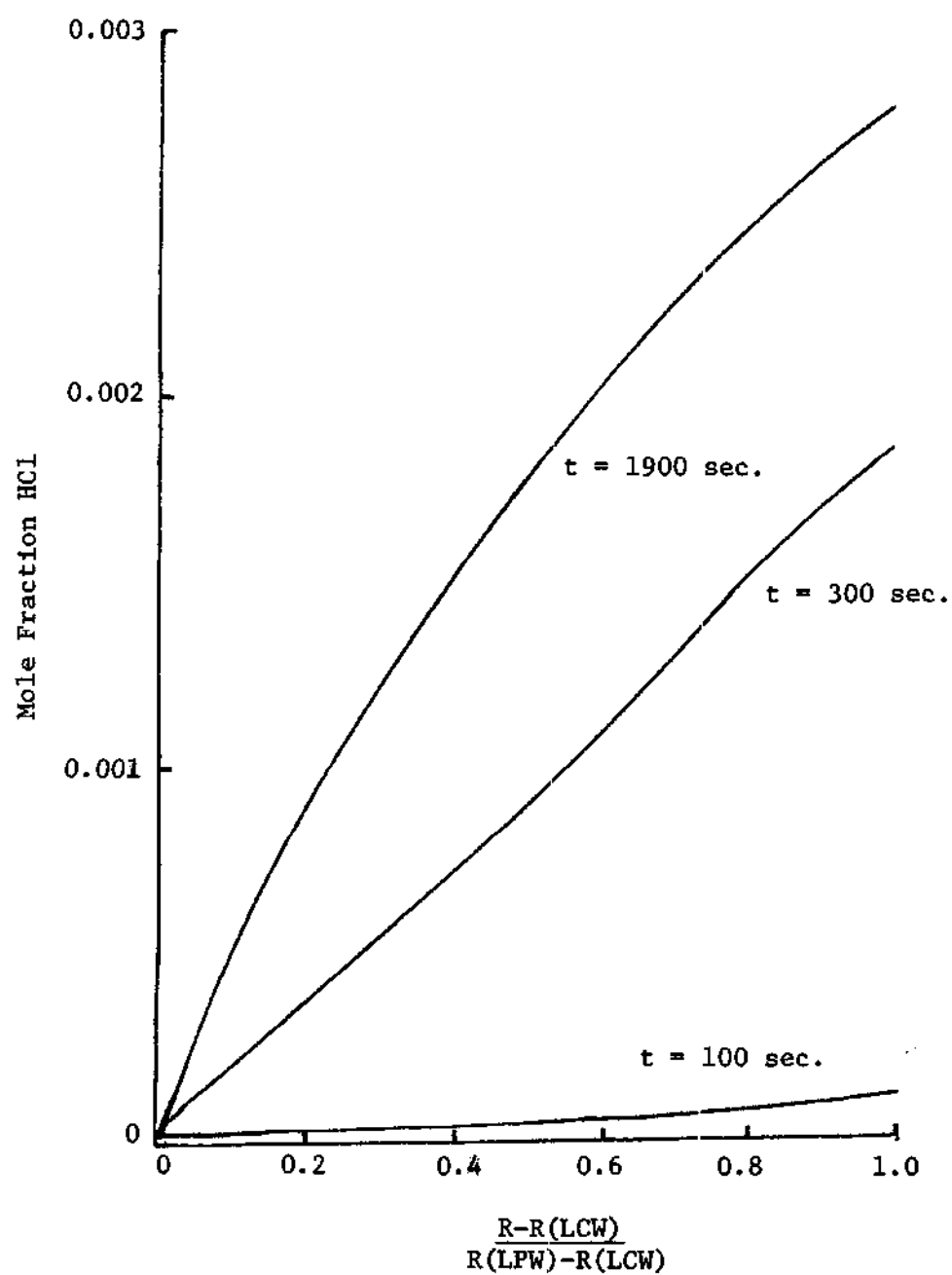


Figure 2. Mole Fraction of HCl versus Station at Times
Shown for the Multicomponent Case.

Table 6. Results of the Solution for the Case Where All Binary Diffusivities are Equal with No Knudsen Diffusion After 100 Seconds

STATION	RADIUS (IN)	TEMPERATURE (DEG F)	K (BTU/FT-HR)	RPC (LB/CUFT)	CP (BTU/LB-F)	V (FT/SEC)	ETA	DELTA (ATM/FT)
1	9.0000	300.0000	8.4618+01	145.4000	.2146	-6.475-07	5.10E-01	.0000
2	.5000	300.0000	8.4618+01	145.4000	.2146	-6.12E-07	5.10E-01	.0000
3	1.0000	300.0000	8.4618+01	145.4000	.2146	-5.51E-07	5.10E-01	.0000
4	1.5000	300.0000	8.4618+01	145.4000	.2146	-4.90E-07	5.10E-01	.0000
5	2.0000	300.0000	8.4618+01	145.4000	.2146	-4.40E-07	5.10E-01	.0000
6	2.5000	300.0000	8.4618+01	145.4000	.2146	-4.10E-07	5.10E-01	.0000
7	3.0000	300.0000	8.4618+01	145.4000	.2146	-4.00E-07	5.10E-01	.0000
8	3.5000	300.0000	8.4618+01	145.4000	.2146	-4.00E-07	5.10E-01	.0000
9	4.0000	300.0000	8.4618+01	145.4000	.2146	-4.00E-07	5.10E-01	.0000
10	4.5000	300.0000	8.4618+01	145.4000	.2146	-4.00E-07	5.10E-01	.0000
11	4.7500	300.0000	8.4618+01	145.4000	.2146	-4.00E-07	5.10E-01	.0000
12	5.0000	300.0000	8.4618+01	145.4000	.2146	-4.00E-07	5.10E-01	.0000
13	5.5000	300.0000	8.4618+01	145.4000	.2146	-4.00E-07	5.10E-01	.0000
14	6.0000	300.0000	8.4618+01	145.4000	.2146	-4.00E-07	5.10E-01	.0000
15	6.5000	300.0000	8.4618+01	145.4000	.2146	-4.00E-07	5.10E-01	.0000
16	7.0000	300.0000	8.4618+01	145.4000	.2146	-4.00E-07	5.10E-01	.0000
17	7.5000	300.0000	8.4618+01	145.4000	.2146	-4.00E-07	5.10E-01	.0000
18	8.0000	300.0000	8.4618+01	145.4000	.2146	-4.00E-07	5.10E-01	.0000
19	8.5000	300.0000	8.4618+01	145.4000	.2146	-4.00E-07	5.10E-01	.0000
20	9.0000	300.0000	8.4618+01	145.4000	.2146	-4.00E-07	5.10E-01	.0000
21	9.5000	300.0000	8.4618+01	145.4000	.2146	-4.00E-07	5.10E-01	.0000
22	10.0000	300.0000	8.4618+01	145.4000	.2146	-4.00E-07	5.10E-01	.0000
23	10.5000	300.0000	8.4618+01	145.4000	.2146	-4.00E-07	5.10E-01	.0000
24	11.0000	300.0000	8.4618+01	145.4000	.2146	-4.00E-07	5.10E-01	.0000
25	11.5000	300.0000	8.4618+01	145.4000	.2146	-4.00E-07	5.10E-01	.0000
26	12.0000	300.0000	8.4618+01	145.4000	.2146	-4.00E-07	5.10E-01	.0000
27	12.5000	300.0000	8.4618+01	145.4000	.2146	-4.00E-07	5.10E-01	.0000
28	13.0000	300.0000	8.4618+01	145.4000	.2146	-4.00E-07	5.10E-01	.0000
29	13.5000	300.0000	8.4618+01	145.4000	.2146	-4.00E-07	5.10E-01	.0000

Table 6 (Continued). Results of the Solution for the Case Where All Binary Diffusivities are Equal with No Knudsen Diffusion After 100 Seconds

STATION	D1X (SQRT/HR)	D2M (SQRT/HR)	D3M (SQRT/HR)	MOFLX1 (MOLE/FT ² /HR)	MOFLX2 (MOLE/FT ² /HR)	MOFLX3 (MOLE/FT ² /HR)	TOTPOF (MOLE/FT ² /HR)
11	1.204E+00	1.174E+00	1.174E+00	5.391E-07	-5.850E-07	4.692E-08	-2.458E-14
12	1.075E+00	1.075E+00	1.075E+00	5.118E-07	-5.550E-07	4.472E-08	-1.633E-14
13	1.075E+00	1.075E+00	1.075E+00	4.617E-07	-5.320E-07	4.033E-08	-3.355E-15
14	1.075E+00	1.075E+00	1.075E+00	4.147E-07	-4.521E-07	3.739E-08	-4.933E-15
15	1.075E+00	1.075E+00	1.075E+00	3.765E-07	-4.131E-07	3.456E-08	-3.211E-15
16	1.075E+00	1.075E+00	1.075E+00	3.500E-07	-3.635E-07	3.242E-08	2.476E-15
17	1.075E+00	1.075E+00	1.075E+00	3.438E-07	-3.758E-07	3.199E-08	5.678E-15
18	1.075E+00	1.075E+00	1.075E+00	3.642E-07	-3.925E-07	3.373E-08	5.137E-15
19	1.075E+00	1.075E+00	1.075E+00	4.317E-07	-4.711E-07	3.932E-08	2.035E-15
20	1.075E+00	1.075E+00	1.075E+00	5.984E-07	-6.191E-07	5.169E-08	-2.349E-15
21	1.119E+00	1.119E+00	1.119E+00	7.896E-07	-8.555E-07	6.873E-08	7.875E-17
22	1.237E+00	1.237E+00	1.237E+00	1.133E-06	-1.235E-06	9.766E-08	1.248E-15
23	1.631E+00	1.631E+00	1.631E+00	1.544E-06	-1.675E-06	1.310E-07	-3.552E-14
24	2.040E+00	2.040E+00	2.040E+00	1.724E-06	-1.969E-06	1.456E-07	-3.759E-14

STATION	X1	X2	X3	TES11	TES12	TES13	XEO	LINGER
11	.990961332	.990000462	.0090191256	9.746E-04	9.746E-04	9.746E-04	1.893E-17	1.759E-17
12	.990961332	.990000462	.0090191256	1.000E+00	1.000E+00	1.000E+00	1.893E-17	1.759E-17
13	.990961332	.990000462	.0090191256	1.000E+00	1.000E+00	1.000E+00	1.893E-17	1.759E-17
14	.990961332	.990000462	.0090191256	1.000E+00	1.000E+00	1.000E+00	1.893E-17	1.759E-17
15	.990961332	.990000462	.0090191256	1.000E+00	1.000E+00	1.000E+00	1.893E-17	1.759E-17
16	.990961332	.990000462	.0090191256	1.000E+00	1.000E+00	1.000E+00	1.893E-17	1.759E-17
17	.990961332	.990000462	.0090191256	1.000E+00	1.000E+00	1.000E+00	1.893E-17	1.759E-17
18	.990961332	.990000462	.0090191256	1.000E+00	1.000E+00	1.000E+00	1.893E-17	1.759E-17
19	.990961332	.990000462	.0090191256	1.000E+00	1.000E+00	1.000E+00	1.893E-17	1.759E-17
20	.990961332	.990000462	.0090191256	1.000E+00	1.000E+00	1.000E+00	1.893E-17	1.759E-17
21	.990961332	.990000462	.0090191256	1.000E+00	1.000E+00	1.000E+00	1.893E-17	1.759E-17
22	.990961332	.990000462	.0090191256	1.000E+00	1.000E+00	1.000E+00	1.893E-17	1.759E-17
23	.990961332	.990000462	.0090191256	1.000E+00	1.000E+00	1.000E+00	1.893E-17	1.759E-17
24	.990961332	.990000462	.0090191256	1.000E+00	1.000E+00	1.000E+00	1.893E-17	1.759E-17

Table 7. Results of the Solution for the Case Where All Binary Diffusivities are Equal with No Knudsen Diffusion After 1000 Seconds

STATION	RADIUS (IN)	TEMPERATURE (DEG F)	K (BTU/FT/HR)	R/C (LB/CLFT)	CP (BTU/LB/F)	V (FT/SEC)	ETA	DELP (ATM/FT)
1	0.0000	302.73219	8.4618+01	145.4000	.2147			
2	.5000	302.73219	8.4618+01	145.4000	.2147			
3	1.0000	302.74922	8.4618+01	145.4000	.2147			
4	1.5000	302.76552	8.4618+01	145.4000	.2147			
5	2.0000	302.82118	8.4618+01	145.4000	.2147			
6	2.5000	302.88172	8.4618+01	145.4000	.2147			
7	3.0000	303.05279	8.4618+01	145.4000	.2147			
8	3.5000	303.22762	8.4618+01	145.4000	.2147			
9	4.0000	303.43652	8.4618+01	145.4000	.2147			
10	4.5000	303.62486	8.4618+01	145.4000	.2147			
11	4.7500	303.81209	9.5628+01	.0074	2.4719	-1.765-05	5.10E-01	.0000
12	5.0000	309.65687	9.2438+01	.0073	2.4702	-1.693-05	5.10E-01	.0000
13	5.5000	321.97759	9.1355+01	.0072	2.4677	-1.568-05	5.10E-01	.0000
14	6.0000	337.20794	8.9298+01	.0071	2.4668	-1.472-05	5.10E-01	.0000
15	6.5000	355.81123	8.7198+01	.0070	2.4685	-1.392-05	5.10E-01	.0000
16	7.0000	382.76231	8.4578+01	.0068	2.4732	-1.343-05	5.10E-01	.0000
17	7.5000	417.44091	8.1348+01	.0065	2.4920	-1.312-05	5.10E-01	.0000
18	8.0000	452.68927	7.7472+01	.0062	2.4959	-1.338-05	5.10E-01	.0000
19	8.5000	521.79391	7.3618+01	.0058	2.5161	-1.308-05	5.10E-01	.0000
20	9.0000	597.30049	6.8098+01	.0054	2.5441	-1.238-05	5.10E-01	.0000
21	9.5000	691.50133	6.2938+01	.0050	2.5810	-1.38E-05	5.10E-01	.0000
22	10.0000	805.18497	5.7848+01	.0045	2.5279	-1.458-05	5.10E-01	.0000
23	10.5000	935.96310	5.3158+01	.0041	2.5839	-1.528-05	5.10E-01	.0000
24	10.7500	991.60554	5.1480+01	.0040	2.7081	-1.55E-05	5.10E-01	.0000
25	11.0000	992.45166	3.3008+01	248.3000	.3017			
26	11.5000	994.85697	3.3008+01	248.3000	.3017			
27	12.0000	997.23092	3.3008+01	248.3000	.3017			
28	12.5000	999.54693	3.3008+01	248.3000	.3017			
29	12.6000	1000.00000	3.3008+01	248.3000	.3017			

Table 7 (Continued). Results of the Solution for the Case Where All Binary Diffusivities are Equal with No Knudsen Diffusion After 1000 Seconds

STATION	DCM (SOFT/HR)	DCM (SOFT/HR)	DCM (SOFT/HR)	MOFLX1 (MOLE/FT ² /HR)	MOFLX2 (MOLE/FT ² /HR)	MOFLX3 (MOLE/FT ² /HR)	TOIMOF (MOLE/FT ² /HR)
1	9.300E-01	9.300E-01	9.300E-01	1.820E-05	-1.980E-05	1.900E-06	-4.266E-13
2	9.300E-01	9.300E-01	9.300E-01	1.730E-05	-1.802E-05	1.515E-06	-2.686E-13
3	9.300E-01	9.300E-01	9.300E-01	1.670E-05	-1.700E-05	1.363E-06	-6.824E-15
4	9.300E-01	9.300E-01	9.300E-01	1.448E-05	-1.572E-05	1.241E-06	-1.216E-14
5	9.300E-01	9.300E-01	9.300E-01	1.336E-05	-1.449E-05	1.131E-06	-2.794E-15
6	9.300E-01	9.300E-01	9.300E-01	1.247E-05	-1.351E-05	1.044E-06	-3.132E-15
7	9.300E-01	9.300E-01	9.300E-01	1.182E-05	-1.259E-05	9.595E-07	-4.533E-15
8	9.300E-01	9.300E-01	9.300E-01	1.096E-05	-1.183E-05	8.941E-07	-1.142E-14
9	9.300E-01	9.300E-01	9.300E-01	1.029E-05	-1.112E-05	8.266E-07	-1.233E-14
10	9.300E-01	9.300E-01	9.300E-01	9.730E-06	-1.050E-05	7.750E-07	-5.049E-15
11	9.300E-01	9.300E-01	9.300E-01	9.231E-06	-9.952E-06	7.215E-07	-7.115E-15
12	9.300E-01	9.300E-01	9.300E-01	8.941E-06	-9.514E-06	6.825E-07	-2.008E-15
13	9.300E-01	9.300E-01	9.300E-01	8.309E-06	-9.066E-06	6.374E-07	-1.454E-15
14	9.300E-01	9.300E-01	9.300E-01	8.225E-06	-8.349E-06	6.230E-07	-2.132E-15

STATION	X1	X2	X3	TEST1	TEST2	TEST3	K20	DINDEX
1	9.93752593	0.000003517	0.000704459	9.746E-01	9.746E-01	9.746E-01	2.392E-17	1.457E-17
2	9.93752593	0.000003517	0.000704459	1.000E+00	1.000E+00	1.000E+00	3.674E-17	6.935E-10
3	9.93752593	0.000003517	0.000704459	1.000E+00	1.000E+00	1.000E+00	9.779E-17	1.552E-08
4	9.93752593	0.000003517	0.000704459	1.000E+00	1.000E+00	1.000E+00	2.396E-16	6.249E-08
5	9.93752593	0.000003517	0.000704459	1.000E+00	1.000E+00	1.000E+00	9.269E-16	1.403E-07
6	9.93752593	0.000003517	0.000704459	1.000E+00	1.000E+00	1.000E+00	3.920E-15	2.762E-07
7	9.93752593	0.000003517	0.000704459	1.000E+00	1.000E+00	1.000E+00	2.688E-14	4.423E-07
8	9.93752593	0.000003517	0.000704459	1.000E+00	1.000E+00	1.000E+00	4.035E-12	8.674E-07
9	9.93752593	0.000003517	0.000704459	1.000E+00	1.000E+00	1.000E+00	8.125E-11	1.165E-06
10	9.93752593	0.000003517	0.000704459	1.000E+00	1.000E+00	1.000E+00	1.983E-09	1.364E-06
11	9.93752593	0.000003517	0.000704459	1.000E+00	1.000E+00	1.000E+00	4.963E-08	1.909E-06
12	9.93752593	0.000003517	0.000704459	1.000E+00	1.000E+00	1.000E+00	1.033E-06	1.372E-06
14	9.93752593	0.000003517	0.000704459	1.000E+00	1.000E+00	1.000E+00	2.433E-06	1.909E-06

Table 8. Results of the Solution for the Case Where All Binary Diffusivities are Equal with No Knudsen Diffusion After 1900 Seconds

STATION	RADIUS (IN)	TEMPERATURE (DEG F)	K (BTU/FT-HR)	P/C (LL/CUFT)	CP (BTU/LE/F)	V (FT/SEC)	ETA	DELTA (ATM/FT)
1	0.0500	321.42592	8.4618+01	145.4000	.2194			
2	.5000	321.42592	8.4618+01	145.4000	.2194			
3	1.0000	321.42594	8.4618+01	145.4000	.2194			
4	1.5000	321.54794	8.4618+01	145.4000	.2194			
5	2.0000	321.66010	8.4618+01	145.4000	.2194			
6	2.5000	321.80553	8.4618+01	145.4000	.2194			
7	3.0000	321.98265	8.4618+01	145.4000	.2195			
8	3.5000	322.19558	8.4618+01	145.4000	.2195			
9	4.0000	322.44213	8.4618+01	145.4000	.2195			
10	4.5000	322.72123	8.4618+01	145.4000	.2195			
11	5.0000	322.87343	8.4618+01	.0078	2.4751	-1.70E-05	5.10E-01	.0000
12	5.5000	337.61769	8.9221-01	.0077	2.4769	-1.70E-05	5.10E-01	.0000
13	6.0000	369.03879	8.5933-01	.0074	2.4819	-1.61E-05	5.10E-01	.0000
14	6.5000	402.35141	8.2721-01	.0072	2.4884	-1.54E-05	5.10E-01	.0000
15	7.0000	438.30935	7.9492-01	.0069	2.4971	-1.49E-05	5.10E-01	.0000
16	7.5000	476.54635	7.6132-01	.0066	2.5082	-1.45E-05	5.10E-01	.0000
17	8.0000	520.21961	7.2773-01	.0063	2.5226	-1.42E-05	5.10E-01	.0000
18	8.5000	578.21959	6.9263-01	.0060	2.5404	-1.40E-05	5.10E-01	.0000
19	9.0000	638.83822	6.5693-01	.0057	2.5622	-1.40E-05	5.10E-01	.0000
20	9.5000	707.60081	6.2143-01	.0053	2.5882	-1.42E-05	5.10E-01	.0000
21	10.0000	784.48591	5.8681-01	.0050	2.6186	-1.43E-05	5.10E-01	.0000
22	10.5000	868.60744	5.5423-01	.0047	2.6531	-1.43E-05	5.10E-01	.0000
23	11.0000	958.13556	5.2433-01	.0044	2.6908	-1.43E-05	5.10E-01	.0000
24	11.5000	1054.42372	5.0000-01	.0043	2.7064	-1.50E-05	5.10E-01	.0000
25	12.0000	1168.24955	3.0000+01	248.3000	.3017			
26	12.5000	1298.85541	3.0000+01	248.3000	.3017			
27	13.0000	1446.31494	3.0000+01	248.3000	.3017			
28	13.5000	1612.72053	3.0000+01	248.3000	.3017			
29	14.0000	1800.00000	3.0000+01	248.3000	.3017			

Table 8 (Continued). Results of the Solution for the Case Where All Binary Diffusivities are Equal with No Knudsen Diffusion After 1900 Seconds

STATION	DEM (SQFT/HR)	DEM (SQFT/HR)	DEM (SQFT/HR)	MOFLX1 (MOLE/FT ² /HR)	MOFLX2 (MOLE/FT ² /HR)	MOFLX3 (MOLE/FT ² /HR)	TOTMOF (MOLE/FT ² /HR)
1	3.6345-01	8.5535-01	4.5535-01	1.9285-05	-2.0985-05	1.7735-06	-8.0802-13
12	3.7-01-01	8.7485-01	2.7185-01	1.8335-05	-1.9345-05	1.6125-06	-5.2155-13
13	3.1115-01	9.7115-01	9.3115-01	1.5685-05	-1.5115-05	1.4485-06	-3.2105-14
14	3.3075-01	9.3075-01	9.9575-01	1.5335-05	-1.6555-05	1.3195-06	-1.7455-14
15	1.0005-00	1.0005-00	1.0005-00	1.4135-05	-1.5335-05	1.2015-06	6.6415-15
16	1.1535-00	1.1535-00	1.1535-00	1.3195-05	-1.4295-05	1.1185-06	-8.5535-16
17	1.1535-00	1.1535-00	1.1535-00	1.2375-05	-1.3295-05	1.0175-06	-4.8195-15
18	1.2315-00	1.2315-00	1.2315-00	1.1575-05	-1.2525-05	9.4745-07	-2.2505-14
19	1.3035-00	1.3035-00	1.3035-00	1.0795-05	-1.1725-05	8.7545-07	-1.9945-14
20	1.6725-00	1.6725-00	1.6725-00	1.0315-05	-1.1135-05	8.2255-07	2.5855-15
21	1.5635-00	1.5635-00	1.5635-00	9.7125-06	-1.0485-05	7.6325-07	-1.4505-18
22	2.0325-00	2.0325-00	2.0325-00	9.3035-06	-1.1505-05	7.2315-07	-1.1205-14
23	2.5125-00	2.5125-00	2.5125-00	8.7965-06	-9.4695-06	6.7275-07	-2.9385-12
24	2.4275-00	2.4275-00	2.4275-00	8.3465-06	-9.3545-06	6.5815-07	-4.2585-12

STATION	X1	X2	X3	TEST1	TEST2	TEST3	KEO	INDEX
1	3900229325	0000000000	0001432930	9.7465-01	9.7465-01	9.7465-01	9.2425-17	4.7755-17
12	9900000000	0000000000	0001894848	1.0005-00	1.0005-00	1.0005-00	2.4785-16	7.1695-10
13	9900000000	0000000000	0001000597	1.0005-00	1.0005-00	1.0005-00	1.7425-15	1.5235-08
14	9900000000	0000000000	0003273092	1.0005-00	1.0005-00	1.0005-00	1.1765-14	6.0005-08
15	9900000000	0000000000	0005050117	1.0005-00	1.0005-00	1.0005-00	8.1265-14	1.4685-07
16	9900000000	0000000000	0005029003	1.0005-00	1.0005-00	1.0005-00	5.9245-13	2.5855-07
17	9900000000	0000000000	0000100503	1.0005-00	1.0005-00	1.0005-00	4.6705-12	4.1565-07
18	9900000000	0000000000	0000000000	1.0005-00	1.0005-00	1.0005-00	3.5545-11	3.9435-07
19	9900000000	0000000000	0000000000	1.0005-00	1.0005-00	1.0005-00	3.5545-11	3.9435-07
20	9900000000	0000000000	0000000000	1.0005-00	1.0005-00	1.0005-00	3.2475-09	3.9555-07
21	9900000000	0000000000	0000000000	1.0005-00	1.0005-00	1.0005-00	2.4745-08	3.9555-07
22	9900000000	0000000000	0000000000	1.0005-00	1.0005-00	1.0005-00	2.3545-07	3.9555-07
23	9900000000	0000000000	0000000000	1.0005-00	1.0005-00	1.0005-00	2.3545-07	3.9555-07
24	9900000000	0000000000	0000000000	1.0005-00	1.0005-00	1.0005-00	3.3545-06	3.9555-07

Table 9. Results of the Solution for the Case Where All Binary Diffusivities are Equal with No Knudsen Diffusion After 2000 Seconds

STATION	RADIUS (IN)	TEMPERATURE (DEG F)	K (BTU/FT/HR)	RPC (LG/CLFT)	CP (BTU/LB/FT)	V (FT/SEC)	ETA	DELP (ATM/FT)
1	0.0000	324.30680	8.461E+01	145.4000	.2155	-2.23E-05	5.10E-01	.0000
2	.5000	324.30680	8.461E+01	145.4000	.2155	-1.74E-05	5.10E-01	.0000
3	1.0000	324.30680	8.461E+01	145.4000	.2155	-2.52E-05	5.10E-01	.0000
4	1.5000	324.30680	8.461E+01	145.4000	.2155	-7.12E-06	5.10E-01	.0000
5	2.0000	324.30680	8.461E+01	145.4000	.2155	-2.23E-05	5.10E-01	.0000
6	2.5000	324.30680	8.461E+01	145.4000	.2155	-2.27E-05	5.10E-01	.0000
7	3.0000	324.30680	8.461E+01	145.4000	.2155	1.43E-05	5.10E-01	.0000
8	3.5000	324.30680	8.461E+01	145.4000	.2155	-2.57E-05	5.10E-01	.0000
9	4.0000	324.30680	8.461E+01	145.4000	.2155	2.63E-05	5.10E-01	.0000
10	4.5000	324.30680	8.461E+01	145.4000	.2155	-3.05E-05	5.10E-01	.0000
11	5.0000	324.30680	8.461E+01	145.4000	.2155	3.92E-05	5.10E-01	.0000
12	5.5000	324.30680	8.461E+01	145.4000	.2155	-3.60E-05	5.10E-01	.0000
13	6.0000	324.30680	8.461E+01	145.4000	.2155	-3.17E-04	5.10E-01	.0000
14	6.5000	324.30680	8.461E+01	145.4000	.2155			
15	7.0000	324.30680	8.461E+01	145.4000	.2155			
16	7.5000	324.30680	8.461E+01	145.4000	.2155			
17	8.0000	324.30680	8.461E+01	145.4000	.2155			
18	8.5000	324.30680	8.461E+01	145.4000	.2155			
19	9.0000	324.30680	8.461E+01	145.4000	.2155			
20	9.5000	324.30680	8.461E+01	145.4000	.2155			
21	10.0000	324.30680	8.461E+01	145.4000	.2155			
22	10.5000	324.30680	8.461E+01	145.4000	.2155			
23	11.0000	324.30680	8.461E+01	145.4000	.2155			
24	11.5000	324.30680	8.461E+01	145.4000	.2155			
25	12.0000	324.30680	8.461E+01	145.4000	.2155			
26	12.5000	324.30680	8.461E+01	145.4000	.2155			
27	13.0000	324.30680	8.461E+01	145.4000	.2155			
28	13.5000	324.30680	8.461E+01	145.4000	.2155			
29	14.0000	324.30680	8.461E+01	145.4000	.2155			

Table 9 (Continued) Results of the Solution for the Case Where All Binary Diffusivities are Equal with No Knudsen Diffusion After 2000 Seconds

STATION	DI* (SCFT/HR)	DCM (SCFT/HR)	DCM (ICFT/HR)	MOFLX1 (MOLE/FT ² /HR)	MOFLX2 (MOLE/FT ² /HR)	MOFLX3 (MOLE/FT ² /HR)	TOTROP (MOLE/FT ² /HR)
11	8.658E-01	8.658E-01	8.658E-01	2.204E-05	-2.225E-05	1.212E-06	-8.532E-13
12	8.728E-01	8.728E-01	8.728E-01	1.922E-05	-2.227E-05	1.745E-06	-8.476E-13
13	9.345E-01	9.345E-01	9.345E-01	2.364E-05	-2.514E-05	1.862E-06	-2.429E-14
14	1.001E+00	1.001E+00	1.001E+00	2.532E-05	-1.613E-05	2.813E-06	-2.443E-14
15	1.076E+00	1.076E+00	1.076E+00	2.184E-05	-2.392E-05	2.075E-06	1.038E-14
16	1.162E+00	1.162E+00	1.162E+00	2.017E-05	-1.242E-05	3.775E-06	2.733E-15
17	1.262E+00	1.262E+00	1.262E+00	2.145E-05	-2.442E-05	2.733E-06	-8.577E-15
18	1.370E+00	1.370E+00	1.370E+00	4.380E-06	-9.130E-06	4.033E-06	-3.244E-14
19	1.518E+00	1.518E+00	1.518E+00	2.289E-05	-2.535E-05	2.683E-06	-3.033E-14
20	1.689E+00	1.689E+00	1.689E+00	5.427E-07	-3.867E-06	5.324E-06	-3.913E-15
21	1.867E+00	1.867E+00	1.867E+00	2.352E-05	-2.352E-05	2.733E-06	3.113E-15
22	2.080E+00	2.080E+00	2.080E+00	-2.318E-06	-2.977E-06	5.793E-06	-4.663E-15
23	2.314E+00	2.314E+00	2.314E+00	2.414E-05	-2.684E-05	2.733E-06	-3.123E-12
24	2.412E+00	2.412E+00	2.412E+00	1.170E-04	-1.194E-04	-7.944E-06	-4.522E-12

STATION	X1	X2	X3	TEST1	TEST2	TEST3	REQ	DIR*EX
11	.9999999137	.80000003924	.0090391849	9.746E-01	9.746E-01	9.746E-01	1.126E-16	5.744E-17
12	.9999999137	.80000003924	.0090391849	1.000E+00	1.000E+00	1.000E+00	1.126E-16	5.744E-17
13	.9999999137	.80000003924	.0090391849	1.000E+00	1.000E+00	1.000E+00	2.123E-15	1.233E-16
14	.9999999137	.80000003924	.0090391849	1.000E+00	1.000E+00	1.000E+00	1.126E-16	1.233E-16
15	.9999999137	.80000003924	.0090391849	1.000E+00	1.000E+00	1.000E+00	1.126E-16	1.233E-16
16	.9999999137	.80000003924	.0090391849	1.000E+00	1.000E+00	1.000E+00	1.126E-16	1.233E-16
17	.9999999137	.80000003924	.0090391849	1.000E+00	1.000E+00	1.000E+00	1.126E-16	1.233E-16
18	.9999999137	.80000003924	.0090391849	1.000E+00	1.000E+00	1.000E+00	1.126E-16	1.233E-16
19	.9999999137	.80000003924	.0090391849	1.000E+00	1.000E+00	1.000E+00	1.126E-16	1.233E-16
20	.9999999137	.80000003924	.0090391849	1.000E+00	1.000E+00	1.000E+00	1.126E-16	1.233E-16
21	.9999999137	.80000003924	.0090391849	1.000E+00	1.000E+00	1.000E+00	1.126E-16	1.233E-16
22	.9999999137	.80000003924	.0090391849	1.000E+00	1.000E+00	1.000E+00	1.126E-16	1.233E-16
23	.9999999137	.80000003924	.0090391849	1.000E+00	1.000E+00	1.000E+00	1.126E-16	1.233E-16
24	.9999999137	.80000003924	.0090391849	1.000E+00	1.000E+00	1.000E+00	1.126E-16	1.233E-16

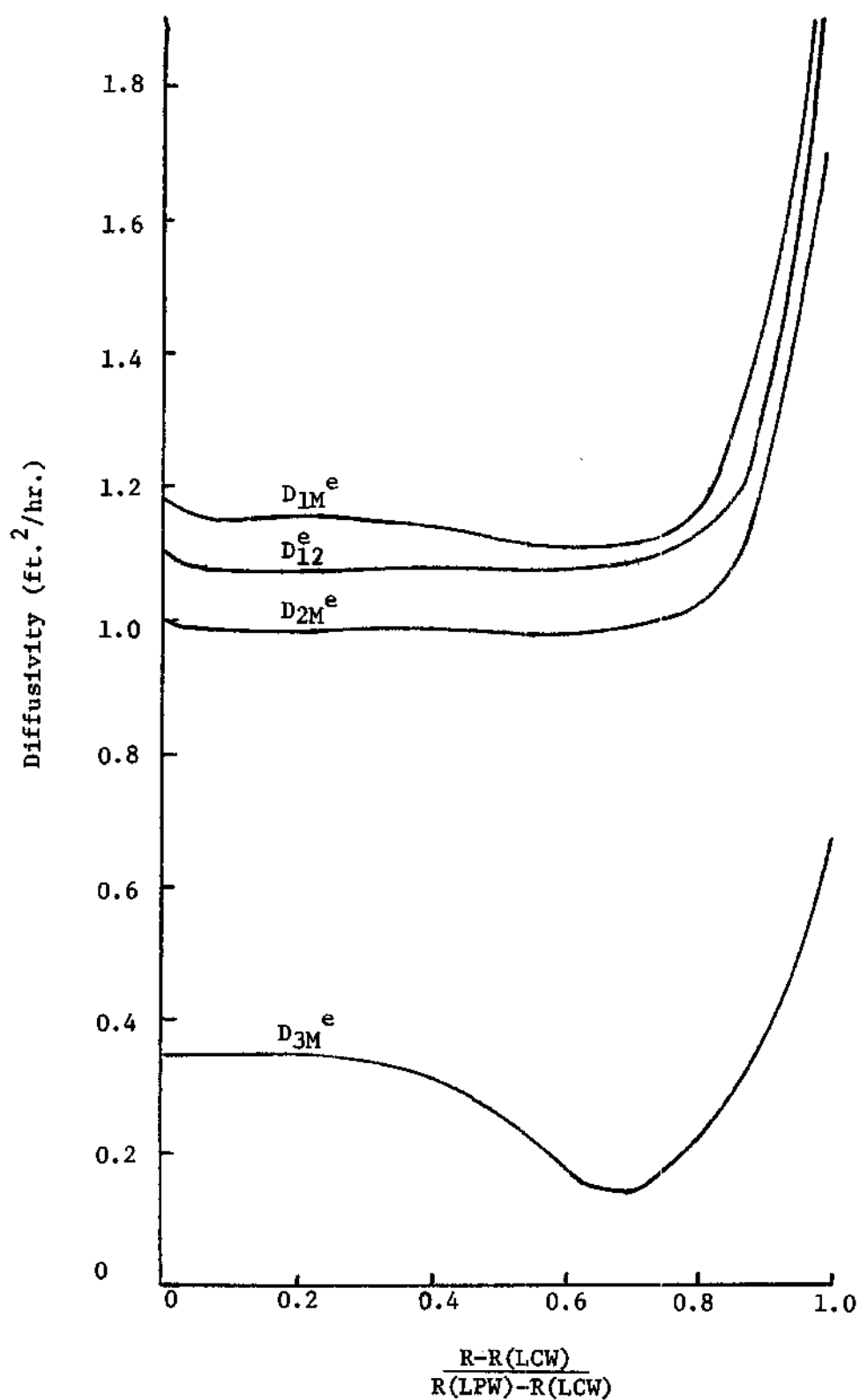


Figure 3. Comparison of Diffusivity for the Multicomponent Case and the Case of Equal Binary Diffusivities After 300 Seconds.

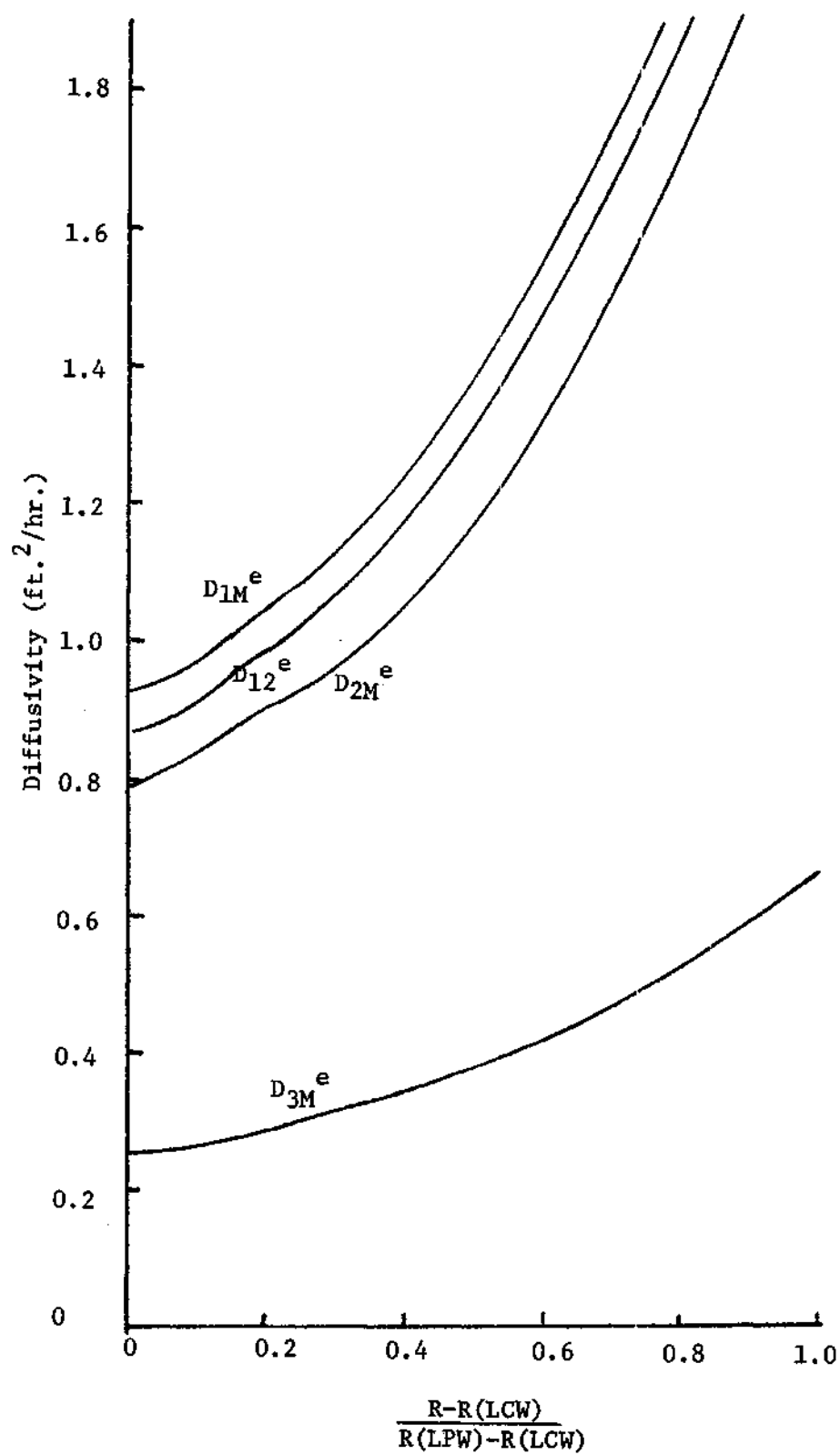


Figure 4. Diffusivity versus Station After 1,900 Seconds.

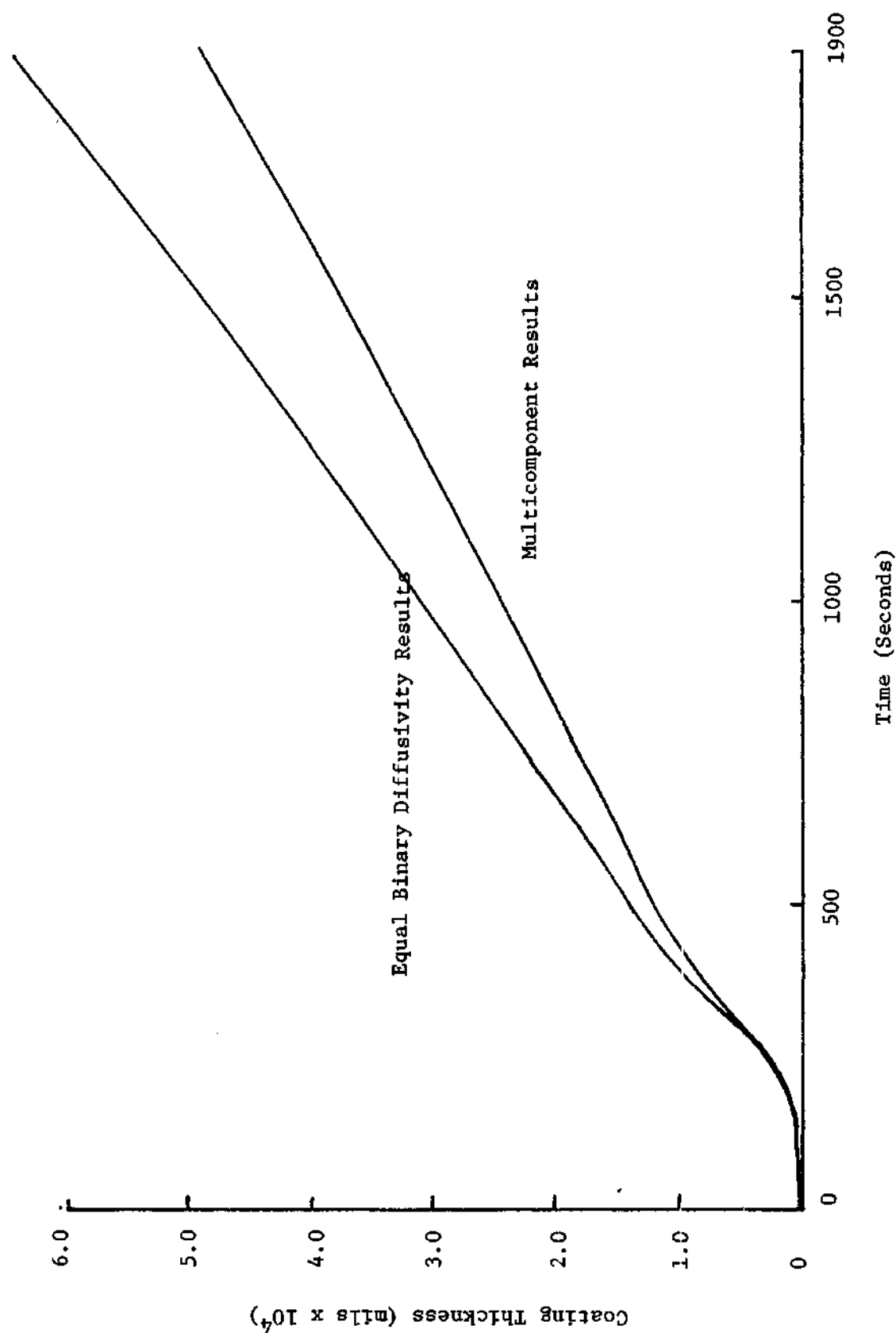


Figure 5. Comparison of Coating Deposited versus Time for Diffusion Cases with No Knudsen Diffusion.

concentration profiles, diffusivity, and coating deposition. The mole fraction of HCl is plotted in Figure 6 versus station for several times and for several pore radii for the multicomponent case. Results after 100 seconds could not be distinguished for any pore radii studied. After 300 seconds, runs with pore radii less than $50,000 \text{ \AA}$ produced oscillations in the HCl profiles indicating instability. Diffusion moduli were also consistently greater than 0.5 further indicating instability. More will be said about this indicator in the next section. After 1,900 seconds results are only available for pore radii equal to $90,000 \text{ \AA}$ and $50,000 \text{ \AA}$. Other runs with smaller pore radii were so unstable that indefinite numbers had already been produced in the calculations, thus stopping the run through an error exit on the computer. Figure 7 is a plot of similar results for the special case for equal binary diffusivities. As with results for the multicomponent case, the HCl profile is very similar after 100 seconds for all pore radii studied. After 300 seconds, results for a pore radius of 30.7 \AA are not valid. Much smaller pore radii can be studied for the special case of equal binary diffusivity because the multicomponent effect does not magnify the problem.

In order to show the Knudsen diffusion effect on diffusivity, effective diffusivities are plotted in Figure 8 for the different pore radii at 1,900 seconds for the special case of equal binary diffusivity. Because all binary diffusivities are equal to $D_{1,2}$, the difference in the effective diffusivity values is a result of the Knudsen component.

The effect of pore radius on the amount of coating deposited versus time is shown for each case and for each different pore radius in Figures 9 and 10. Broken line curves represent results from unstable

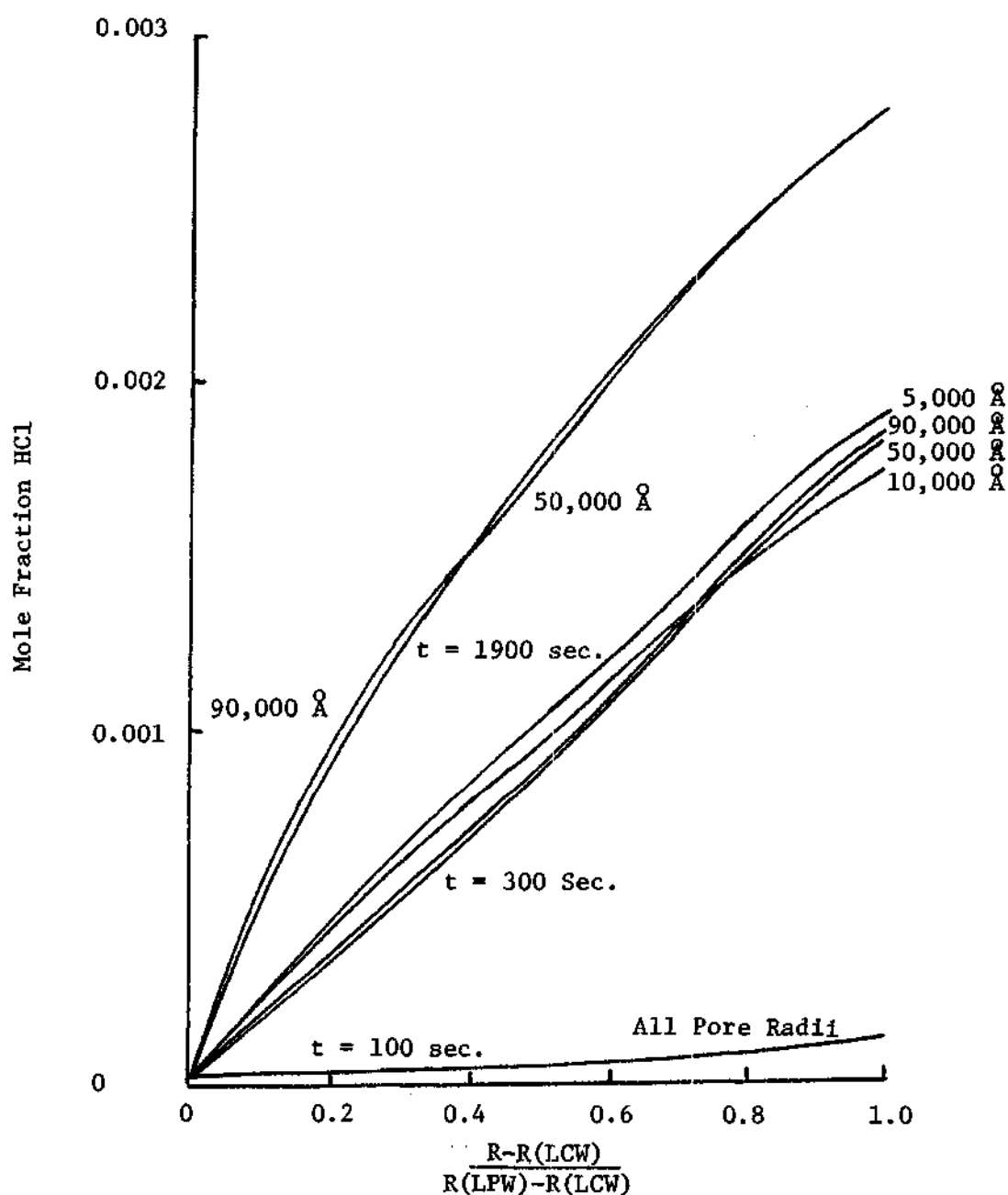


Figure 6. Mole Fraction of HCl versus Station for Times and Pore Radii Shown for the Multicomponent Case.

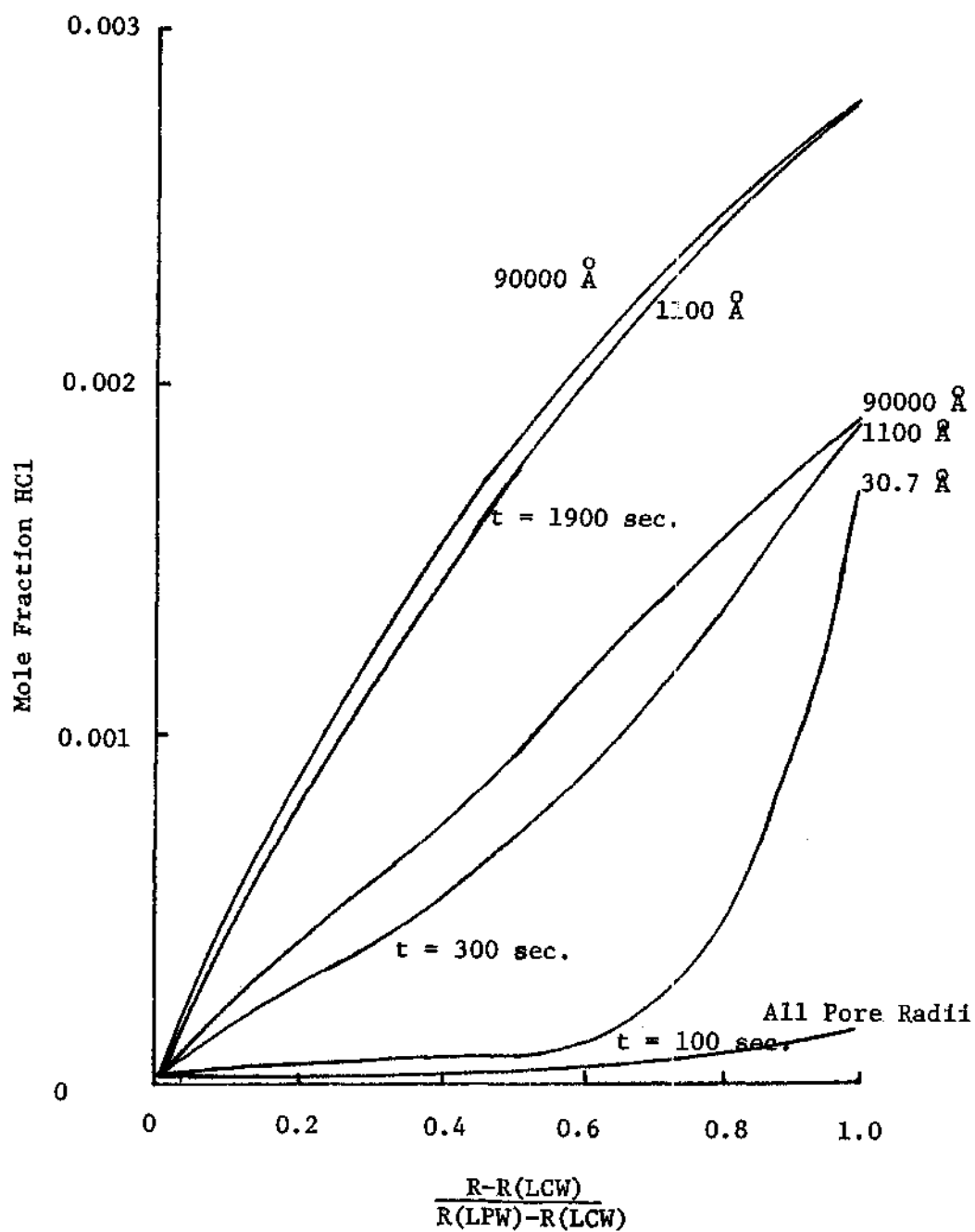


Figure 7. Mole Fraction of HCl versus Station for Times and Pore Radii Shown for the Equal Binary Diffusivities Case.

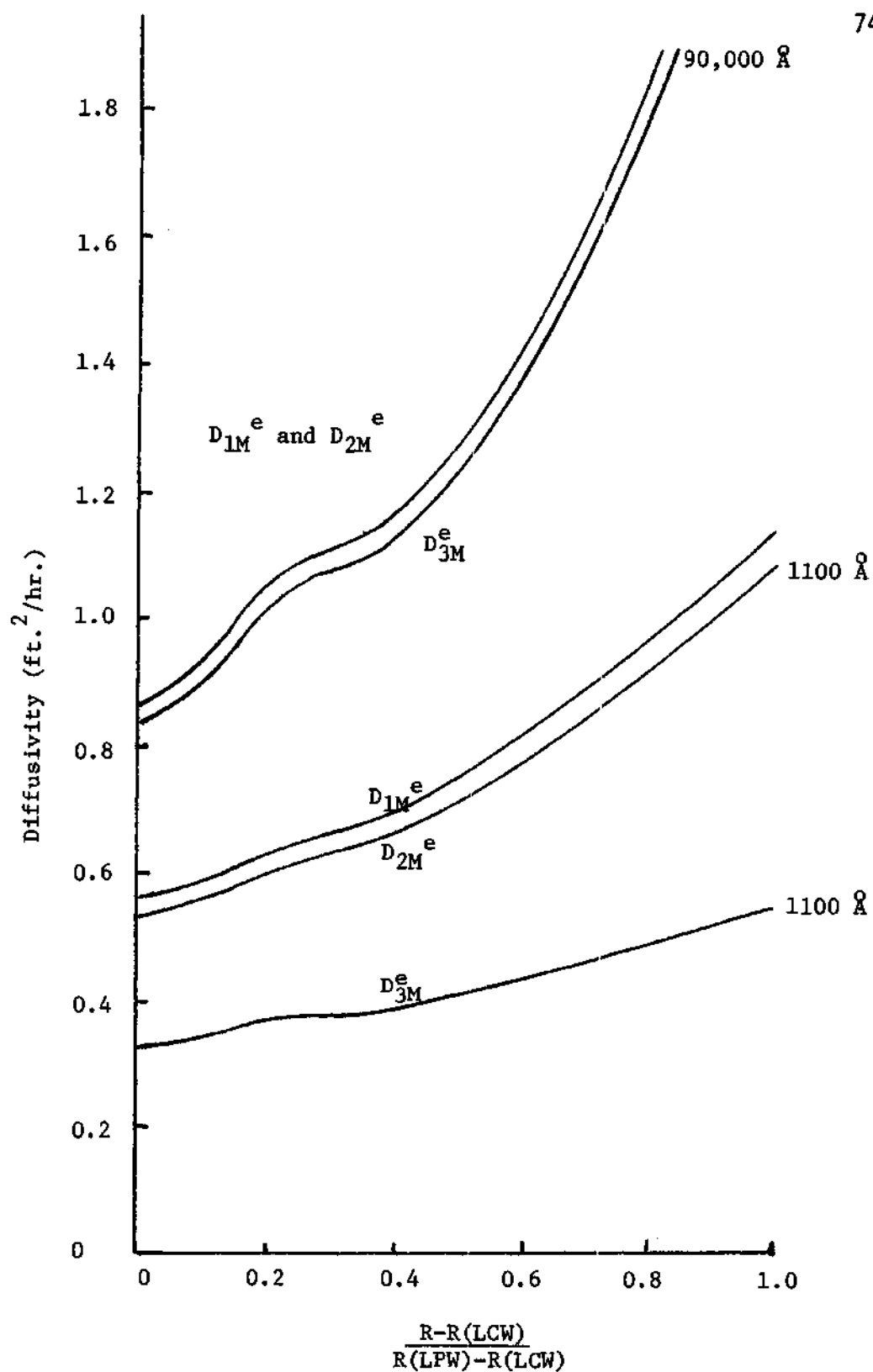


Figure 8. Diffusivity versus Station for Pore Radii

Shown at 1,900 Seconds.

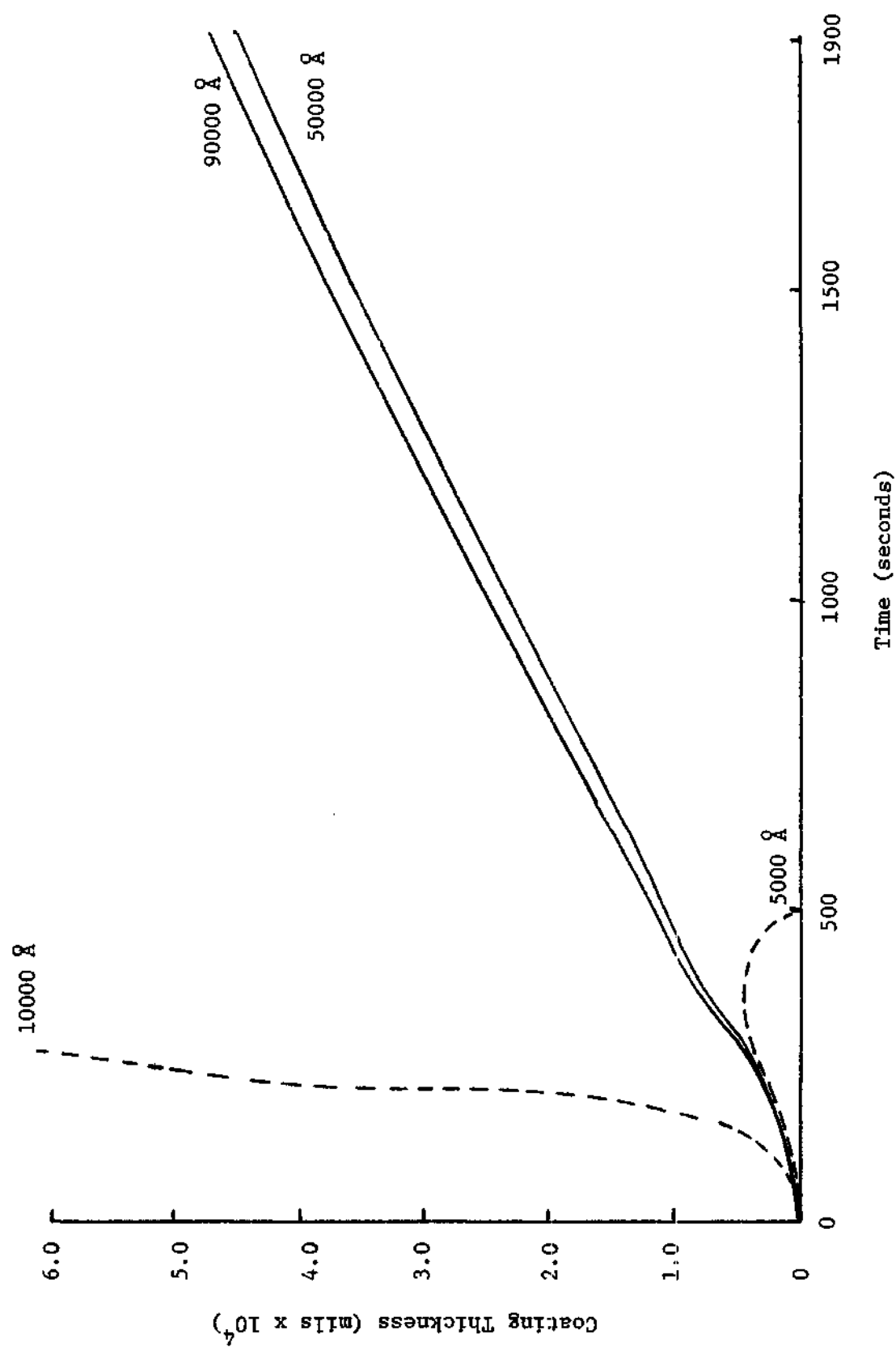


Figure 9. Coating Thickness versus Time for Pore Radii Shown for the Multicomponent Case.

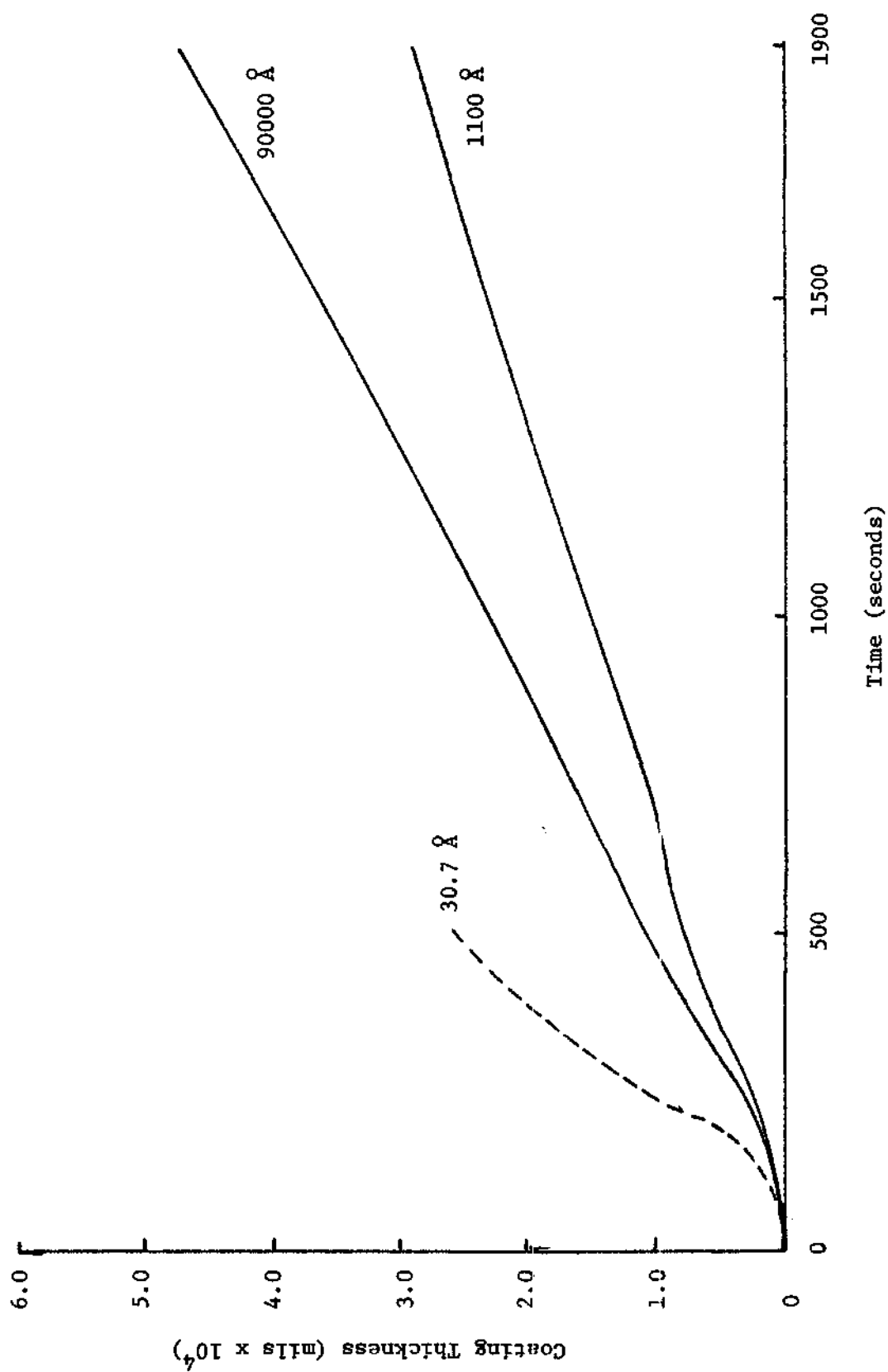


Figure 10. Coating Thickness versus Time for Pore Radii Shown for the Equal Binary Diffusivities Case.

solutions.

Accuracy of Results

The accuracy of results to the solutions discussed above is a function of time spacing, distance step size, and stability. As was previously mentioned, runs with smaller step sizes will provide more accurate solutions provided stability is maintained. Due to lack of computer time, results with smaller step sizes were not obtained. Stability was checked on each run by monitoring stability moduli for both heat and mass transfer as was discussed in Chapter III. Should any modulus exceed 0.5, the value of the modulus, the iteration, and the station were printed as a warning.

One good method to test accuracy of the numerical solutions is to compare results with those from an analytical solution. Unfortunately, such solutions are not available for this pack cementation problem. However, for very early times, the Arnold solution reported in Bird et al.²⁹ can be assumed to approximate results expected from the numerical solutions. In Figure 11, results of Arnold are compared to the multicomponent case and the special case of equal binary diffusivities. If the assumptions are made that at 1900 seconds the multicomponent solution has reached steady state and that the bulk flow term is negligible, a simple analytical solution results. The product of $\rho \delta_{im}^e$ was fitted to a curve of the form $a + br^2$ for this solution. Results of the steady state solution and those for the multicomponent case at 1900 seconds are shown in Figure 12.

In the macroscopic sense a test for accuracy is that the product of the radius and coating thickness deposited should be little less than the product of the core radius and the thickness of core material depleted. Results at 1900 seconds for the multicomponent case are $5.1606 (10^{-3})$.

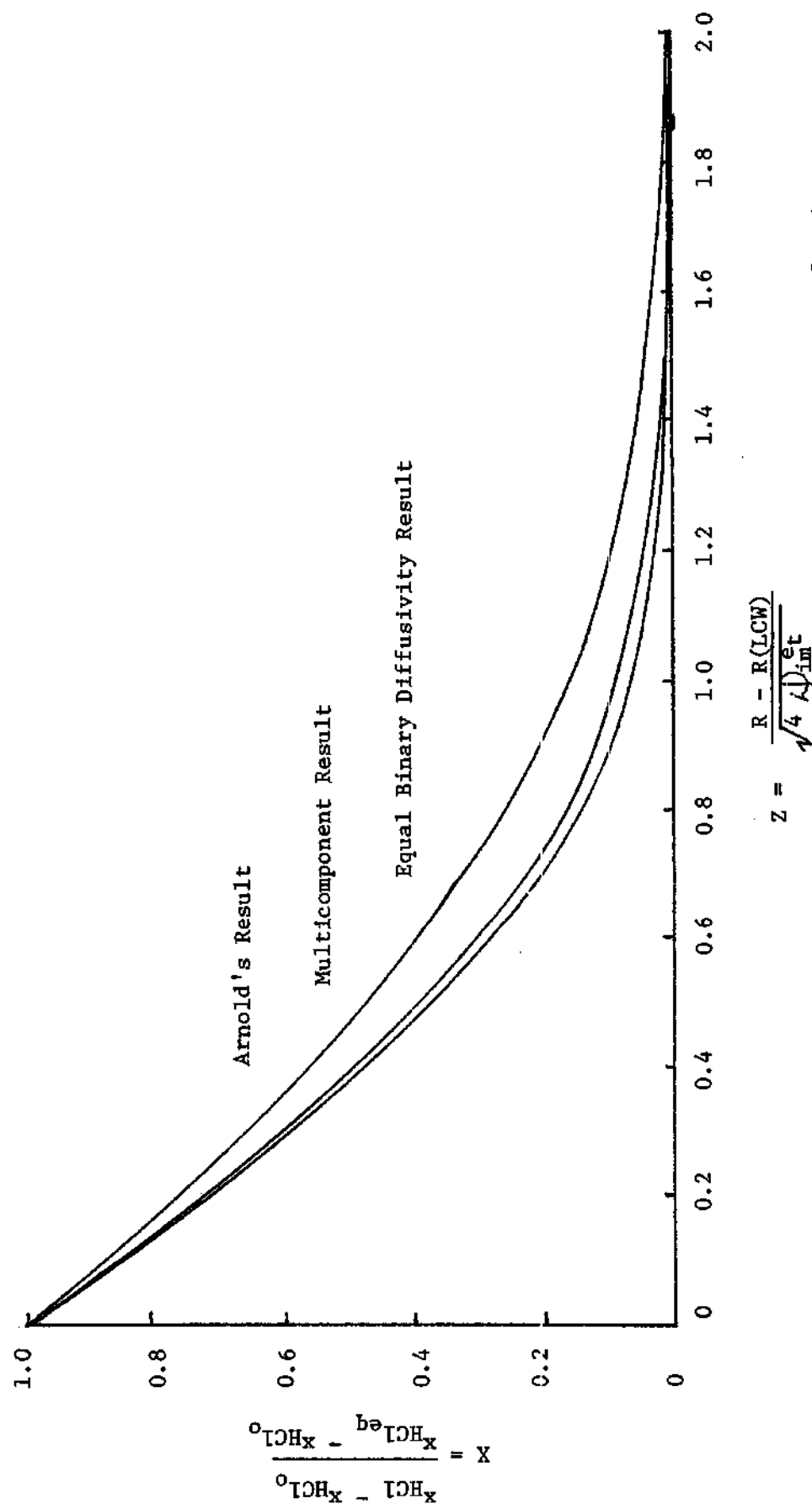


Figure 11. Arnold Solution versus the Multicomponent Solution at Early Times.

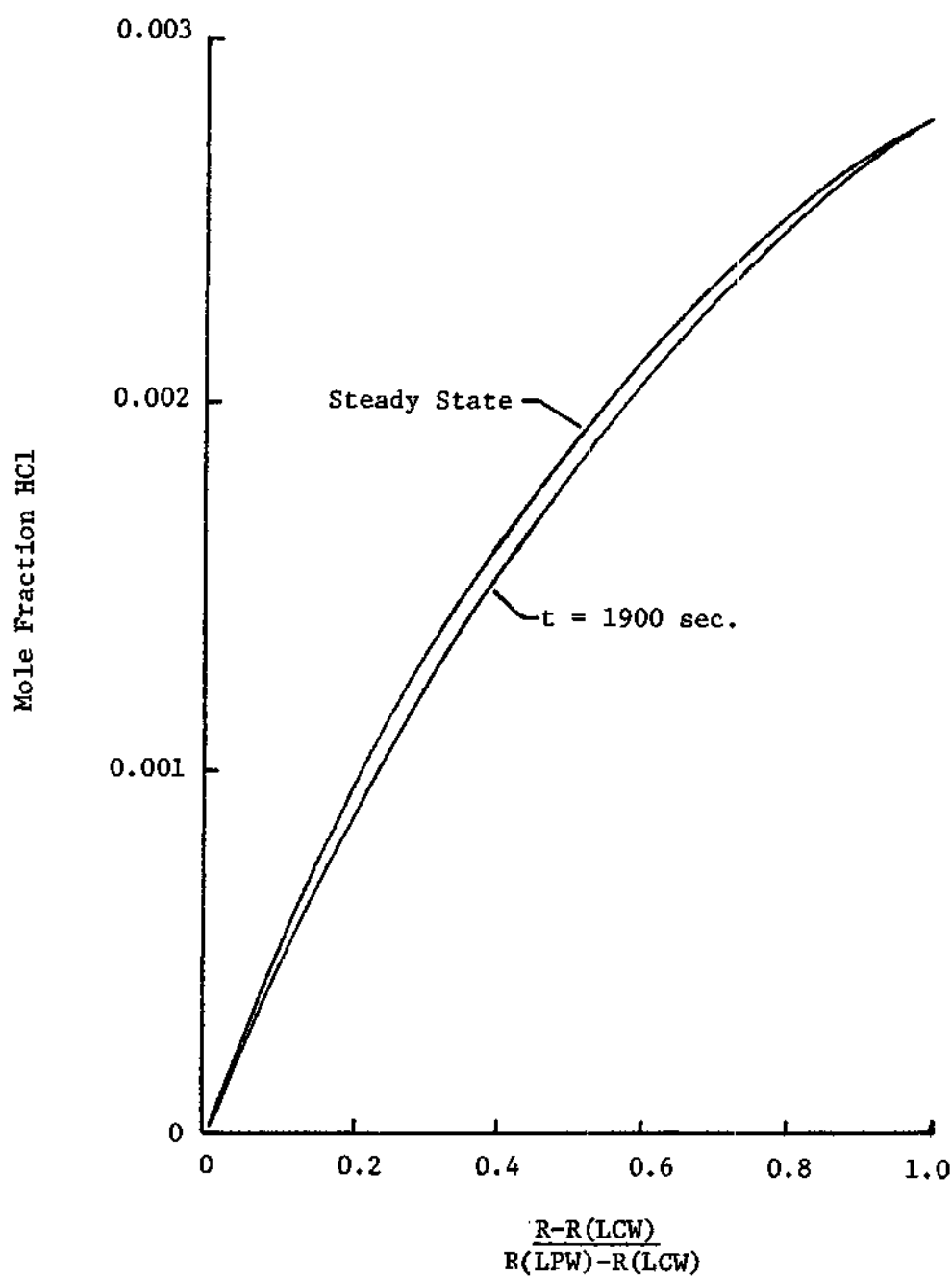


Figure 12. Steady State Solution versus the Multicomponent Solution at 1900 Seconds.

mil-inches and $5.4102(10^{-3})$ mil-inches respectively.

Perhaps the most significant measure of the accuracy of results from solutions presented herein concern the values listed in various tables under the heading "TEST." This parameter represents the ratio of the molar concentration gradient as calculated from the Stephan-Maxwell equation to the same gradient as calculated from the numerical solution. Since the Stephan-Maxwell equation is exact, the fact that values for the "TEST" parameters are very close to unity is indicative that the numerical solution is both reasonable and accurate.

CHAPTER V

CONCLUSIONS AND RECOMMENDATIONS

The most important conclusion reached from the work discussed herein is that the model chosen for multicomponent diffusion will provide a successful solution for initial value problems in multicomponent mass transfer. The second important conclusion is that the assumption of equal binary diffusivities will provide a reasonable solution, thus greatly simplifying calculations. And finally, Knudsen diffusion can be a significant contribution to mass transfer in porous medium.

Several areas of further work and development in this area are evident from the results of this thesis. A nested iterative scheme to better calculate the molar concentrations in the porous media when deposition occurs should be developed. Laboratory experiments should be conducted to provide actual data for comparison with the model. And finally, experimental work to better relate porous media properties to transport properties should be conducted.

APPENDIX I

CONTINUITY EQUATION FOR POROUS MATERIAL

Consider a small volume of porous material, V_p , composed of substrate particles covered with a thin coating and a gas-filled void. Let the mass of the substrate particle be defined as:

$$m_{p_0} = \rho_{p_0} V_{p_0} \quad (A1-1)$$

where V_{p_0} is the volume of porous media occupied by the substrate particles

ρ_{p_0} is the density of the substrate.

and the mass of the coating be defined as:

$$m_c = \rho_c (V_p - V_{p_0}) \quad (A1-2)$$

where ρ_c is the density of the substrate coating

V_p is the volume of the porous media occupied by the solid particles.

The density of the solid composite may be calculated as follows:

$$\rho_p = \frac{m_{p_0} + m_c}{V_p} \quad (A1-3)$$

$$= \frac{\rho_{p_0} V_{p_0} + \rho_c (V_p - V_{p_0})}{V_p} \quad (A1-4)$$

$$= \rho_c + \frac{V_{p_0}}{V_p} (\rho_{p_0} - \rho_c) \quad (A1-5)$$

If the porosities of the media are defined as:

$$\epsilon_{p_0} = \frac{V_{p_0}}{V_t} \quad (\text{A1-6})$$

and
$$\epsilon_p = \frac{V_p}{V_t} \quad (\text{A1-7})$$

where V_t is the total volume of porous media

Then
$$\frac{V_{p_0}}{V_p} = \frac{\epsilon_{p_0}}{\epsilon_p} \quad (\text{A1-8})$$

And ρ_p becomes:

$$\rho_p = \rho_c + (\rho_{p_0} - \rho_c) \frac{\epsilon_{p_0}}{\epsilon_p} \quad (\text{A1-9})$$

Now the continuity equation for a two-phase mixture of solid composite and gas is written as follows:

$$\frac{\partial \rho_t}{\partial t} + \nabla \cdot \bar{n} = 0 \quad (\text{A1-10})$$

where ρ_t is the density of the porous medium

\bar{n} is the mass flux in the porous medium.

But ρ_t is $\epsilon_p \rho_p + \epsilon \rho$, where ϵ is the gas filled volume and ρ is the density of the gas. Also $\bar{n}_t = \bar{n}_p + \sum_{i=1}^N \bar{n}_i^e$ where \bar{n}_i^e is the mass flux of the gas species i . Assuming that the mass flux of the composite, \bar{n}_p , is zero, the continuity equation becomes

$$\frac{\partial}{\partial t}(\epsilon_p \rho_p) + \frac{\partial}{\partial t}(\epsilon \rho) + \nabla \cdot \sum_{i=1}^N \bar{n}_i^e = 0 \quad (\text{A1-11})$$

Now
$$\epsilon_p \rho_p = \epsilon_p \rho_c + (\rho_{p_0} - \rho_c) \epsilon_{p_0} \quad (\text{A1-12})$$

For a coating with a constant density, the time derivative of $\epsilon_p \rho_p$ will be:

$$\frac{\partial}{\partial t}(\epsilon_p \rho_p) = \rho_c \frac{\partial \epsilon_p}{\partial t} \quad (\text{A1-13})$$

And the continuity equation for the porous medium becomes

$$\frac{\partial}{\partial x}(\epsilon \rho) + \rho_c \frac{\partial \epsilon_p}{\partial x} + \nabla \cdot \bar{n}^e = 0 \quad (\text{A1-14})$$

APPENDIX II

BINARY DIFFUSION COEFFICIENT FOR POROUS MEDIA

Evans, Watson, and Mason have proposed a model for the binary diffusion equation in porous media which begins with a modified form of the Stefan-Maxwell equation for constant temperature and pressure.³⁷ Evans et al. proposed their relation in terms of molecules rather than the customary molecular qualities. In addition, these workers have treated the solid particles of the porous medium as large molecules with a zero mole velocity. The general form of this equation is given below.

$$\sum_{\substack{j=1 \\ j \neq i}}^{v'} \frac{n_i n_j}{n'^2 D_{ij}^{e'}} (\bar{v}_j - \bar{v}_i) = \frac{1}{n'} \frac{\partial n_i}{\partial z} \quad (\text{A2-1})$$

where n_i is the number of molecules of species i for the total unit volume of solid and gas
 n' is the total number of molecules, solid and gas, for the total unit volume
 $D_{ij}^{e'}$ is the effective diffusion coefficient
 \bar{v}_i is mass velocity of species i .
 v' is the number of gas and solid i species.

In this equation, effects of the porous media on the diffusion path are incorporated in the definition of the diffusion coefficient as follows:

$$D_{ij}^{e'} = \frac{\epsilon}{\tau} D_{ij}' \quad (\text{A2-2})$$

where ϵ' is the porosity
 τ is the tortuosity
 $D_{ij}^{e'}$ is the binary diffusion coefficient.

If the molecular flux of species i , \bar{N}_i is defined as the product $n_i \bar{V}$, then equation A2-1 may be rearranged to give:

$$\sum_{\substack{j=1 \\ j \neq i}}^{\nu'} (n' D_{ij}^{e'})^{-1} (n_i \bar{N}_j - n_j \bar{N}_i) = \frac{\partial n_i}{\partial z} \quad (\text{A2-3})$$

For two gaseous species and one solid species p equation A2-3 becomes:

$$n_i \bar{N}_j - n_j \bar{N}_i \frac{D_{ij}^{e'}}{D_{ij}^{e'}} + n_i \bar{N}_p - n_p \bar{N}_i \frac{D_{ip}^{e'}}{D_{ip}^{e'}} = n' \frac{\partial n_i}{\partial z} \quad (\text{A2-4})$$

Assuming that the solid species p has a zero mass velocity, \bar{N}_p would also be equal to zero. Equation A2-4 could then be arranged to give:

$$\bar{N}_i \left(1 + \frac{n_p}{n} \frac{D_{ij}^{e'}}{D_{ip}^{e'}} \right) = - \frac{n'}{n} D_{ij}^{e'} \frac{\partial n_i}{\partial z} + \frac{n_i}{n} \bar{N} \quad (\text{A2-5})$$

If δ_i is defined as follows:

$$\delta_i = \left(1 + \frac{n_p}{n} \frac{D_{ij}^{e'}}{D_{ip}^{e'}} \right)^{-1} \quad (\text{A2-6})$$

Then equation A2-5 may be arranged to give:

$$\bar{N}_i = - D_i^e \frac{\partial n_i}{\partial z} + \frac{n_i}{n} \delta_i \bar{N} \quad (\text{A2-7})$$

where

$$D_i^e = \frac{n'}{n} D_{ij}^{e'} \delta_i \quad (\text{A2-8})$$

and

$$n' D_{ij}^{e'} = \left(\frac{16}{3} \frac{\pi}{\epsilon} \left(\frac{\bar{m}}{2\pi kT} \right)^{\frac{1}{2}} \pi \Omega_{ij} \Omega_{ij} \right)^{-1} \quad (\text{A2-9})$$

The quantity $n' D_{ip}^{e'}$ is calculated from a modification of equation A2-9. For a mixture of a gas and solid, the reduced mass \bar{m} may be approximated by the mass of the gas species, m_i . The collision diameter reduces to the radius of the solid particle and the collision integral becomes $(1 + \frac{a_i \pi}{8})$. The term a_i is the fraction of species i diffusely scattered by the solid and for most gases is approximately equal to unit. Therefore, the diffusivity for interaction between the solid and gas is given below:

$$n' D_{ip}^{e'} = \left(\frac{16}{3} \frac{\pi}{\epsilon} \left(\frac{m_i}{2\pi kT} \right)^{\frac{1}{2}} \pi R_p^2 \left(1 + \frac{a_i \pi}{8} \right) \right)^{-1} \quad (\text{A2-10})$$

This equation is used by Evans et al. to represent the effect of Knudsen diffusion.

APPENDIX III

COMPARISON OF VARIOUS FORMS FOR THE BINARY
DIFFUSION EQUATION IN POROUS MEDIA

Evans, Watson and Mason have proposed the following equations for the binary diffusion equation in porous media.³⁷

$$\bar{N}_i = -D_i^e \frac{\partial n_i}{\partial z} + \frac{n_i}{n} \delta_i \bar{N} \quad (\text{A3-1})$$

where
$$D_i^e = \frac{n'}{n} D_{ij}^{e'} \delta_i \quad (\text{A3-2})$$

and
$$\delta_i = \left(1 + \frac{n_p}{n} \frac{D_{ij}^{e'}}{D_{ip}^{e'}}\right)^{-1} \quad (\text{A3-3})$$

If the mole fraction of species i, v_i , is defined as the ratio $\frac{n_i}{n}$ then equation A3-1 may be rearranged to give:

$$\bar{N}_i = \frac{-D_i^e \frac{\partial n_i}{\partial z}}{1 - \alpha v_i \delta_i} \quad (\text{A3-4})$$

where
$$\alpha = 1 + \frac{\bar{N}}{\bar{N}_i} \quad (\text{A3-5})$$

Because $n' D_{ij}^{e'}$ is equal to $n D_{ij}^e$, equation A3-2 may be rearranged to

give:

$$\delta_i = \frac{D_i^e}{D_j^e} \quad (\text{A3-6})$$

Combining this result with equation A3-4 and rearranging yields:

$$\bar{N}_i = \frac{-D_j^e \frac{\partial n_i}{\partial z}}{1 + \frac{D_j^e}{D_p^e} - \alpha \kappa_i} \quad (\text{A3-7})$$

Equation A3-7 is the form suggested by Rothfield⁴¹ and Scott⁴².

APPENDIX IV

MULTICOMPONENT DIFFUSION EQUATION FOR POROUS MEDIA

For non-constant pressure and temperature, the Stephan-Maxwell equation written in the terminology of Evans et al. is given as follows:

$$\sum_{\substack{i=1 \\ i \neq j}}^{p'} \frac{n_i n_j}{n'^2} (D_{ij}^{e'})^{-1} (\bar{v}_j^e - \bar{v}_i^e) = \nabla \left(\frac{n_i}{n'} \right) \quad (\text{A4-1a})$$

where

$$n' = n + n_p \quad (\text{A4-1b})$$

$$n = \sum_{i=1}^p n_i \quad (\text{A4-1c})$$

$$D_{ij}^{e'} = \frac{\epsilon}{\tau} \phi_{ij}' \quad (\text{A4-1d})$$

$$\phi_{ij}' = \left(\frac{16}{3} n' \left(\frac{\bar{m}}{2\pi k T} \right)^{\frac{1}{2}} \pi \sigma_{ij}^e \Omega_{ij} \right)^{-1} \quad (\text{A4-1e})$$

- and
- n_i is the molecules per unit total volume of the gas species i
 - n_p is the molecules per unit total volume of the solid species
 - \bar{v}_i^e is the apparent molecular average velocity for the gas species i or the solid species p .

By dividing the number of molecules per unit volume by Avogadro's number

equation A3-1a may be converted to an equation based on the number of moles per unit total volume as follows:

$$\sum_{\substack{j=1 \\ j \neq i}}^{J'} \frac{c_i c_j}{c'} (c' D_{ij}^e)^{-1} (\bar{v}_j^e - \bar{v}_i^e) = \nabla \left(\frac{c_i}{c'} \right) \quad (\text{A4-2})$$

This equation is further expanded to give:

$$\sum_{\substack{j=1 \\ j \neq i}}^{J'} \frac{c_i c_j}{c'} (c' D_{ij}^e)^{-1} (\bar{v}_j^e - \bar{v}_i^e) = \frac{1}{c'} \nabla c_i - \frac{1}{c'} \frac{c_i}{c'} \nabla c' \quad (\text{A4-3})$$

If the molar flux of gas species i is defined as:

$$\bar{N}_i^e = c_i \bar{v}_i^e \quad (\text{A4-4})$$

equation A3-3 becomes:

$$\sum_{\substack{j=1 \\ j \neq i}}^{J'} \frac{c_i c_j}{c'} (c' D_{ij}^e)^{-1} \left(\frac{\bar{N}_j^e}{c_j} - \frac{\bar{N}_i^e}{c_i} \right) = \frac{1}{c'} \nabla c_i - \frac{1}{c'} \frac{c_i}{c'} \nabla c' \quad (\text{A4-5})$$

If only one species exists in the solid phase, the term which accounts for the interaction between the solid and the gas species i may be separated from the summation in equation A3-5 and the mass fraction of the gas species i substituted for the ratio of c_i to c to give:

$$\sum_{\substack{i=1 \\ i \neq j}}^J \frac{c}{c'} (c' d_{ij}^e)^{-1} (x_i \bar{N}_j^e - x_j \bar{N}_i^e) - (c' d_{ip}^e)^{-1} \left(\frac{c_p}{c'} \bar{N}_i^e - \frac{c_i}{c'} \bar{N}_p^e \right) \quad (\text{A4-6a})$$

$$\frac{c_i}{c'} \bar{N}_p^e = \frac{c}{c'} \nabla x_i + \frac{x_i}{c} \nabla c - \frac{c}{c'} \frac{x_i}{c'} \nabla c' \quad (\text{A4-6b})$$

where $x_i = \frac{c_i}{c}$ (4-6b)

Now $\Delta c'$ equals Δc because the number of solid molecules does not change.

In addition, c' may be factored and canceled to give:

$$\sum_{\substack{i=1 \\ i \neq j}}^J c (c' d_{ij}^e)^{-1} (x_i \bar{N}_j^e - x_j \bar{N}_i^e) + (c' d_{ip}^e)^{-1} (c_i \bar{N}_p^e - c_p \bar{N}_i^e) = c \nabla x_i + x_i \left(1 - \frac{c}{c'}\right) \nabla c \quad (\text{A4-7})$$

For most situations $\frac{c}{c'}$ is nearly unity. Thus, equation A4-7 becomes:

$$\nabla x_i = \sum_{\substack{i=1 \\ i \neq j}}^J (c' d_{ij}^e)^{-1} (x_i \bar{N}_j^e - x_j \bar{N}_i^e) + (c' d_{ip}^e)^{-1} \left(\frac{c_i}{c} \bar{N}_p^e - \frac{c_p}{c} \bar{N}_i^e \right) \quad (\text{A4-8})$$

APPENDIX V

MULTICOMPONENT ENERGY CONSERVATION EQUATION
FOR POROUS MEDIA

Neglecting kinetic and potential energy, the equation for energy conservation of a homogeneous mixture is:

$$\frac{\partial}{\partial t}(\rho \hat{H}_t) + \nabla \cdot \rho \vec{v}_e \hat{H}_t = -\nabla \cdot \vec{q} + \frac{\partial P}{\partial t} \quad (\text{A5-1})$$

where \hat{H}_t is the enthalpy of the mixture.

Assuming that the porous medium is a mixture of solid and gases which may be represented by the "dusty gas" model used in previous derivations, equation A5-1 may be modified to give equation A5-2 below. As with other relations based on this model, the velocity of the solid is assumed to be zero. In addition, the solid is assumed to be incompressible so that changes in pressure only occur in the void volume.

$$\frac{\partial}{\partial t}(\epsilon \rho \hat{H}) + \frac{\partial}{\partial t}(\epsilon_p \rho_p \hat{H}_p) + \nabla \cdot \rho \vec{v}_e \hat{H} = -\nabla \cdot \vec{q} + \frac{\partial}{\partial t}(\epsilon P) \quad (\text{A5-2})$$

where \hat{H} is the enthalpy for the gas mixture
 \hat{H}_p is the enthalpy for the solid phase.

Equation A5-2 can be expanded to give:

$$\epsilon \rho \frac{\partial \hat{H}}{\partial t} + \hat{H} \frac{\partial}{\partial t}(\epsilon \rho) + \frac{\partial}{\partial t}(\epsilon_p \rho_p \hat{H}_p) + \nabla \cdot \rho \vec{v}_e \hat{H} = -\nabla \cdot \vec{q} + \frac{\partial}{\partial t}(\epsilon P) \quad (\text{A5-3})$$

According to the continuity equation:

$$\frac{\partial}{\partial t}(\epsilon \rho) + \nabla \cdot \rho \vec{v}_c = - \frac{\partial}{\partial t}(\epsilon_p \rho_p) \quad (\text{A5-4})$$

Inserting this result in equation A5-3 and combining terms yields:

$$\epsilon \rho \frac{\partial \hat{H}}{\partial t} + \frac{\partial}{\partial t}(\epsilon_p \rho_p \hat{H}_p) - \hat{H} \frac{\partial}{\partial t}(\epsilon_p \rho_p) + \rho \vec{v}_c \cdot \nabla \hat{H} = - \nabla \cdot \vec{q} + \epsilon \frac{\partial P}{\partial t} + \rho \frac{\partial E}{\partial t} \quad (\text{A5-5})$$

If the solid material is composed of a substrate particle and a coating of a single species and if the density of the coating does not change with time, the derivative of the product $\epsilon_p \rho_p$ with respect to time can be represented as shown in equation A5-6. Details of this derivation are shown in Appendix I.

$$\frac{\partial}{\partial t}(\epsilon_p \rho_p) = - \rho_c \frac{\partial E}{\partial t} \quad (\text{A5-6})$$

Inserting these results into equation A5-5 yields:

$$\epsilon \rho \frac{\partial \hat{H}}{\partial t} + \frac{\partial}{\partial t}(\epsilon_p \rho_p \hat{H}_p) + \rho_c \hat{H} \frac{\partial E}{\partial t} = - \rho \vec{v}_c \cdot \nabla \hat{H} - \nabla \cdot \vec{q} + \epsilon \frac{\partial P}{\partial t} + \rho \frac{\partial E}{\partial t} \quad (\text{A5-7})$$

In order to express the energy equation in terms of temperature, the following equation is used:

$$A = \sum_{i=1}^N \omega_i \hat{H}_i \quad (\text{A5-7a})$$

where
$$\hat{H}_i = \int_{T_b}^T c_{p_i} dT + \hat{H}_i^{\circ} \quad (\text{A5-7b})$$

and \hat{H}_i° is the enthalpy of the gas species i at the base temperature

T_b is the base temperature.

The relation describing the enthalpy of the solid phase can also be expanded to give:

$$\epsilon_p \rho_p \hat{H}_p = \epsilon_{p_0} \rho_{p_0} \hat{H}_{p_0} + (\epsilon_p - \epsilon_{p_0}) \rho_c \hat{H}_c \quad (\text{A5-8a})$$

where
$$\hat{H}_c = \int_{T_b}^T c_{p_c} dT + \hat{H}_c^{\circ} \quad (\text{A5-8b})$$

and
$$\hat{H}_{p_0} = \int_{T_b}^T c_{p_p} dT + \hat{H}_{p_0}^{\circ} \quad (\text{A5-8c})$$

Assuming that the density of the solid substrate and of the coating are constant in time, application of these definitions for the individual enthalpies to equation A5-7 results in a conservation of energy equation based on the local temperature of the porous media. This equation is given below:

$$\begin{aligned} \epsilon_p \rho_p \frac{\partial T}{\partial t} + \epsilon_p \sum_{i=1}^N \hat{H}_i \frac{\partial w_i}{\partial t} + \epsilon_{p_0} \rho_{p_0} c_{p_{p_0}} \frac{\partial T}{\partial t} + (\epsilon_p - \epsilon_{p_0}) \rho_c c_{p_c} \frac{\partial T}{\partial t} \\ - \rho_c \hat{H}_c \frac{\partial \epsilon}{\partial t} + \rho_c \hat{H}_c^{\circ} \frac{\partial \epsilon}{\partial t} = - \rho \nabla_e \cdot \nabla \hat{H} - \nabla \cdot \bar{q} + \epsilon \frac{\partial p}{\partial t} + \rho \frac{\partial \epsilon}{\partial t} \end{aligned} \quad (\text{A5-9})$$

Now the flux of energy into the system, \bar{q} , can be expanded as follows:

$$\bar{q} = -k_e \nabla T + \sum_{i=1}^N \hat{H}_i \bar{j}_i^e \quad (\text{A5-10})$$

Inserting these results into equation A5-9 and combining terms yields the following equation for energy conservation in porous media:

$$\begin{aligned} & (\epsilon_p c_p + \epsilon_p \rho_p c_{p0} + (\epsilon_p - \epsilon_p) \rho_c c_c) \frac{\partial T}{\partial t} + \rho_c (\hat{H} - \hat{H}_c) \frac{\partial x}{\partial t} \quad (\text{A5-11}) \\ & + \epsilon_p \sum_{i=1}^N \hat{H}_i \frac{\partial \omega_i}{\partial t} = -\rho \bar{v}_e c_p \cdot \nabla T - \rho \bar{v}_e \cdot \sum_{i=1}^N \hat{H}_i \nabla \omega_i \\ & - \nabla \cdot \sum_{i=1}^N \hat{H}_i \bar{j}_i + \nabla \cdot k_e \nabla T + \epsilon \frac{\partial p}{\partial t} + \rho \frac{\partial x}{\partial t} \end{aligned}$$

APPENDIX VI

CALCULATION OF THE SUBSURFACE TEMPERATURE

$T(L, t)$ is defined as the temperature of the grid point just inside the shell surface. In the algorithm arranged for solution of this problem, the spacing between this point and the surface can be very much smaller than the spacing for the other grids. As a result, space derivative calculations can be inaccurate. In addition, the value for the surface temperature is specified or experimentally determined. As a result, the value calculated for $T(L, t)$ must be consistent with the value for the heat flux at this point as implied by specification of the surface temperature. In order to provide increased accuracy and to satisfy the constraint on the heat flux, an implicit equation is used to calculate $T(L, t)$. This method is possible at this point because the value of the surface temperature is known at all times. The equation is developed below:

$$T(L, t + \Delta t) = T(L, t) + \frac{\Delta t}{2} \left(\frac{\partial T}{\partial x} \Big|_t + \frac{\partial T}{\partial x} \Big|_{t + \Delta t} \right) \quad (\text{A6-1})$$

where $\frac{\partial T}{\partial x} \Big|_t$ is the time derivative of temperature at time

$\frac{\partial T}{\partial x} \Big|_{t + \Delta t}$ is the time derivative of temperature at time

The equation for the time derivative of temperature at time $t + \Delta t$ is given below. This equation uses values for all physical and transport properties evaluated at the previous time, t . In this respect, the use of this

method is not totally implicit, but the values for these variables will not change significantly in the range of the calculation.

$$\frac{\partial T}{\partial t} / t + \Delta t = \left(\frac{2}{\Delta s \Delta r} \left(\frac{T(s, t + \Delta t)}{\Delta s} + \frac{T(L-1, t + \Delta t)}{\Delta r} \right) - \frac{2T(L, t + \Delta t)}{\Delta s \Delta r} \right) \alpha_s(L, t) \quad (A6-2)$$

$$+ \left(\frac{\partial k_s}{\partial r} + \frac{k_s(L, t)}{R(L)} \right) \frac{1}{\Delta r \Delta s} \left(\left(\frac{\Delta r}{\Delta s} T(s, t + \Delta t) - \frac{\Delta s}{\Delta r} T(L-1, t + \Delta t) \right) - \left(\frac{\Delta r}{\Delta s} - \frac{\Delta s}{\Delta r} \right) T(L, t + \Delta t) \right) / \rho(L, t) c_p(L, t)$$

where $T(s, t + \Delta t)$ is the temperature at the surface at time $t + \Delta t$

$\alpha_s(L, t)$ is the thermal of diffusivity

$T(L-1, t + \Delta t)$ is the temperature two points inside the surface at time $t + \Delta t$

Δr is the spacing for a normal grid

Δs is the spacing for the last grid point and surface.

$$\text{and } \frac{\partial k_s}{\partial r} = \left(\frac{\Delta r}{\Delta s} k_s(L+1, t) - \frac{\Delta s}{\Delta r} k_s(L-1, t) \right) / (\Delta r \Delta s) - k_s(L, t) \frac{\Delta r - \Delta s}{\Delta r \Delta s} \quad (A6-2b)$$

Application of equation A6-2a and A6-2b to A6-1 yields after rearranging terms:

$$T(L, t + \Delta t) = \left(T(L, t) + \frac{\Delta t}{2} \frac{\partial T}{\partial t} / t + \frac{\Delta t}{2} \left(\frac{1}{\Delta s \Delta r} \right) \left(\frac{\alpha_s(L, t)}{R(L)} \right. \right. \quad (A6-3)$$

$$+ \left. \frac{\partial k_s}{\partial r} / \left(\rho(L, t) c_p(L, t) \right) \right) \left(\frac{\Delta r}{\Delta s} T(L+1, t + \Delta t) - \frac{\Delta s}{\Delta r} T(L-1, t + \Delta t) \right) +$$

$$2\alpha_s(L, t) \left(\frac{T(L+1, t + \Delta t)}{\Delta s} + \frac{T(L-1, t + \Delta t)}{\Delta r} \right) / \left(1 + \frac{\Delta t}{2} \left(\frac{1}{\Delta r \Delta s} \right) \right)$$

$$\left(\left(\frac{\alpha_s(L, t)}{R(L)} + \frac{\partial k_s}{\partial r} / \left(\rho(L, t) c_p(L, t) \right) \right) \left(\frac{\Delta r}{\Delta s} - \frac{\Delta s}{\Delta r} \right) + 2\alpha_s(L, t) \left(\frac{1}{\Delta s} + \frac{1}{\Delta r} \right) \right)$$

APPENDIX VII

INTERFACE CONTINUITY EQUATION AND
THICKNESS CALCULATION

Because chemical reaction may consume or deposit solid silicon at an interface, the distance between the solid surface and the first node point in the porous medium will vary and a gap will form. As a result, a special calculation for grid thickness and the continuity equation must be developed. As was previously stated, storage terms are necessary because the interface is treated as a volume element in a numerical solution. The derivations begin with the continuity equation. Dimensions used in these derivations are shown in Figure 13.

$$\frac{\partial}{\partial t} (2\pi R_c L_o \Delta c r_{si} + 2\pi R_c L_o (\Delta r_p - \Delta r_p_o) \rho + 2\pi R_c L_o \Delta r_p_o \epsilon \rho + 2\pi R_c L_o \Delta r_p_o (\epsilon_p - \epsilon_p_o) \rho_p) = -2\pi (R_c + \Delta r_p) L_o \rho \bar{v}_e|_{LCWP1} \quad (A7-1)$$

Dividing by $2\pi R_c L_o$ yields:

$$\frac{\partial}{\partial t} (\Delta c r_{si} + (\Delta r_p - \Delta r_p_o) \rho + \Delta r_p_o \epsilon \rho + \Delta r_p_o (\epsilon_p - \epsilon_p_o) \rho_p) = -\frac{R_c (LCWP1)}{R_c} \rho \bar{v}_e|_{LCWP1} \quad (A7-2)$$

But, Δr_p_o is the initial distance from the interface to the node point just inside the porous media which is constant; so

$$\rho_{si} \frac{\partial \Delta c r_{si}}{\partial t} + (\Delta r_p + \epsilon \Delta r_p_o - \Delta r_p_o) \rho \frac{\partial \Delta r_p}{\partial t} + \rho \frac{\partial \Delta r_p}{\partial t} + \Delta r_p_o (\rho_p \epsilon_p) \frac{\partial \epsilon}{\partial t} = -\frac{R_c (LCWP1)}{R_c} \rho \bar{v}_e|_{LCWP1} \quad (A7-3)$$

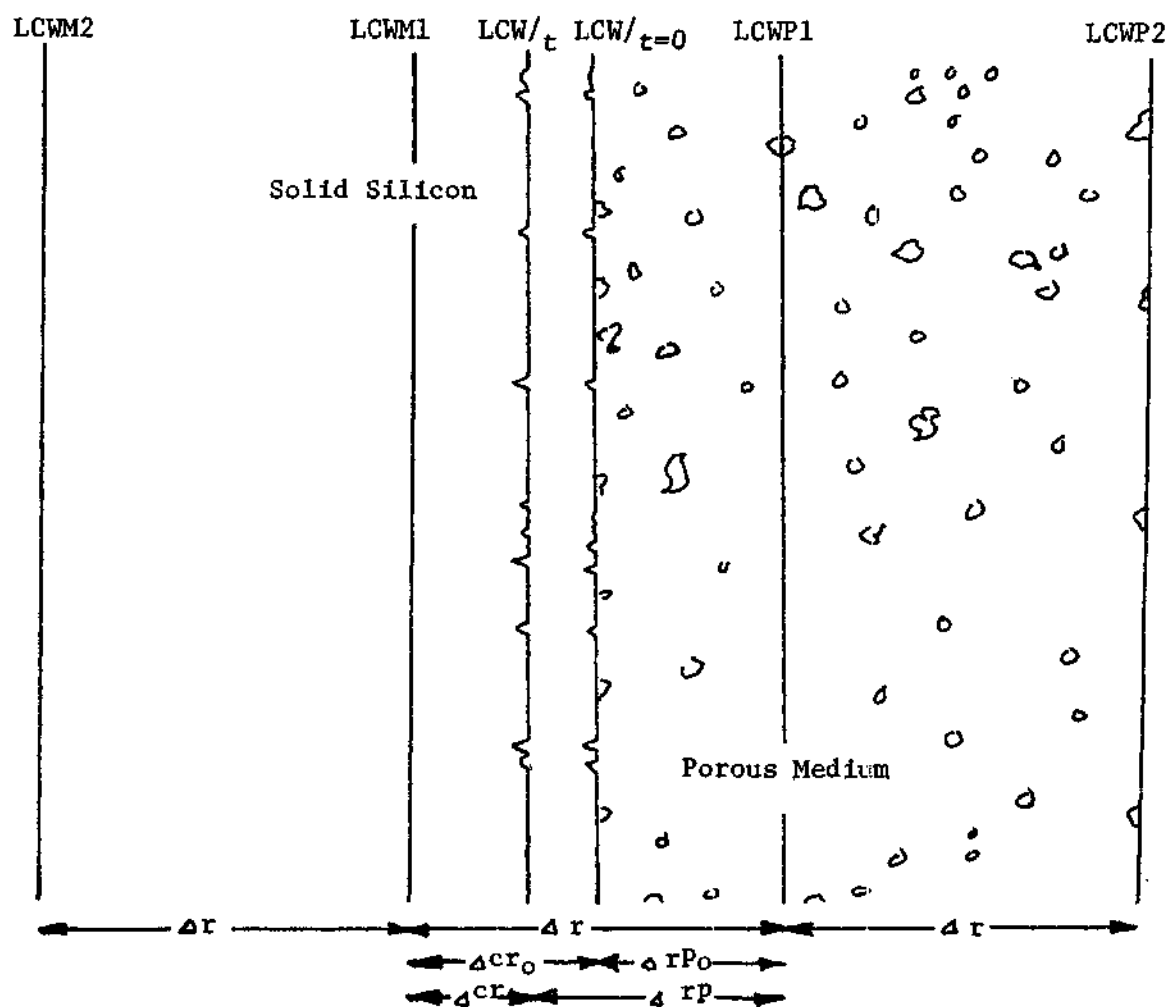


Figure 13. Schematic Representation of the Porous Media--Core Gap.

Expanding and combining terms yields:

$$\rho_{si} \frac{\partial \Delta cr}{\partial t} + (\Delta r p + \epsilon \Delta r p_0 - \Delta r p_0) \frac{\partial p}{\partial t} + \rho \frac{\partial \Delta r p}{\partial t} + \Delta r p_0 \rho_{si} \frac{\partial \epsilon p}{\partial t} = - \frac{R(LCWPI)}{R_c} \rho \bar{v}_e /_{LCWPI} \quad (A7-4)$$

But $\Delta cr = \Delta r - \Delta r p$ and Δr is constant so:

$$(\Delta r + \epsilon \Delta r p_0 - \Delta r p_0) \frac{\partial p}{\partial t} + (\rho - \rho_{si}) \frac{\partial \Delta r p}{\partial t} + (\rho - \rho_{si}) \Delta r p_0 \frac{\partial \epsilon}{\partial t} = - \frac{R(LCWPI)}{R_c} \rho \bar{v}_e /_{LCWPI} \quad (A7-5)$$

Combining terms and dividing by $\Delta r p$ gives the final form of the continuity equation used in this work.

$$\left(1 + \frac{\Delta r p_0}{\Delta r p} (\epsilon - 1)\right) \frac{\partial p}{\partial t} + \frac{\rho - \rho_{si}}{\Delta r p} \frac{\partial \Delta r p}{\partial t} + (\rho - \rho_{si}) \frac{\partial \epsilon}{\partial t} = - \frac{R(LCWPI)}{R_c \Delta r p} \rho \bar{v}_e /_{LCWPI} \quad (A7-6)$$

Results of a similar derivation for the other interface are:

$$\epsilon \frac{\partial p}{\partial t} + (\rho - \rho_{si}) \frac{\partial \epsilon}{\partial t} - (\epsilon p - \rho_{si} \frac{1 + \epsilon - \epsilon_0}{\Delta r p}) \frac{\partial \Delta r p}{\partial t} = \frac{R(LPWMI)}{R_p \Delta r p} \rho \bar{v}_e /_{LPWMI} \quad (A7-7)$$

The thickness of the partial grid between the core and the first node point in the porous medium will change due to depletion of the core.

The thickness of this partial grid is calculated from a mass balance on the species, silicon, in the original grid as follows:

$$\frac{\partial}{\partial t} (2\pi R_c L_0 \Delta r p_0 (\epsilon_p - \epsilon_p) \rho_{si} - 2\pi R_c L_0 (\Delta r p - \Delta r p_0) \rho_{si}) = 2\pi R_c L_0 \Delta r p r_{si} \quad (A-8)$$

The last term in equation A7-8 represents the net generation (or depletion) of silicon in the grid of thickness $\Delta r p$. The other term represents depletion in the porous material and the depletion of the core to form a gap. Dividing by $2\pi R_c L_0$ and expanding terms gives:

$$\Delta r p_0 \rho_{si} \frac{\partial \epsilon_p}{\partial t} - \rho_{si} \frac{\partial \Delta r p}{\partial t} = \Delta r p r_{si} \quad (A7-9)$$

But $\epsilon_p = 1 - \epsilon$ so equation A9-8 becomes:

$$-\Delta r p_0 \rho_{si} \frac{\partial \epsilon}{\partial t} - \rho_{si} \frac{\partial \Delta r p}{\partial t} = \Delta r p r_{si} \quad (A7-10)$$

Solving for $\frac{\partial \Delta r p}{\partial t}$ yields:

$$\frac{\partial \Delta r p}{\partial t} = - \frac{\Delta r p r_{si} + \rho_{si} \Delta r p_0 \frac{\partial \epsilon}{\partial t}}{\rho_{si}} \quad (A7-11)$$

A similar equation can be derived for the shell interface. The results are shown below:

$$\frac{\partial \Delta p_i}{\partial \lambda} = - \frac{\Delta p_i \gamma_{3i} + \rho_{3i} \Delta p_i \frac{\partial E}{\partial \lambda}}{\rho_{3i} (E - E_0 + 1)} \quad (A7-12)$$

APPENDIX VIII

CALCULATION OF INTERFACE MASS FRACTIONS

BOUNDARY CONDITIONS

In the solution to a differential equation, derivatives of the mass fluxes at the solid boundary must be zero. Also, a boundary has zero thickness so there is no storage term in the mass balance. For a finite difference approximation, a finite volume is used so a storage term and a flux term are needed. For the interface between the core and the porous medium, the following mass balance applies:

$$\frac{\partial}{\partial t}(2\pi R_c \Delta r p_o L_o w_{ie} + 2\pi R_c (\Delta r p - \Delta r p_o) L_o \rho w_i) + 2\pi R(L_{cw} p_i) L_o \bar{n}_i^e / L_{cw} p_i = 2\pi R_c L_o \Delta r p r_i \quad (A8-1)$$

where R_c is the radius of the interface
 $R(L_{cw} p_i)$ is the radius at $L_{cw} p_i$
 $L_{cw} p_i$ is one point beyond the interface
 $\Delta r p$ is the thickness of the interval between L_{cw} and $L_{cw} p_i$
 $\Delta r p_o$ is the initial value for $\Delta r p$.

Equation A8-1 can be expanded to give:

$$\Delta r p \frac{\partial}{\partial t}(\epsilon \rho w_i) + \epsilon \rho w_i \frac{\partial \Delta r p}{\partial t} + (\Delta r p - \Delta r p_o) \frac{\partial}{\partial t}(\rho w_i) + \rho w_i \frac{\partial \Delta r p}{\partial t} + \frac{R(L_{cw} p_i)}{R_c} \bar{n}_i^e / L_{cw} p_i = \Delta r p r_i \quad (A8-2)$$

In the algorithm for the problem at hand, $\omega_i(\text{LCW}, t)$ is calculated from a Taylor's series as follows:

$$\omega_i(\text{LCW}, t+\Delta t) = \omega_i(\text{LCW}, t) + \frac{\Delta t}{2} \left(\frac{\partial \omega_i}{\partial t} \Big|_t + \frac{\partial \omega_i}{\partial t} \Big|_{t+\Delta t} \right) \quad (\text{A8-3})$$

As with the calculation of the subsurface temperature (see Appendix VI), the fact that Δr_p can be very small, thus producing inaccurate derivatives, warrants the use of an implicit solution for $\omega_i(\text{LCW}, t+\Delta t)$. The derivative $\frac{\partial \omega_i}{\partial t} \Big|_{t+\Delta t}$ is obtained from equation A8-2 and is shown in the expanded form below:

$$\begin{aligned} \frac{\partial \omega_i}{\partial t} \Big|_{t+\Delta t} = & \left(\frac{\Delta r_p}{\Delta r_p} r_i \Big|_t - \omega_i(\text{LCW}, t+\Delta t) \left(E(\text{LCW}, t) + \frac{\Delta r_p}{\Delta r_p} - 1 \right) \frac{\partial p}{\partial t} \Big|_t \right. \\ & - \rho(\text{LCW}, t+\Delta t) \omega_i(\text{LCW}, t+\Delta t) \left(\frac{\partial E}{\partial t} \Big|_t + \frac{\partial \Delta r_p}{\partial t} \Big|_t / \Delta r_p \right) - \bar{n}_i^e(\text{LCW}, t) \\ & \left. \frac{R(\text{LCWPI})}{\Delta r_p R(\text{LCW})} \right) / \left(\rho(\text{LCW}, t+\Delta t) E(\text{LCW}, t+\Delta t) + \frac{\Delta r_p}{\Delta r_p} - 1 \right) \end{aligned} \quad (\text{A8-4})$$

Insertion of equation A8-4 into A8-3 and collecting terms yields the following equation for $\omega_i(\text{LCW}, t+\Delta t)$:

$$\begin{aligned} \omega_i(\text{LCW}, t+\Delta t) = & \left(\omega_i(\text{LCW}, t) + \frac{\Delta t}{2} \frac{\partial \omega_i}{\partial t} \Big|_t + \frac{\Delta t}{2} \left(\frac{\Delta r_p}{\Delta r_p} r_i \Big|_t \right. \right. \\ & + \frac{R(\text{LCWPI})}{R(\text{LCW})} \left(\rho(\text{LCWPI}, t+\Delta t) \bar{n}_i^e(\text{LCWPI}, t+\Delta t) / M_w(\text{LCWPI}, t+\Delta t) \right. \\ & \left. \left. \left((\chi_i(\text{LCWPI}, t+\Delta t) - \chi_i(\text{LCWPI}, t+\Delta t)) \frac{\Delta r_p}{\Delta r} + \frac{\Delta r}{\Delta r_p} \chi_i(\text{LCWPI}, t+\Delta t) \right) \right) \right. \end{aligned} \quad (\text{A8-5})$$

$$\begin{aligned}
 & 1/(\Delta r + \Delta r_p) + \chi_i(LCWPI, t+\Delta t) \bar{N}^e(LCWPI, t+\Delta t) M_i / \Delta r_p) / \\
 & (\rho(LCW, t+\Delta t) (E(LCW, t) + \frac{\Delta r_p}{\Delta r_p} - 1))) / (1 + \frac{\Delta t}{2} (\frac{R(LCWPI)}{R(LCW)} \\
 & \rho(LCW, t+\Delta t) \bar{M}_m^e(LCWPI, t+\Delta t) / M_w(LCWPI, t+\Delta t) (\frac{\Delta r}{\Delta r_p} / \\
 & (\Delta r + \Delta r_p)) M_w(LCW, t+\Delta t) / \Delta r_p + (E(LCW, t) + \frac{\Delta r_p}{\Delta r_p} - 1) \\
 & \frac{\partial \rho}{\partial t} / \rho + \rho(LCW, t+\Delta t) (\frac{\partial E}{\partial t} / E + \frac{\partial \Delta r_p}{\partial t} / \Delta r_p) / (\rho(LCW, t+\Delta t) \\
 & (E(LCW, t) + \frac{\Delta r_p}{\Delta r_p} - 1)))
 \end{aligned}
 \tag{A8-5}$$

Cont'd

A similar equation can be developed for the interface between the porous medium and the shell. The results are:

$$\begin{aligned}
 & w_i(LPWI, t+\Delta t) = (w_i(LPWI, t) + \frac{\Delta t}{2} \frac{\partial w_i}{\partial t} / \rho + \frac{\Delta t}{2} (r_i / \rho + \\
 & \frac{R(LPWI)}{R(LPWI)} \frac{M_i}{\Delta r_p} \rho(LPWI, t+\Delta t) \bar{M}_m^e(LPWI, t+\Delta t) / M_w(LPWI, t+\Delta t) \\
 & (\chi_i(LPWI, t+\Delta t) \frac{\Delta r}{\Delta r_p} + \chi_i(LPWI, t+\Delta t) - \chi_i(LPWI, t+\Delta t) \\
 & \frac{\Delta r}{\Delta r_p}) / (\Delta r + \Delta r_p) + \chi_i(LPWI, t+\Delta t) \bar{N}^e(LPWI, t+\Delta t))) / \\
 & (E(LPWI, t) \rho(LPWI, t+\Delta t))) / (1 + \frac{\Delta t}{2} (\frac{R(LPWI)}{R(LPWI)} \rho(LPWI, t+\Delta t) \\
 & \bar{M}_m^e(LPWI, t+\Delta t) / M_w(LPWI, t+\Delta t) (\frac{\Delta r}{\Delta r_p} / (\Delta r + \Delta r_p)) \\
 & M_w(LPWI, t+\Delta t) / \Delta r_p + \rho(LPWI, t+\Delta t) (\frac{\partial E}{\partial t} / E + E(LPWI, t) \\
 & \frac{\partial \Delta r_p}{\partial t} / \Delta r_p) + E(LPWI, t) \frac{\partial \rho}{\partial t} / \rho) / (E(LPWI, t) \rho(LPWI, t+\Delta t)))
 \end{aligned}
 \tag{A8-6}$$

APPENDIX IX

CALCULATION OF INTERFACE TEMPERATURE

BOUNDARY CONDITIONS

The calculation of the interface boundary condition is based on an energy balance over a portion of the porous section on one side of the interface. To improve the accuracy of the numerical solution, an implicit calculation of the interface temperature values is used. The method used to calculate $T(LW)$, the temperature of the interface between the core and the porous medium, is shown below. Results for a similar derivation are also given for $T(LPW)$, the temperature at the other interface. The derivation begins with the following energy balance:

$$\begin{aligned} \frac{\partial}{\partial t}(\epsilon_p \Delta r_p \hat{U}) + \frac{\partial}{\partial t}(\epsilon_p \rho_p \Delta r_p \hat{U}_p) + \frac{\partial}{\partial t}((\epsilon_p - \epsilon_p) \rho_c \Delta r_p \hat{U}_c) + \quad (A9-1) \\ \frac{\partial}{\partial t}((\Delta r_p - \Delta r_p) \rho \hat{U}) + \frac{\partial}{\partial t}(\rho_c \Delta r_c \hat{U}_c) = \frac{R(LWP)}{R(LW)} \sum_{i=1}^N \tilde{n}_i^e(LWP) \\ \hat{A}_i(LWP) + \left(\frac{R(LWP)}{R(LW)} \tilde{q}_{in} - \frac{R(LWP)}{R(LW)} \tilde{q}_{out} \right) \end{aligned}$$

The first term is the accumulation of internal energy of the gas phase in the partial increment next to the interface. The second term is the accumulation of internal energy of the porous substrate next to the interface. The third term represents the accumulation of internal energy on the core material deposited on the porous substrate. The fourth term is the change in internal energy of the gas in the gap between the core and porous

medium. The fifth term is the accumulation of internal energy of the core material near the interface. The remaining two terms represent the flux of energy due to diffusion and conduction. For the problem at hand, the density of the solids does not change in time and the internal energy of the solid can be represented in terms of \hat{c}_p so Equation A9-1 becomes:

$$\begin{aligned} & \frac{\partial}{\partial t}(\epsilon_p \Delta r_p \hat{U}) + \frac{\partial}{\partial t}(\rho(\Delta r_p - \Delta r_p_0) \hat{U}) + \epsilon_p \rho_p \Delta r_p_0 c_p \frac{\partial T}{\partial t} + \quad (A9-2) \\ & (\epsilon_p - \epsilon_p_0) \rho_c \Delta r_p_0 c_p \frac{\partial T}{\partial t} - \rho_c \Delta r_p_0 \hat{U}_c \frac{\partial \epsilon}{\partial t} + \Delta r_p \rho_c c_p \frac{\partial T}{\partial t} + \rho_c \hat{U}_c \frac{\partial \Delta r}{\partial t} \\ & = - \frac{R(LCWPI)}{R_c} \left(\sum_{i=1}^N \bar{n}_i^e(LCWPI) \hat{H}_i(LCWPI) \right) + \frac{R(LCWMI)}{R_c} \bar{q}_{in} - \frac{R(LCWPI)}{R_c} \bar{q}_{out} \end{aligned}$$

Substituting the definition for \hat{U} and expanding and combining terms gives:

$$\begin{aligned} & \Delta r_p \frac{\partial}{\partial t}(\epsilon_p \hat{H}) - \Delta r_p \frac{\partial}{\partial t}(\epsilon_p) + \epsilon_p \left(\hat{H} - \frac{P}{\rho} \right) \frac{\partial \Delta r_p}{\partial t} + (\Delta r_p - \Delta r_p_0) \frac{\partial}{\partial t}(\hat{H} \rho) \quad (A9-3) \\ & - (\Delta r_p - \Delta r_p_0) \frac{\partial \rho}{\partial t} + \rho \left(\hat{H} - \frac{P}{\rho} \right) \frac{\partial \Delta r_p}{\partial t} + (\epsilon_p \rho_p \Delta r_p_0 c_p + (\epsilon_p - \epsilon_p_0) \rho_c \Delta r_p_0 c_p + \\ & \rho_c \Delta r_p c_p) \frac{\partial T}{\partial t} - \rho_c \Delta r_p_0 \hat{U}_c \frac{\partial \epsilon}{\partial t} + \rho_c \hat{U}_c \frac{\partial \Delta r}{\partial t} + \rho \left(\hat{H} - \frac{P}{\rho} \right) \frac{\partial \Delta r_p}{\partial t} = - \frac{R(LCWPI)}{R_c} \sum_{i=1}^N \bar{n}_i^e(LCWPI) \\ & \hat{H}_i(LCWPI) + \frac{R(LCWMI)}{R_c} \bar{q}_{in} - \frac{R(LCWPI)}{R_c} \bar{q}_{out} \end{aligned}$$

Application of the definition of \hat{H} and expansion of terms gives:

$$\begin{aligned} & \Delta r_p \hat{H} \rho \frac{\partial \epsilon}{\partial t} + \Delta r_p \hat{H} \epsilon \frac{\partial \rho}{\partial t} - \Delta r_p \rho \epsilon \frac{\partial \rho}{\partial t} - \Delta r_p \rho \frac{\partial \epsilon}{\partial t} + \epsilon \rho \left(\hat{H} - \frac{P}{\rho} \right) \frac{\partial \Delta r_p}{\partial t} \quad (A9-4) \\ & + (\Delta r_p - \Delta r_p_0) \hat{H} \frac{\partial \rho}{\partial t} - (\Delta r_p - \Delta r_p_0) \rho \frac{\partial \hat{H}}{\partial t} + \rho \left(\hat{H} - \frac{P}{\rho} \right) \frac{\partial \Delta r_p}{\partial t} + (\epsilon_p \rho_p + (\Delta r_p - \Delta r_p_0) \rho_c) \rho \frac{\partial T}{\partial t} \end{aligned}$$

$$\begin{aligned}
 & + \epsilon_p \rho_0 \Delta r_0 c_p + (\epsilon_p - \epsilon_0) \rho_c \Delta r_0 c_p + \rho_c \Delta r c_p \left) \frac{\partial T}{\partial t} - \quad (A9-4) \\
 & \rho_c \Delta r_0 \left(\hat{H}_c - \frac{P}{\rho_c} \right) \frac{\partial \epsilon}{\partial t} + \rho_c \left(\hat{H}_c - \frac{P}{\rho_c} \right) \frac{\partial \Delta r}{\partial t} = - \frac{R(LCW)}{R_c} \sum_{i=1}^N \bar{n}_i^e(LCW) \hat{H}_i(LCW) \\
 & + \frac{R(LCW)}{R_c} \bar{q}_{in} - \frac{R(LCW)}{R_c} \bar{q}_{out}
 \end{aligned}$$

Assuming $\frac{\partial \Delta r}{\partial t}$ is $-\frac{\partial r}{\partial t}$ and combining terms based on derivatives yields:

$$\begin{aligned}
 & (\Delta r (\hat{H}_p - P) - \Delta r_0 (\hat{H}_c \rho_c - \frac{1}{0.3676})) \frac{\partial \epsilon}{\partial t} + \hat{H} (\Delta r (1.01\epsilon) - \Delta r) \quad (A9-5) \\
 & \frac{\partial P}{\partial t} + (\epsilon (\rho \hat{H} - P) + \hat{H}_p - P - \hat{H}_c \rho_c + \frac{1}{0.3676}) \frac{\partial \Delta r}{\partial t} = (\Delta r (1 + \epsilon) - \Delta r_0) \\
 & \frac{\partial P}{\partial t} + (\epsilon \rho c_p + \rho (\Delta r - \Delta r_0) c_p + \epsilon_p \rho_0 \Delta r_0 c_p + (\epsilon_p - \epsilon_0) \rho_c \Delta r_0 c_p) \\
 & \frac{\partial T}{\partial t} = \frac{R(LCW)}{R_c} \sum_{i=1}^N \bar{n}_i^e(LCW) \hat{H}_i(LCW) + \frac{R(LCW)}{R_c} \bar{q}_{in} - \frac{R(LCW)}{R_c} \bar{q}_{out}
 \end{aligned}$$

For a numerical solution, values for \bar{q} are defined as follows:

$$\bar{q}_{in} = -k(LCW) (T(LCW) - T(LCW_{in})) / \Delta r \quad (A9-6)$$

$$\bar{q}_{out} = -k(LCW) (T(LCW) - T(LCW_{out})) / \Delta r \quad (A9-7)$$

Further, if $T(LCW, t + \Delta t)$ is defined as:

$$T(LCW, t + \Delta t) = T(LCW, t) + \Delta t \left. \frac{\partial T}{\partial t} \right|_{t+\Delta t} \quad (A9-8)$$

then an implicit numerical solution for $T(LCW, t + \Delta t)$ can be found as follows:

$$\begin{aligned}
 T(LCW, t+\Delta t) = & (T(LCW, t) + \frac{\Delta t}{2} (- \frac{R(LCWPI)}{R_c} \sum_{i=1}^N \hat{H}_i^0(LCWPI, (A9-9) \\
 & t+\Delta t) \hat{H}_i(LCWPI, t+\Delta t) + \frac{R(LCWMI)}{R_c \Delta cr} k(LCW, t+\Delta t) T(LCWMI, t+\Delta t) \\
 & + \frac{R(LCWPI)}{R_c \Delta rp} k(LCWPI, t+\Delta t) T(LCWPI, t+\Delta t) - ARGETA \frac{\partial E}{\partial t} \\
 & - ARG RHO \frac{\partial p}{\partial t} - ARG DRP \frac{\partial \Delta rp}{\partial t} + ARG P \frac{\partial p}{\partial t}) / ERC) / \\
 & (1 + \frac{\Delta t}{2} (\frac{R(LCWMI)}{R_c \Delta cr} k(LCWMI) + \frac{R(LCWPI)}{R_c \Delta rp} k(LCWPI)) / ERC)
 \end{aligned}$$

where

$$\begin{aligned}
 ARGETA = & \Delta rp (\hat{H}(LCW, t+\Delta t) \rho(LCW, t+\Delta t) \\
 & - P(LCW, t) - \Delta rp_0 (\hat{H}_c(LCW, t+\Delta t) \rho_c(LCW, t+\Delta t) \\
 & - \frac{1}{0.3676})
 \end{aligned}$$

$$ARG RHO = \hat{H}(LCW, t+\Delta t) (\Delta rp + \epsilon(LCW, t) \Delta rp - \Delta rp_0)$$

$$\begin{aligned}
 ARG DP = & (p(LCW, t+\Delta t) \hat{H}(LCW, t+\Delta t) - P(LCW, t)) \\
 & (\epsilon(LCW, t) + 1) - \rho_c(LCWMI, t+\Delta t) \hat{H}_c(LCWMI, t+\Delta t) \\
 & + \frac{1}{0.3676}
 \end{aligned}$$

$$\begin{aligned}
 ERC = & \Delta rp \epsilon(LCW, t) \rho(LCW, t+\Delta t) c_p(LCW, t+\Delta t) \\
 & (\Delta rp - \Delta rp_0) + (1 - \epsilon_0) \rho_0 \Delta rp_0 c_{p_0}(LCW, t+\Delta t) + \\
 & (\epsilon_0 - \epsilon(LCW, t)) \rho_c(LCW, t+\Delta t) \Delta rp_0 c_{p_c}(LCW, t+\Delta t) \\
 & + \rho_c(LCWMI, t+\Delta t) c_{p_c}(LCWMI, t+\Delta t) \Delta cr.
 \end{aligned}$$

A similar equation can be derived for the interface between the porous medium and the shell. The results of that derivation are:

$$\begin{aligned}
 T(LPW, t+\Delta t) = & \left(T(LPW, t) + \frac{\Delta t}{2} \left(\frac{R(LPWMI)}{R_p} \sum_{i=1}^N \tilde{n}_i^c \right. \right. & (A9-9) \\
 & (LPWMI, t+\Delta t) \hat{H}_i(LPWMI, t+\Delta t) + \frac{R(LPWMI)}{R_p \Delta \rho_0} k(LPWMI, t+\Delta t) \\
 & T(LPWMI, t+\Delta t) + \frac{R(LPWMI)}{R_p \Delta \rho_0} k(LPWMI, t+\Delta t) T(LPWMI, t+\Delta t) - \\
 & ARGETA \frac{\partial E}{\partial t} - ARG RHO \frac{\partial \rho}{\partial t} - ARGPR \frac{\partial \Delta p}{\partial t} + ARG P \frac{\partial \rho}{\partial t} \Big) / ERC \Big) / \\
 & \left(1 + \frac{R(LPWMI)}{R_p \Delta \rho_0} k(LPWMI, t+\Delta t) + \frac{R(LPWMI)}{R_p \Delta \rho_0} \right) \frac{\Delta t}{2} / ERC \Big)
 \end{aligned}$$

where

$$\begin{aligned}
 ARGETA &= \Delta p_r (\hat{H}(LPW, t+\Delta t) \rho(LPW, t+\Delta t) \\
 &\quad - \frac{\rho(LPW, t)}{0.3676} - \Delta \rho_0 (\rho_c(LPW, t+\Delta t) \hat{H}_c(LPW, \\
 &\quad t+\Delta t) - \frac{1}{0.3676}) \\
 ARG RHO &= E(LPW, t) \hat{H}(LPW, t+\Delta t) \Delta p_r \\
 ARGPR &= E(LPW, t) (\rho(LPW, t+\Delta t) \hat{H}(LPW, \\
 &\quad t+\Delta t) - \frac{\rho(LPW, t)}{0.3676}) - (\rho_c(LPW, t+\Delta t) \hat{H}_c(LPW, \\
 &\quad t+\Delta t) - \frac{1}{0.3676}) \\
 ARG P &= E(LPW, t) \Delta p_r / 0.3676 \\
 ERC &= E(LPW, t) \rho(LPW, t+\Delta t) c_p(LPW, \\
 &\quad t+\Delta t) \Delta p_r + (1 - \epsilon_0) \rho_B(LPW) \Delta \rho_0 c_p(LPW,
 \end{aligned}$$

$$\begin{aligned}
& t + \Delta t) + \Delta r_{SD} \rho(LPW, t + \Delta t) c_p(LPW, \\
& t + \Delta t) + (E_0 - E(LPW, t)) \rho_c(LPW, t + \Delta t) \\
& \Delta p_{r0} + c_p(LPW, t + \Delta t) + (\Delta p_r - \Delta p_{r0}) \\
& c_p(LPW, t + \Delta t) \rho_c(LPW, t + \Delta t)
\end{aligned}$$

APPENDIX X

CALCULATION OF THE OVERALL DIFFUSIVITY
AND OVERALL THERMAL CONDUCTIVITY FOR THE
CORE INTERFACE

Because the interface between the core and the porous medium may recede as a result of depletion of the core material, a special calculation must be made for the diffusivity and the thermal conductivity in the interval just beyond the interface. These calculations are based on a model which treats the intervals as a composite material composed of the gap, formed by recession of the core, and the porous material. The geometry and nomenclature used for this derivation are shown in Figure 13 with Δr_p as the portion of the increment representing the gap and with Δr_p as the portion representing the porous medium. The derivation for the diffusivity will be shown first.

If the assumption can be made that for any instant, the molar flux relative to the molar-average velocity in the gap is equal to that in the porous medium just beyond the gap and is only slightly dependent on distance over that interval, an overall diffusivity can be calculated as follows:

$$-r \left(\frac{\rho}{M_w} \sum_{i=1}^n \frac{\partial x_i}{\partial r} \right) \bigg|_{R_c + \Delta r_p} = -r \left(\frac{\rho}{M_w} \sum_{i=1}^n \frac{\partial x_i}{\partial r} \right) \bigg|_{R_c + \Delta r_p} \quad (\text{A10-1})$$

Upon integration, the following equations result:

$$x_i / R_c + \Delta r p - \Delta r p_0 - x_i / R_c = \frac{-R_c \bar{J}_i^{*e} \ln \left(\frac{R_c + \Delta r p - \Delta r p_0}{R_c} \right)}{\frac{\rho}{M_w} \Delta r p / R_c + \Delta r p - \Delta r p_0} \quad (\text{A10-2a})$$

$$\text{and } x_i / R_c + \Delta r p - x_i / R_c + \Delta r p - \Delta r p_0 = \frac{-R_c \bar{J}_i^{*e} \ln \left(\frac{R_c + \Delta r p}{R_c + \Delta r p - \Delta r p_0} \right)}{\frac{\rho}{M_w} \Delta r p / R_c + \Delta r p} \quad (\text{A10-2b})$$

Adding equations A10-2a and A10-2b and rearranging terms yields:

$$x_i / R_c + \Delta r p - x_i / R_c = -R_c \bar{J}_i^{*e} \left(\frac{\ln \left(\frac{R_c + \Delta r p}{R_c + \Delta r p - \Delta r p_0} \right)}{\frac{\rho}{M_w} \Delta r p / R_c + \Delta r p} + \frac{\ln \left(\frac{R_c + \Delta r p - \Delta r p_0}{R_c} \right)}{\frac{\rho}{M_w} \Delta r p / R_c + \Delta r p - \Delta r p_0} \right) \quad (\text{A10-3})$$

This equation can be further rearranged to give:

$$\bar{J}_i^{*e} = -\frac{\rho}{M_w} \left(\frac{\ln \left(\frac{R_c + \Delta r p}{R_c + \Delta r p - \Delta r p_0} \right)}{\Delta r p / R_c + \Delta r p} + \frac{\ln \left(\frac{R_c + \Delta r p - \Delta r p_0}{R_c} \right)}{\Delta r p / R_c + \Delta r p - \Delta r p_0} \right)^{-1} \frac{x_i / R_c + \Delta r p - x_i / R_c}{R_c} \quad (\text{A10-4})$$

If equation A10-4 is multiplied and divided by the space increment for the interval under consideration, a derivative can be created. If the remaining terms are collected, an overall diffusivity results as shown by equation A10-5a and A10-5b.

$$\bar{J}_i^{*e} = -\frac{\rho}{M_w} \Delta r p \frac{\partial x_i}{\partial r} \quad (\text{A10-5a})$$

where

$$\bar{\omega}_m^e = \left(\frac{\ln\left(\frac{R_c + \Delta r p}{R_c + \Delta r p - \Delta r p_0}\right)}{\omega_m^e|_{R_c + \Delta r p}} + \frac{\ln\left(\frac{R_c + \Delta r p - \Delta r p_0}{R_c}\right)}{\omega_m^e|_{R_c + \Delta r p - \Delta r p_0}} \right) \frac{\Delta r p}{R_c} \quad (\text{A10-5b})$$

A similar logic can be used to derive an equation for the overall thermal conductivity for the composite formed from the gap and the porous medium in the interval just beyond the core interface. In this case, the heat flux in the gap is assumed to be independent of distance for the interval and the flux in the gap is assumed to equal that in the porous medium. This relation is represented as follows:

$$-r k_e \left| \frac{\partial T}{\partial r} \right|_{R_c + \Delta r p - \Delta r p_0} = -r k_e \left| \frac{\partial T}{\partial r} \right|_{R_c + \Delta r p} = R_c \bar{q} \quad (\text{A10-6})$$

Upon integration, the following equations result:

$$T|_{R_c + \Delta r p - \Delta r p_0} - T|_{R_c} = R_c \bar{q} \frac{\ln\left(\frac{R_c + \Delta r p - \Delta r p_0}{R_c}\right)}{k_e|_{R_c + \Delta r p - \Delta r p_0}} \quad (\text{A10-7a})$$

and

$$T|_{R_c + \Delta r p} - T|_{R_c + \Delta r p - \Delta r p_0} = R_c \bar{q} \frac{\ln\left(\frac{R_c + \Delta r p}{R_c + \Delta r p - \Delta r p_0}\right)}{k_e|_{R_c + \Delta r p}} \quad (\text{A10-7b})$$

Adding equation A10-7a and A10-7b yields:

$$\frac{T|_{R_c + \Delta r p} - T|_{R_c}}{\Delta r p} = -R_c \bar{q}_f \left(\frac{\ln\left(\frac{R_c + \Delta r p}{R_c + \Delta r p \cdot \Delta r p_0}\right)}{k_e|_{R_c + \Delta r p}} + \frac{\ln\left(\frac{R_c + \Delta r p \cdot \Delta r p_0}{R_c}\right)}{k_e|_{R_c + \Delta r p \cdot \Delta r p_0}} \right)^{-1} \quad (\text{A10-8})$$

Equation A10-8 can be represented as a derivative equation by multiplying and dividing by $\Delta r p$. The overall thermal conductivity is then obtained by collecting terms as follows:

$$\bar{q}_f = -\bar{k}_e \frac{\partial T}{\partial r} \quad (\text{A10-9a})$$

where

$$\bar{k}_e = \left(\frac{\ln\left(\frac{R_c + \Delta r p}{R_c + \Delta r p \cdot \Delta r p_0}\right)}{k_e|_{R_c + \Delta r p}} + \frac{\ln\left(\frac{R_c + \Delta r p \cdot \Delta r p_0}{R_c}\right)}{k_e|_{R_c + \Delta r p \cdot \Delta r p_0}} \right)^{-1} \frac{\Delta r p}{R_c} \quad (\text{A10-9b})$$

APPENDIX XI

COMPUTER PROGRAM

Nomenclature

Program MAIN

Subroutine DIFF

NOMENCLATURE FOR THE COMPUTER PROGRAM

Real Variables:

ALPHAC (I)	Thermal diffusivity for the core material
ALPHAS (I)	Thermal diffusivity for the shell material
ARG	Argument used in time loop limit definition
ARGETA	Argument used in energy equation for either interface
ARGLP	Argument used in space loop limit definition
ARGGP	Argument used in energy equation for either interface
ARGPR	Argument used in energy equation for core interface
ARGRHO	Argument used in energy equation for either interface
ARGRP	Argument used in energy equation for shell interface
ARGX2	Argument used to calculate y_2 from equilibrium expression
CAPX (II)	Dimensionless concentration variable used in the Arnold Solution
CCA	Argument used in initial value calculation for the Arnold Solution
CCB	Argument used in initial value calculation for the Arnold Solution
CB0	Interpolation variable used in center line temperature profile calculation
CBI	Same as above
CB2	Same as above
C1D1	Constant for diffusion collision integral calculation
C1D2	Same as above

CIV1	Constant for viscosity collision integral calculation
CLAMB	Argument used in initial value calculation for the Arnold Solution
COATTH	Coating thickness at the shell-porous medium interface
COAT1	Coating thickness at the shell-porous medium interface during iteration J
COLIND (II, JJ)	Collision integral for diffusivity
COLINV (II)	Collision integral for viscosity
CONTH	Constant used in pressure calculation equal to
COREDP	Thickness of core depleted
CORE1	Thickness of core depleted during iteration J
CP (I)	Mixture Heat capacity
CPC	Heat capacity of the core material
CPC1	Constant for core heat capacity calculation
CPC2	Same as above
CPC3	Same as above
CPG (II)	Heat capacity of gas species II
CPG1 (II)	Constant for gas species II heat capacity calculation
CPG2 (II)	Same as above
CPG3 (II)	Same as above
CPG4 (II)	Same as above
CPG5 (II)	Same as above
CPP (I)	Heat capacity of the porous substrate material
CPP1	Constant for porous material heat capacity calculation
CPP2	Same as above
CPP3	Same as above

CPP0	Initial value of CPP
CPS	Heat capacity of shell material
CPS1	Constant for shell material heat capacity calculation
CPS2	Same as above
CPS3	Same as above
CS0	Interpolation variable used in surface temperature profile calculation
CS1	Same as above
CS2	Same as above
C00	Interpolation variable for centerline and surface temperature profile calculation
C01	Same as above
C02	Same as above
C10	Same as above
C11	Same as above
C12	Same as above
C20	Same as above
C21	Same as above
C22	Same as above
DEGF	Point out variable for temperature
DELCR	Partial space increment between the last node in the core and the core radius
DELCRL	Old value of DELCR
DELCRO	Initial value of DELCR
DELK (I)	First derivative of K with respect to r
DELKC (I)	First derivative of KC with respect to r
DELKS (I)	First derivative of KS with respect to r
DELKDT	First derivative of the product $K(I)*DEL(T(I))$ with respect to r at either interface

DELN1E (I)	First derivative of the mass flux of species 1 with respect to r
DELN2E (I)	First derivative of the mass flux of species 2 with respect to r
DELN3E (I)	First derivative of the mass flux of species 3 with respect to r
DELP (I)	First derivative of the pressure with respect to r
DELPR	Partial space increment between the porous medium and the node just inside the porous medium
DELPRL	Old value of DELPR
DELPRO	Initial value of DELPR
DELR	Space increment
DELROV (I)	First derivative of the produce $\text{RHO}(I) \cdot V(I)$ with respect to r
DELRP	Partial space increment between the core radius and the node just inside the porous medium
DELRPL	Old value of DELRP
DELRPO	Initial value of DELRP
DELRS	Partial space increment between the porous medium radius and node just inside the shell
DELRSO	Initial value of DELRS
DELS	Space increment variable for the shell energy equation calculation equal to either DELR or DELSR
DELSR	Partial space increment between the last node in the shell and the shell radius
DELSUM (I)	First derivative of the sum of the product $\text{AG}(II) \cdot V \text{ FLUXJII}(I)$ with respect to r
DELT (I)	First derivative of $T(t)$ with respect to r
DELTAU	Time increment
DELVA	Space increment variable for the porous medium calculations equal to either DELR or DELPR

DELVAB	Same as above equal to either DELR or DELRP
DELW1 (I)	First derivative of W(1) with respect to r
DELW2 (I)	Same as above
DELW3 (I)	Same as above
DELX	Space increment variable for the shell energy equation calculation equal to either DELRS or DELR
DELX1 (I)	First derivative of X1(I) with respect to r
DELX2 (I)	First derivative of X2(I) with respect to r
DELX3 (I)	First derivative of X3(i) with respect to r
DG (II, JJ)	Binary diffusivity for the gas pair II, JJ
DIF (II, JJ)	Argument used in the multicomponent diffusivity calculation
DIFOPT	Diffusion model option indicator
DINDEX (I)	Index used to determine whether deposition should occur
DIST	Printout variable for radius
DIVN1E (I)	Divergence of N1E (I) with respect to r
DIVN2E (I)	Divergence of N2E (I) with respect to r
DIVN3E (I)	Divergence of N3E (I) with respect to r
DIVROV (I)	Divergence of the product RHO(I)*V(L)
DK (II)	Knudsen diffusivity for species II
DM (II,I)	Multicomponent effective diffusivity
DMOD1	Diffusion stability modulus for species 1
DMOD2	Diffusion stability modulus for species 2
DMOD3	Diffusion stability modulus for species 3
DPRDOT	Change in time of the partial increment DELPR
DRDS	Ratio of either DELR/DELS or DELX/DELS

DRLIM	Smallest value of the partial increment at the surface accepted equal to 0.01 DELR
DRPDOT	Change in time of the partial increment DELRP
DSDR	Ratio of either DELS/DELX or DELS/DELR
DTAU10	Variable used in surface and core temperature profile calculation
DTAU20	Variable used in surface and core temperature profile calculation
DTAU21	Variable used in surface and core temperature profile calculation
DTL1	Argument used in shell energy equation calculation
DTL2	Argument used in shell energy equation calculation
DUMM	Dummy variable equal to 1.0/3.0
DX	Sum of mole fractions for normalization
D1M (I)	Multicomponent diffusivity for species 1
D2M (I)	Multicomponent diffusivity for species 2
D3M (I)	Multicomponent diffusivity for species 3
E (II)	Lennard-Jones constant for gas species II
EOVERK(II, JJ)	Lennard-Jones constant for the gas species pair II, JJ
EPS (I)	Emissivity of porous particles
EQUIX (II)	Initial equilibrium concentration of gas species II at the core interface
ERC	Argument used in energy equation calculation for porous medium
ESP	Input value of EPS (I)
ETA (I)	Void fraction or porosity of the porous media
ETADOT (I)	First derivative of ETA (I) with respect to time
ETADTL (I)	Old value of ETADOT (I)
ETALAS (I)	Old value of ETA (I)

ETA0	Initial value of ETA (I)
F (I)	Function used to calculate P (I) equal to $ETA(I) * MW(I) * RAD(I) * WBARI / T(I)$
FACTK (I)	Argument used to calculate KE (I)
FLUX	Output variable for the heat flux at the shell interface
FLUXJ1 (I)	Mass flux of gas species 1
FLUXJ2 (I)	Mass flux of gas species 2
FLUXJ3 (I)	Mass flux of gas species 3
GEN1 (I)	Rate of production of species 1, H_2
GEN2 (I)	Rate of production of species 2, HCl
GEN3 (I)	Rate of production of species 3, $HSiCl_3$
GEN4 (I)	Rate of production of species 4, $Si()$
H (I)	Mixture enthalpy
HC (I)	Enthalpy of core material
HCO	Initial value of HC (I)
HEADG2	Input variable for heading
HEADG3	Input variable for heading
HEADG4	Input variable for heading
HEADG5	Input variable for heading
HEADG6	Input variable for heading
HEADG7	Input variable for heading
HG (II)	Enthalpy of gas species II
HGVAPO (I)	Heat of vaporization of gas species I at 298° K
HS (I)	Enthalpy of shell
HS0	Initial value of HS (I)
KAPPA (I)	Permeability of porous medium

K (I)	Thermal conductivity
KC (I)	Thermal conductivity of core material
KE (I)	Effective thermal conductivity of porous medium
KEQ (I)	Equilibrium constant
KEQ1	Constants used to calculate KEQ (I)
KEQ2	Constants used to calculate KEQ (I)
KG (II)	Thermal conductivity of gas species II
KLAS (I)	Old value of K (I)
KLCW	Thermal conductivity of the core at station LCW
KM (I)	Mixture thermal conductivity
KP (I)	Thermal conductivity of the porous material
KR (I)	Effective thermal conductivity of the porous material due to radiation
KRO (I)	Thermal conductivity due to radiation of the porous material used to calculate KR(I)
KS (I)	Thermal conductivity of the shell
KSLPW	Thermal conductivity of the shell at station LPW
LAPLT (I)	Second derivative of T (I) with respect to r
LOGKEQ	Natural logarithm of KEQ (I)
M (II)	Molecular weight of gas species II
MBAR (II)	Function of M (II) used to calculate D (II, JJ)
ME1	Atomic weight of element 1
ME2	Atomic weight of element 2
ME3	Atomic weight of element 3
MOFLX (II, I)	Molar flux of gas species I
MP	Molecular weight of porous material
MU (I)	Mixture viscosity of gas species II

MW (I)	Mixture molecular weight
MW0	Initial value of MW (I)
M1	Molecular weight of gas species 1
M2	Molecular weight of gas species 2
M3	Molecular weight of gas species 3
N1E (I)	Mass flux of gas species 1
N2E (I)	Mass flux of gas species 2
N3E (I)	Mass flux of gas species 3
N1ELAS (I)	Old value of N1E (I)
N2ELAS (I)	Old value of N2E (I)
N3ELAS (I)	Old value of N3E (I)
OUTD	Print out value of RAD (I)
OUTTIME	Print out value of TIME
OUTP	Print out value of P (I)
OUTVR	Print out value of V (I)
P (I)	Pressure
PDOT (I)	First derivative of P(T) with respect to t
PARTD	Porous material particle diameter
PHI (I)	Function of molecular weight and viscosity used in mixture property calculation
PI	Constant equal to 3.14159
PLAS (I)	Old value of P (I)
PORER	Porous material pore radius
P0	Initial value of P (I)
R	Universal gas constant
RAD (I)	Radius

RADC	Radius of the core
RADIUS	Radius of the shell
RADP	Radius of the porous material
RHO (I)	Mixture density
RHOC (I)	Density of the core
RHOC1 (I)	Constant used to calculate RHOC (I)
RHOC2	Constant used to calculate RHOC (I)
RHOC3	Constant used to calculate RHOC (I)
RHODOT (I)	Change in time of the mixture density
RHOLAS (I)	Old value of RHO (I)
RHOP (I)	Density of the porous material
RHOP0	Initial value of RHOP (I)
RHOS (I)	Density of the shell
RHOS1	Constant used to calculate RHOS (I)
RHOS2	Constant used to calculate RHOS (I)
RHOS3	Constant used to calculate RHOS (I)
RHOVW (I)	Product of RHO (I) and V (I) at the shell interface
RINC	Argument used in pressure calculation equal to either 2*DELR or DELR + DELRP
RZ (I)	Dimensionless space and time variable used in the Arnold Solution
SIG (II)	Lennard-Jones constant for gas species II
SIGSQ (II,JJ)	Mixture Lennard-Jones constant for the gas species pair II, JJ
SMDF	Argument used to calculate TOT MOF (I)
SUM	Argument used to calculate TDOT (I)
SUMDIF (I)	Argument used to calculate DM (II,JJ)

SUMGEL (I)	Old value of SUMGEN (I)
SUMGEN (I)	Sum used to determine if all coating has been removed
SUML3 (I)	Old value of SUM3 (I)
SUMXPH	Argument used to calculate mixture physical properties
SUM1 (I)	Argument used to calculate TDOT (I)
SUM2 (I)	Argument used to calculate TDOT (I)
SUM3 (I)	Argument used to calculate TDOT (I)
SUM4C	Argument used to calculate TDOT(I) in the core interface
SUM4S	Argument used to calculate TDOT(I) in the shell interface
SO	Specific surface of porous material
T (I)	Temperature
TAU	Time limit of computer run
TAU0	Value of time used in surface and centerline profile interpolation routine
TAU1	Value of time used in surface and centerline profile interpolation routine
TAU2	Value of time used in surface and centerline profile interpolation routine
TBASE	Base temperature for thermodynamic calculations equal to 70.0°F
TB (J)	Centerline temperature
TB0	Value of TB (I) used in centerline temperature interpolation routine
TB1	Value of TB (I) used in centerline temperature interpolation routine
TB2	Value of TB (I) used in centerline temperature interpolation routine
TCC1	Constant used to calculate KC (I)

TCC2	Constant used to calculate KC (I)
TCC3	Constant used to calculate KC (I)
TCP1	Constant used to calculate KP (I)
TCP2	Constant used to calculate KP (I)
TCP3	Constant used to calculate KP (I)
TCS1	Constant used to calculate KS (I)
TCS2	Constant used to calculate KS (I)
TCS3	Constant used to calculate KS (I)
TDOT (I)	Change in time of T (I)
TEST1 (I)	Ratio of DELX1 to value predicted by Stefan-Maxwell equation
TEST2 (I)	Ratio of DELX2 to value predicted by Stefan-Maxwell equation
TEST3 (I)	Ratio of DELX3 to value predicted by Stefan-Maxwell equation
TIME	Cumulative value of time since calculation began
TIME 2	Value of time used in surface and centerline temperature equation
TINIT	Initial value for the temperature profile
TLAS (I)	Old value of T (I)
TMOD (I)	Temperature stability modulus
TOPT	Input data printout option
TOTMOF (I)	Total mole flux
TR	Reduced temperature used to calculate DG(II,JJ)
TSURF	Surface temperature
TSO	Value of TSURF used in surface temperature interpolation routine
TSI	Value of TSURF used in surface temperature interpolation routine

TS2	Value of TSURF used in surface temperature interpolation routine
V (I)	Velocity
VLAS (I)	Old value of V (I)
VRGRDT	Product of V(I)*
W	Sum of mass fractions
W1 (I)	Mass fraction of species 1
W2 (I)	Mass fraction of species 2
W3 (I)	Mass fraction of species 3
W1INIT	Initial value of W1 (I)
W2INIT	Initial value of W2 (I)
W3INIT	Initial value of W3 (I)
W1LAS (I)	Old value of W1 (I)
W2LAS (I)	Old value of W2 (I)
W3LAS (I)	Old value of W3 (I)
W1DOT (I)	First derivative of W1 with respect to t
W2DOT (I)	First derivative of W2 with respect to t
W3DOT (I)	First derivative of W3 with respect to t
WBAR1	Elemental mass fraction of gas species 1
W3DT	Old value of W3DOT(I)
X(II,I)	Mole fraction of gas species II
XCPG	Argument used to calculate GP
XHG	Argument used to calculate H
XINIT (II,I)	Initial value of X(II,I)
XK	Argument used to calculate KM (I)
XLAMB	Argument used to calculate initial values for Arnold Solution

XLAS (II,I)	Old value of X(II,I)
XMU	Argument used to calculate MU (I)
XPHI	Argument used to calculate PHI (I)
Integers:	
I	Integer used to indicate position
ICT1	Integer used to determine if reaction has occurred
II	Integer used to indicate species
IMINUS	I-1
IPLUS	I+1
IPR	Integer used to indicate station next to shell interface inside the porous medium
IRP	Integer used to indicate station next to core interface inside the porous medium
I1	I+1
I2	I+2
J	Integer used to indicate time
JJ	Integer used to indicate species
JJEND	Integer used to indicate end of run
JJJ	Integer used to indicate time
JPLUS	J+1
JPRINT	Integer used in print routine
KK	Integer used to indicate species
KKK	Integer used to indicate species
LC	Integer used to indicate station next to core inside the core
LCPLUS	LC + 1
LCW	Integer used to indicate the core interface
LCUM1	LCW - 1

LCWM2	$LCW - 2$
LCWP1	$LCW + 1$
LCWP2	$LCW + 2$
LMINUS	$LS - 1$
LP	Integer used to indicate the station next to the shell interface inside the porous medium
LPW	Integer used to indicate the shell interface
LPWM1	$LPW - 1$
LPWM2	$LPW - 2$
LPWP1	$LPW + 1$
LPWP2	$LPW + 2$
LS	Integer used to indicate the surface
N	Integer used to indicate time
NPRINT	Integer used to indicate time in the print routine
NR	$LPW + 1$
NRE	$LS - 1$
NT	Integer used to indicate the number of input temperature profile data points.

PROGRAM MAIN

```

PROGRAM MAIN(DATA,OUTPUT,TAPES=DATA,TAPES=OUTPUT)
COMMON I,KKK,J,LCH,LP,DIFORT
COMMON TOTMOF(50),RHOP(50)
COMMON MPAF(10,10),PLAS(50),SIGSO(10,10),M(10),MM(50)
COMMON RHO(50),MOFLY(10,50),DOVERK(10,10),TLAS(50)
COMMON XLAS(10,50),DM(10,50),DIM(50),DEM(50),DEM(50),STALAS(50)
COMMON OK(10,50),OG(10,10),COLIND(10,10),DIF(10,10),SUMDIF(10,50)
COMMON MP,POPER,CID1,CID2,CILT(50),RAD(50)
COMMON DELRP,DELPR0,DELPR,CLPR0
DIMENSION WILAS(50),W2LAS(50),W3LAS(50),W1(50),W2(50),W3(50)
DIMENSION COLINV(10),MUG(10),MU(50)
DIMENSION CPG(10),CPG1(10),CPG2(10),CPG3(10),CP(50)
DIMENSION CPC(50),CPP(50),CPS(50),HS(10),H(50)
DIMENSION KG(10),K(50),KP(50),KS(50),KC(50),ALPHAC(50),ALPHAS(50)
DIMENSION T(50),VLAS(50),V(50)
DIMENSION LAPLT(50),TDOT(50),DELKC(50),DELK(50)
DIMENSION DELP(50),P(50),ETA(50),KM(50),RHOC(50)
DIMENSION W1DOT(50),W2DOT(50),W3DOT(50),RHODOT(50)
DIMENSION VSGPT(50),HGVAP0(10),HC(50),HS(50)
DIMENSION LOGKEQ(50),KEQ(50),PLVROV(50)
DIMENSION PHI(10,10),XPHI(10)
DIMENSION DELW1(50),DELW2(50),DELW3(50)
DIMENSION CPG4(10),CPG5(10),EPS(50),KP(50)
DIMENSION KPO(50),FACTK(50),KE(50),DELK5(50)
DIMENSION DELX1(50),DELX2(50),DELX3(50)
DIMENSION N1E(50),N2E(50),N3E(50),N1ELAS(50),N2ELAS(50),N3ELAS(50)
DIMENSION DELN1E(50),DELN2E(50),DELN3E(50)
DIMENSION FLUXJ1(50),FLUXJ2(50),FLUXJ3(50)
DIMENSION DELRCV(50),ETADOT(50),SUMGEN(50),SUMGEL(50),TOT1(50)
DIMENSION GEN1(50),GEN2(50),GEN3(50),GEN4(50)
DIMENSION SUM1(50),SUM2(50),SIG(10),E(10),KAPPA(50)
DIMENSION SUM3(50),KLAS(50),TEST1(50),TEST2(50),TEST3(50)
DIMENSION SUML7(50),X(10,50),DELSUM(50)
DIMENSION STADTL(50),DINDEX(50),F(50),RHOLAS(50),RHOS(50)
DIMENSION DIVN1E(50),DIVN2E(50),DIVN3E(50)
DIMENSION CMCO1(50),CMCO2(50),CMCO3(50),TMC0(50)
DIMENSION EQUIX(10),RZ(10,50),XINIT(10),CAPX(10,50)

```

C

```

REAL LAPLT,M,KLAS,KEQ,KM,MUG,MU
REAL K,KS,KC,KP,KPO,KE,KEQ2,KEQ3,LOGKEQ,M1,M2,M3
REAL N1E,N2E,N3E,N1ELAS,N2ELAS,N3ELAS,MOFLX
REAL MPAP,MH,KE,KG,KAPPA,KLCH,KSLPW
REAL ME,ME1,ME2,ME3,MW0

```

C

```

DATA R/1.997/,V(1)/0.0/,VSGDOT(1)/0.0/,PI/3.14159/,TRASE/70.0/

```

C

C

```

INPUT FORMATS

```

C

```

2 FORMAT(12A6)
11 FORMAT(2F10.1)

```

C

C

```

OUTPUT FORMATS

```

C

```

51 FORMAT(1H1)
52 FORMAT(12A6)
53 FORMAT(/,17X,10HINPUT DATA,/,
1 9X,22HINITIAL TEMPERATURE = ,F6.1,6H DEG F,/,

```



```

2 9X,224TOTAL RADIUS      = ,F6.3,34 IN./,
3 9X,224CORE RADIUS       = ,F6.3,34 IN./,
4 9X,224P.MEDIA RADIUS    = ,F6.3,34 IN./,
5 9X,224CORE RADIUS       = ,F6.1,44 ANG./,
6 9X,224PARTICLE DIAM.    = ,F6.3,44 MIC./,
7 9X,224PERMISSIVITY      = ,F6.3,./,
8 9X,224DELTA-R SPACING   = ,F6.3,34 IN./,
9 9X,224TIME LIMIT        = ,F6.1,44 SEC./,
1 9X,224TIME INCREMENT    = ,F6.3,44 SEC./,
2 9X,224INTERPOLATION POINTS = ,I3,./,
3 9X,224PINT.FACTOR       = ,J5,./,
4 9X,224INITIAL POROSITY   = ,F6.3,./,
5 9X,224SPECIES           = ,I3),
55 FORMAT(/,9X,354HEAT CAPACITY EQUATION COEFFICIENTS./,
1 11X,74HCP1 = ,1PE10.3,2X,74HCP2 = ,E10.3,2X,74HCP3 = ,E10.3,./,
2 11X,74HCP1 = ,E10.3,2X,74HCP2 = ,E10.3,2X,74HCP3 = ,E10.3,./,
3 11X,74HCP1 = ,E10.3,2X,74HCP2 = ,E10.3,2X,74HCP3 = ,E10.3,./,
4 15X,34HCP1,8X,34HCP2,8X,34HCP3,8X,34HCP4,8X,34HCP5,./,
5 6X,6HH2 ,E10.3,1X,E10.3,1X,E10.3,1X,E10.3,1X,E10.3,./,
6 6X,6HHCL ,E10.3,1X,E10.3,1X,E10.3,1X,E10.3,1X,E10.3,./,
7 6X,6HSHCL3,E10.3,1X,E10.3,1X,E10.3,1X,E10.3,1X,E10.3,./,
55 FORMAT(/,9X,424THERMAL CONDUCTIVITY EQUATION COEFFICIENTS./,
1 11X,74HCC1 = ,1PE10.3,2X,74HCC2 = ,E10.3,2X,74HCC3 = ,E10.3,./,
2 11X,74HCC1 = ,E10.3,2X,74HCC2 = ,E10.3,2X,74HCC3 = ,E10.3,./,
3 11X,74HCC1 = ,E10.3,2X,74HCC2 = ,E10.3,2X,74HCC3 = ,E10.3,./,
55 FORMAT(/,9X,374KINETIC THEORY COEFFICIENTS./,
1 15X,34E/K,15X,6HSIGMA,./,
2 6X,6HH2 ,F10.4,64 DEG K,1X,F6.2,44 ANG./,
3 6X,6HHCL ,F10.4,64 DEG K,1X,F6.2,44 ANG./,
4 6X,6HSHCL3,F10.4,64 DEG K,1X,F6.2,44 ANG./,
59 FORMAT(/,11H END OF RUN./,141)
62 FORMAT(14H,234TIME = ,F6.3,44 SEC./,
1 20H PRESSURE = ,1PE10.3,44 ATM./,
2 20H HEAT FLUX = ,E10.3,11H BTU/FT2/HR./,
3 20H DEPOSITION RATE = ,E10.3,10H LB/HR/FT2./,
4 20H COATING DEPOSITED = ,E10.3,15H MILS./,
5 20H DEPOSITION THIS ITERATION = ,F10.3,11H MILS*1.0E6./,
6 20H CORE DEPLETED = ,E10.3,15H MILS./,
7 20H DEPLETION THIS ITERATION = ,E10.3,11H MILS*1.0E6./,
62 FORMAT(/,9X,174MOLECULAR WEIGHTS./,
1 6X,6HH2 ,F6.1,94 LB/MOLE./,
2 6X,6HHCL ,F6.1,94 LB/MOLE./,
3 6X,6HSHCL3,F6.1,94 LB/MOLE./,
4 6X,6HAL2O3 ,F6.1,94 LB/MOLE./,
64 FORMAT(/,9X,214ELEMENT ATOMIC WEIGHT./,
1 6X,6HH ,F6.1,94 LB/MOLE./,
2 6X,6HCL ,F6.1,94 LB/MOLE./,
3 6X,6HSI ,F6.1,94 LB/MOLE./,
65 FORMAT(/,9X,344INITIAL SPECIES MASS CONCENTRATION./,
1 6X,6HH2 ,F7.5,./,
2 6X,6HHCL ,F7.5,./,
3 6X,6HSHCL3,F7.5,./,
66 FORMAT(/,9X,344INITIAL SPECIES MOLE CONCENTRATION./,
1 6X,6HH2 ,F7.5,./,
2 6X,6HHCL ,F7.5,./,
3 6X,6HSHCL3 ,F7.5,./,
73 FORMAT(/,9X,214DENSITY COEFFICIENTS./,

```

```

1 9X,29HPRASEENTHALPY SOLID.//.
2 9X,16HINITIAL POROSITY.//.
3 6X,8HHCOC1 = .1PE10.3,9H LR/CHFT.//.
4 6X,8HHCOC2 = .E10.3,9H LR/CHFT.//.
5 6X,8HHCOC3 = .E10.3,9H LR/CHFT.//.
6 6X,8HHCOS1 = .E10.3,9H LR/CHFT.//.
7 6X,8HHCOS2 = .E10.3,9H LR/CHFT.//.
8 6X,8HHCOS3 = .E10.3,9H LR/CHFT.//.
9 6X,8HHCOP0 = .E10.3,9H LR/CHFT.//.
1 6X,8HHCOC = .0PE10.4,7H DTU/LR.//.
2 6X,8HHCOS = .F10.4,7H DTU/LR.//.
3 6X,8HHCASE = .1PE10.3,6H DEG.F).
71 FORMAT(//,3X,7HSTATION,5X,5HCAFX1,9X,3HRZ1,11X,5HCAPX2,9X,
1 7HPZ2,11X,5HCAPX3,9X,3HRZ3.//)
72 FORMAT(3X,I3,6X,E10.3,4X,E10.3,4X,E10.3,
1 4X,E10.3,4X,E10.3,4X,E10.3)
A0 FORMAT(//,3X,7HSTATION,3X,6HRAIUS,5X,11HTEMPERATURE,7X,1HK,
1 10X,3HHP0,10X,2HCP,10X,1HV,11X,3HSTA,9X,4HDELP.//.
2 14X,4H(IN),2X,7H(CEG.F),3X,11H(3TU/FT/HR),
3 2X,9H(LR/CHFT),4X,10H(DTU/LR/F),2X,9H(FT/SEC),16X,9H(AT4/FT))
A1 FORMAT(3X,I3,6X,F7.4,5X,F11.5,3X,1PE10.3,0FF10.4,5X,F7.4,4X,
1 1PE10.2,4X,E0.2,4X,0PE7.4)
A2 FORMAT(3X,I3,6X,F7.4,5X,F11.5,3X,1PE10.3,0FF10.4,2X,E10.4)
A5 FORMAT(3X,I3,6X,1PE10.3,4X,E10.3,4X,E10.3,4X,E10.3,4X,E10.3,4X,E10.3,4X,
1 E10.3,4X,E10.3,4X,E10.3)
A7 FORMAT(//,9X,8HCELP0 = .F10.5.//.
1 9X,8HCELP1 = .F10.5.//.
2 9X,8HCELP2 = .F10.5.//.
3 9X,8HCELP3 = .F10.5.//)
A8 FORMAT(11H,1,3X,7HSTATION,6X,3H01M,11X,3H02M,11X,3H03M,7X,
1 6HMOFLX1,3X,6HMOFLX2,9X,6HMOFLX3,9X,6H0TMOF,AX,4HGF0F,//.
2 13X,9H(SOFT/H0),5X,9H(SOFT/H0),6X,9H(SOFT/H0),
3 1X,13H(MOLE/FT2/HR),1X,13H(MOLE/FT2/HR),1X,
4 13H(MOLE/FT2/HR),1X,13H(MOLE/FT2/HR),1X,11H(LR/H0/FT))
A9 FORMAT(//,3X,7HSTATION,AX,24X1,11X,2HX2,11X,2HX3,9X,
1 5HTEST1,6X,5HTEST2,6X,5HTEST3,7X,3HKE0,6X,6HINDEX,//)
92 FORMAT(//,3X,30HWARNING TEMPERATURE MODULUS = .1PE10.3,
1 13H AT ITERATION,6PI5,12H AND STATION,13)
93 FORMAT(//,9X,15HAPARTIAL GRID SPACES AND NODE POINTS.//.
1 6X,5HLC = .I3,2X,5HLP = .I3,2X,5HLS = .I3,2X,
2 5HLCW = .I3,2X,5HLPW = .I3.//)
94 FORMAT(//,9X,24HKINETIC INSOPY CONSTANTS.//.
1 6X,6HCIC1 .F7.4.//,6X,6HCIC2 .F7.4.//.
2 6X,6HCIC3 .F7.4.//,6X,6HCIC4 .F7.4.//)
95 FORMAT(//,9X,7HNEQUILIBRIUM CONSTANT PARAMETERS.//.
1 6X,6HKE01 .E15.5.//,6X,6HKE02 .E15.5,6H(CEG.K)
96 FORMAT(//,3X,24HWARNING DIFFUSION MODULUS = .1PE10.3,
1 12H AT ITERATION,6PI5,12H AND STATION,13)
97 FORMAT(3X,I3,6X,F12.10,1X,F12.10,1X,F12.10,1X,1PE10.3,
1 1X,E10.3,1X,E10.3,1X,E10.3,1X,E10.3)
99 FORMAT(//,9X,40HBINARY DIFFUSIVITIES ARE ALLOWED TO VARY)
99 FORMAT(//,9X,44HALL BINARY DIFFUSIVITIES ARE EQUAL TO D(1,2))
101 FORMAT(//,9X,44HALL BINARY DIFFUSIVITIES ARE EQUAL TO D(1,2).//.
1 9X,29H(THERE IS NO KNUDSEN DIFFUSION)

```

```

C***** ELEMENT 1 *****
C
100 WRITE(6,51)
C
C READ NUMBER OF INPUT POINTS, PRINT FACTOR, NUMBER OF SPECIES
C PRINT OPTION AND DIFFUSIVITY OPTION
C
110 READ(5,*)INT,NPRINT,KKK,TOPT,DIFOPT
C
C CHECK FOR END OF RUN
C
120 IF(INT.LE.0)GO TO 2000
C
C READ AND WRITE OTHER INPUT DATA
C
READ(5,2)HEACNG,HEADG2,HEADG3,HEADG4,HEADG5,HEADG6,HEADG7
WRITE(6,52)HEACNG,HEADG2,HEADG3,HEADG4,HEADG5,HEADG6,HEADG7
IF(DIFOPT=1)125,126,127
125 WRITE(6,99)
GO TO 123
126 WRITE(6,101)
GO TO 123
127 WRITE(6,99)
128 CONTINUE
READ(5,*)PORFR,PARTD,ESP
READ(5,*)RADIUS,DELTA,TINIT,TAU,DELTAU,PADC,PADP
DO 130 KK=1,KKK
READ(5,*)CPG1(KK),CPG2(KK),CPG3(KK),CPG4(KK),CPG5(KK)
READ(5,*)HGVAFD(KK),E(KK),SIG(KK)
130 CONTINUE
READ(5,*)TCC1,TCC2,TCC3,CPC1,CPC2,CPC3
READ(5,*)TCP1,TCP2,TCP3,CPP1,CPP2,CPP3
READ(5,*)TCS1,TCS2,TCS3,CPS1,CPS2,CPS3
READ(5,*)ETA0,W1INIT,W2INIT,W3INIT
WRITE(6,53)TINIT,RADIUS,PADC,PADP,PORFR,PARTD,ESP,
1 CELR,TAU,DELTAU,INT,NPRINT,ETA0,KKK
WRITE(6,65)W1INIT,W2INIT,W3INIT
READ(5,*)M1,M2,M3,ME1,ME2,ME3,MP
READ(5,*)RHOC1,RHOC2,RHOC3,RHOS1,RHOS2,RHOS3,RHOP0,HCO,HSO
READ(5,*)KEQ1,KEQ2
READ(5,*)CID1,CID2,CIV1,CIV2
C FOR COMPLETE INPUT PRINTOUT, TOPT MUST EQUAL 1
IF(TOPT=0)140,140,141
141 CONTINUE
WRITE(6,94)CID1,CID2,CIV1,CIV2
WRITE(6,95)KEQ1,KEQ2
WRITE(6,70)RHOC1,RHOC2,RHOC3,RHOS1,RHOS2,RHOS3,RHOP0,HCO,HSO,TBASE
WRITE(6,63)M1,M2,M3,MP
WRITE(6,64)ME1,ME2,ME3
WRITE(6,55)TCC1,TCC2,TCC3,TCP1,TCP2,TCP3,TCS1,TCS2,TCS3
WRITE(6,56)E(1),SIG(1),E(2),SIG(2),E(3),SIG(3)
WRITE(6,54)CPC1,CPC2,CPC3,CPP1,CPP2,CPP3,CPS1,CPS2,CPS3,
1 CPG1(1),CPG2(1),CPG3(1),CPG4(1),CPG5(1),
2 CPG1(2),CPG2(2),CPG3(2),CPG4(2),CPG5(2),
3 CPG1(3),CPG2(3),CPG3(3),CPG4(3),CPG5(3)
140 CONTINUE
C

```

```

C      READ TIME AND SURFACE TEMPERATURES FOR FIRST INTERVAL
C
      READ(5,11) TAU0,TS0
      READ(5,11) TAU1,TS1
      READ(5,11) TAU2,TS2
C
C      CONVERT TIME UNITS FROM SECONDS TO HOURS
C
      TAL=TAU/3600.0
      DELTAU=DELTAU/3600.0
      TAU0=TAU0/3600.0
      TAU1=TAU1/3600.0
      TAU2=TAU2/3600.0
C
C      CONVERT DISTANCE UNITS FROM INCHES TO FEET
C
      RADIUS=RADIUS/12.0
      RADCC=RADCC/12.0
      RADP=RADP/12.0
      DELR=DELR/12.0
C
C      CONVERT TEMPERATURE UNITS FROM FAHRENHEIT TO RANKINE
C
      TBASE=TBASE+459.6
      TINIT=TINIT+459.6
      TS0=TS0+459.6
      TS1=TS1+459.6
      TS2=TS2+459.6
C
C      COMPUTE LIMIT OF RADIUS AND TOTAL NUMBER OF DISTANCE STATIONS
C
      DPLIM=0.01*DELR
      LS=IFIX(RADIUS/DELR)
      DELSR=RADIUS-FLOAT(LS)*DELR
200 IF (DELSR-DPLIM) 210,210,220
210 DELSR=DELSR+DELR
      LS=LS+1
      GO TO 230
220 LS=LS+2
230 LS=LS+2
      LMI+US=LS-1
      LC=IFIX(RADCC/DELR)
      DELCR=RADCC-FLOAT(LC)*DELR
      DELCR0=DELCR
      LC=LC+1
      ANGLE=(DELCR+RADP-RADCC)
      LP=IFIX(ANGLE/DELR)+LC
      DELER=RADP-FLOAT(LP)*DELR+DELCR
      DELPR0=DELER
      DELPR=DELF-DELER
      DELRP0=DELRP
      DELPS=DELP-DELER
      DELRS0=DELPS
      LP=LP+1
      LPH=LP+1
      LCW=LC+1
      WRITE(6,93) LC,LP,LS,LCW,LPH

```

```

RAD(I)=0.0
DO 231 I=2,LC
  IMINUS=I-1
  RAD(I)=RAD(IMINUS)+DELPR
231 CONTINUE
  RAD(LCH)=RADC
  NR=LCW+1
  DO 232 I=NR,LD
    RAD(I)=RAD(LC)+FLOAT(I-LCH)*DELR
232 CONTINUE
    RAD(LFW)=RADF
    NR=LCW+1
    NRE=LS-1
    DO 233 I=NR,NRE
      RAD(I)=RAD(LF)+FLOAT(I-LFW)*DELR
233 CONTINUE
      RAD(LS)=RADIUS
      DO 300 I=1,LS
        TLAS(I)=TINIT
        RHODCT(I)=0.0
        IF (I-LC) 250,250,260
250 KLAS(I)=TCC1+TCC2/TLAS(I)+TCC3*TLAS(I)
        GO TO 300
260 IF (I-LF) 270,270,280
270 KLAS(I)=TCP1+TCP2/TLAS(I)+TCP3*TLAS(I)
        GO TO 300
280 KLAS(I)=TCS1+TCS2/TLAS(I)+TCS3*TLAS(I)
300 CONTINUE
    KSLFW=KLAS(LFW)

C
C   CALCULATE MOLE FRACTIONS
C
  MW0=1.0/(W1INIT/M1+W2INIT/M2+W3INIT/M3)
  XINIT(1)=W1INIT*MW0/M1
  XINIT(2)=W2INIT*MW0/M2
  XINIT(3)=W3INIT*MW0/M3
  OX=XINIT(1)+XINIT(2)+XINIT(3)
  XINIT(1)=XINIT(1)/OX
  XINIT(2)=XINIT(2)/OX
  XINIT(3)=XINIT(3)/OX
  WRITE(6,66)XINIT(1),XINIT(2),XINIT(3)

C
C   INITIALIZE VARIABLES
C
  DELPRL=DELP20
  DELEFL=DELF20
  DELCRL=DELC20
  DPFCOT=0.0
  DPFCCT=0.0
  PDOT=0.0
  DO 305 I=LCW,LCW
    ETALAS(I)=ETA0
    VLAS(I)=0.0
    W1LAS(I)=W1INIT
    W2LAS(I)=W2INIT
    W3LAS(I)=W3INIT
    MW(I)=MW0

```

```

PLAS(I)=1.0
XLAS(1,I)=XINIT(1)
XLAS(2,I)=XINIT(2)
XLAS(3,I)=XINIT(3)
SUML3(I)=0.0
P=0.7302
PHOLAS(I)=PLAS(I)*MW(I)/(R*TLAS(I))
M1ELAS(I)=0.0
M2ELAS(I)=0.0
M3ELAS(I)=0.0
TOTMOF(I)=0.0
MOFLX(1,I)=0.0
MOFLX(2,I)=0.0
MOFLX(3,I)=0.0
GEN1(I)=0.0
GEN2(I)=0.0
GEN3(I)=0.0
GEN4(I)=0.0
ETAOTL(I)=0.0
RHODOT(I)=0.0
SUMGEL(I)=0.0
ICT1(I)=0
305 CONTINUE
CPP0=CPP1+CPP2*TINIT-CPP3/TINIT**2.0
C
C   CALCULATE THE MULTICOMPONENT CONSTANTS
C
M(1)=M1
M(2)=M2
M(3)=M3
II=0
350 DO 400 II=1,KKK
JJ=0
DO 360 JJ=1,KKK
SIGSQ(II,JJ)=(7.5*(SIG(II)+SIG(JJ)))**2.0
EOVERK(II,JJ)=(E(II)*E(JJ))**0.5
MBAR(II,JJ)=(M(II)*M(JJ))/(M(II)+M(JJ))
360 CONTINUE
400 CONTINUE
C
C   SET REAL TIME COUNTERS AND INTERGERS
C
JJEND=NT-2
JPRINT=NPRINT
ARG=TAU/DELTAU
N=INT(ARG)
IF(NPRINT.EQ.0)GO TO 330
J=N/NPRINT
J=NPRINT*J
IF(J-N)310,330,320
310 N=J+NPRINT
GO TO 330
320 N=J
330 CONTINUE
TIME=0.0
TIME2=0.0
JJJ=2

```

```

C
C      CALCULATE THE INITIAL SURFACE TEMPERATURE
C
DTAU10=TAU1-TAU0
DTAU20=TAU2-TAU0
DTAU21=TAU2-TAU1
C20=1.0/(DTAU10*DTAU20)
C21=1.0/(DTAU10*DTAU21)
C22=1.0/(DTAU20*DTAU21)
C10=C20*(TAU1+TAU2)
C11=C21*(TAU0+TAU2)
C12=C22*(TAU0+TAU1)
C00=C20*TAU1*TAU2
C01=C21*TAU0*TAU2
C02=C22*TAU1*TAU0
CS0=C00*TS0+C02*TS2-C01*TS1
CS1=C10*TS0+C12*TS2-C11*TS1
CS2=C20*TS0+C22*TS2-C21*TS1
TSUPF=CS0

C
C      CALCULATE THE PRESSURE CONSTANT
C
R=0.7302
P0=1.0
WBAR1=ME1/M2*W2INIT+2.0*ME1/M1*W1INIT+PE1/PS*W1INIT
CONTH=ETAP*P0*FWJ/(9*TINIT)*WBAR1*PI*(PAPD**2.0-P4DC**2.0)

C
C      BEGIN FORWARD MARCHING IN TIME
C
ONPME=1.0/3.7
450 GO 1000 J=1,N
JPLUS=J+1
TIME2=TIME2+DELTAU
455 IF (TAU2-TIME2)450,500,500
460 IF (JJJ-JJEND)460,470,500
470 JJJ=JJJ+1
TAU0=TAU1
TAU1=TAU2
TS0=TS1
TS1=TS2
DTAU10=DTAU21
475 GO TO 490
480 JJJ=JJJ+2
TAL0=TAU2
TS0=TS2
PEAQ(5,11)TAU1,TS1
TS1=TS1+459.6
TAU1=TAU1/3500.0
DTAU10=TAU1-TAU0

C
C      UPDATE INPUT SURFACE TEMPERATURE PROFILE
C
490 PEAQ(5,11)TAU2,TS2
TS2=TS2+459.6
TAL2=TAU2/3500.0
DTAU20=TAU2-TAU1
DTAU21=TAU2-TAU1

```

```

C20=1.0/(DTAU10*DTAU20)
C21=1.0/(DTAU10*DTAU21)
C22=1.0/(DTAU20*DTAU21)
C10=C20*(TAU1+TAU2)
C11=C21*(TAU1+TAU2)
C12=C22*(TAU1+TAU2)
C00=C20*TAU1*TAU2
C01=C21*TAU1*TAU2
C02=C22*TAU1*TAU2
CS0=C00*TS0+C02*TS2-C01*TS1
CS1=C10*TS0+C12*TS2-C11*TS1
CS2=C20*TS0+C22*TS2-C21*TS1
500 TLAS(LS)=TSURF
TSURF=CS0+TIME2*(CS2*TIME2-CS1)
T(LS)=TSURF
T(1)=TLAS(2)

C
C***** ELEMENT 2 *****
C
C SOLVE ENERGY EQUATION FOR CORE MATERIAL
C
DO 600 I=2,LC
IPLUS=I+1
IMINUS=I-1
CPC(I)=CPC1+CPC2*TLAS(I)+CPC3/TLAS(I)**2.0
RHOC(I)=RHOC1+RHOC2*TLAS(I)+RHOC3/TLAS(I)**2.0
KC(I)=TCC1+TCC2/TLAS(I)+TCC3*TLAS(I)
K(I)=KC(I)
ALPHAC(I)=KC(I)/(RHOC(I)*CPC(I))
IMQ(I)=ALPHAC(I)*DELTAU/DELR**2.0
IF(I-LC)595,590,595
500 DELVA=DELR
KLCH=TCC1+TCC2/TLAS(LCH)+TCC3*TLAS(LCH)
DELC(I)=((KLCH-KLAS(I))*DELVA/DELR+
1 (KLAS(I)-KLAS(IMINUS))*DELVA/DELR)/(DELVA+DELR)
GO TO 596
595 DELVA=DELR
DELC(I)=((KLAS(IPLUS)-KLAS(I))*DELVA/DELR+
1 (KLAS(I)-KLAS(IMINUS))*DELVA/DELR)/(DELVA+DELR)
595 DELT(I)=((TLAS(IPLUS)-TLAS(I))*DELVA/DELR+
1 (TLAS(I)-TLAS(IMINUS))*DELVA/DELR)/(DELVA+DELR)
LAPLT(I)=2.0/(DELR+DELVA)*((TLAS(IPLUS)-TLAS(I))
1 /DELVA-(TLAS(I)-TLAS(IMINUS))/DELR)
TDOT(I)=ALPHAC(I)*(DELT(I)/RAD(I)+LAPLT(I))+1.0/(RHOC(I)*CPC(I))*
1 DELC(I)*DELT(I)
600 T(I)=TLAS(I)+DELTAU*TDOT(I)
T(1)=T(2)
RHOC(1)=RHOC(2)
CPC(1)=CPC(2)
K(1)=K(2)

C
C***** ELEMENT 3 *****
C
C SOLVE TRANSPORT EQUATIONS FOR POROUS SECTION
C
IRP=LCH+1
IFR=LPH-1

```



```

      LCPLUS=LC+2
      DO 735 I=LCPLUS,LO
      IPLUS=I+2
      IMINUS=I-2
      IF (IMINUS-LCW) 610,610,611
610  DELVAR=DELP
      GO TO 614
611  DELVAR=DELP
614  CONTINUE
      IF (IPLUS-LPW) 615,615,616
615  DELVA=DELR
      GO TO 617
616  DELVA=DELP
617  CONTINUE

C
C      CALCULATE SPACE DERIVATIVES
C
      DELPCV(I)=(PHOLAS(IPLUS)*VLAS(IPLUS)-PHOLAS(I)*VLAS(I))*
1  DELVAR/DELVA+(PHOLAS(I)*VLAS(I)-PHOLAS(IMINUS)*VLAS(IMINUS))*
2  DELVA/DELVAR/(DELVA+DELVAR)
      DIVNOV(I)=DELPV(I)+PHOLAS(I)*VLAS(I)/RAD(I)
      DELX1(I)=((XLAS(1,IPLUS)-XLAS(1,I))*DELVAR/DELVA+
1  (XLAS(1,I)-XLAS(1,IMINUS))*DELVA/DELVAR)/(DELVA+DELVAR)
      DELX2(I)=((XLAS(2,IPLUS)-XLAS(2,I))*DELVAR/DELVA+
1  (XLAS(2,I)-XLAS(2,IMINUS))*DELVA/DELVAR)/(DELVA+DELVAR)
      DELX3(I)=((XLAS(3,IPLUS)-XLAS(3,I))*DELVAR/DELVA+
1  (XLAS(3,I)-XLAS(3,IMINUS))*DELVA/DELVAR)/(DELVA+DELVAR)
      DELH1(I)=(HOLAS(IPLUS)-HOLAS(I))*DELVAR/DELVA
1  +(HOLAS(I)-HOLAS(IMINUS))*DELVA/DELVAR/(DELVA+DELVAR)
      DELH2(I)=(H2LAS(IPLUS)-H2LAS(I))*DELVAR/DELVA
1  +(H2LAS(I)-H2LAS(IMINUS))*DELVA/DELVAR/(DELVA+DELVAR)
      DELH3(I)=(H3LAS(IPLUS)-H3LAS(I))*DELVAR/DELVA
1  +(H3LAS(I)-H3LAS(IMINUS))*DELVA/DELVAR/(DELVA+DELVAR)
      DELN1E(I)=(N1ELAS(IPLUS)-N1ELAS(I))*DELVAR/DELVA+
1  (N1ELAS(I)-N1ELAS(IMINUS))*DELVA/DELVAR/(DELVA+DELVAR)
      DELN2E(I)=(N2ELAS(IPLUS)-N2ELAS(I))*DELVAR/DELVA+
1  (N2ELAS(I)-N2ELAS(IMINUS))*DELVA/DELVAR/(DELVA+DELVAR)
      DELN3E(I)=(N3ELAS(IPLUS)-N3ELAS(I))*DELVAR/DELVA+
1  (N3ELAS(I)-N3ELAS(IMINUS))*DELVA/DELVAR/(DELVA+DELVAR)
      DIVN1E(I)=DELN1E(I)+N1ELAS(I)/RAD(I)
      DIVN2E(I)=DELN2E(I)+N2ELAS(I)/RAD(I)
      DIVN3E(I)=DELN3E(I)+N3ELAS(I)/RAD(I)
      DELK(I)=((KLAS(IPLUS)-KLAS(I))*DELVAR/DELVA+
1  (KLAS(I)-KLAS(IMINUS))*DELVA/DELVAR)/(DELVA+DELVAR)
      DELT(I)=((TLAS(IPLUS)-TLAS(I))*DELVAR/DELVA+
1  (TLAS(I)-TLAS(IMINUS))*DELVA/DELVAR)/(DELVA+DELVAR)
      LAPLT(I)=((TLAS(IPLUS)-TLAS(I))/DELVA+(TLAS(IMINUS)-
1  TLAS(I))/DELVAR)*(2.0/(DELVA+DELVAR))
      DELSUM(I)=((SUML3(IPLUS)*RAD(IPLUS)-SUML3(I)*RAD(I))*
1  DELVAR/DELVA+(SUML3(I)*RAD(I)-SUML3(IMINUS)*RAD(IMINUS))*
2  DELVA/DELVAR)/(DELVA+DELVAR)/RAD(I)

C
C      CALCULATE THE NEW DENSITY AND THE VELOCITY
C
      R=0.7302
      RHC(I)=PLAS(I)*MH(I)/(R*TLAS(I))
      V(I)=(N1ELAS(I)+N2ELAS(I)+N3ELAS(I))/RHC(I)

```

```

C
C      SOLVE SPECIES I CONSERVATION EQUATIONS
C
      RMOCOT(I)=1.0/ETALAS(I)*((RMOFC-RHC(I))*STADTL(I)-DIVRCV(I))
      W1COT(I)=1.0/(ETALAS(I)*RHO(I))*(-W1LAS(I)*(ETALAS(I)*RMODOT(I)
1  +RHC(I)*STADTL(I))-DIVN1E(I)+GEN1(I))
      W2COT(I)=1.0/(ETALAS(I)*RHO(I))*(-W2LAS(I)*(ETALAS(I)*RMODOT(I)
1  +RHC(I)*STADTL(I))-DIVN2E(I)+GEN2(I))
      W3COT(I)=1.0/(ETALAS(I)*RHO(I))*(-W3LAS(I)*(ETALAS(I)*RMODOT(I)
1  +RHC(I)*STADTL(I))-DIVN3E(I)+GEN3(I))
C
C      CALCULATE FLUXES
C
      CALL DIFF
      DMOD1(I)=D1M(I)*DELTAU/DELR**2.0/ETALAS(I)
      DMOD2(I)=D2M(I)*DELTAU/DELP**2.0/ETALAS(I)
      DMOD3(I)=D3M(I)*DELTAU/DELP**2.0/ETALAS(I)
      MOFLX(1,I)=-RHC(I)*D1M(I)/MW(I)*DELX1(I)+XLAS(1,I)*TOTMOF(I)
      MOFLX(2,I)=-RHC(I)*D2M(I)/MW(I)*DELX2(I)+XLAS(2,I)*TOTMOF(I)
      MOFLX(3,I)=-RHC(I)*D3M(I)/MW(I)*DELX3(I)+XLAS(3,I)*TOTMOF(I)
      TOTMOF(I)=MOFLX(1,I)+MOFLX(2,I)+MOFLX(3,I)
      N1E(I)=MOFLX(1,I)*M1
      N2E(I)=MOFLX(2,I)*M2
      N3E(I)=MOFLX(3,I)*M3
      FLUXJ1(I)=N1E(I)-W1LAS(I)*RHO(I)*V(I)
      FLUXJ2(I)=N2E(I)-W2LAS(I)*RHO(I)*V(I)
      FLUXJ3(I)=N3E(I)-W3LAS(I)*RHO(I)*V(I)
C
C      CHECK ACCURACY OF THE DIFFUSION EQUATION
C
      IF(ABS(TOTMOF(I))-0.01630,630,631)
630  TEST1(I)=1.0
      TEST2(I)=1.0
      TEST3(I)=1.0
      GO TO 636
631  CONTINUE
      DO 635 II=1,KKK
      SUMDIF(II,I)=0.0
      DO 634 JJ=1,KKK
      IF(II-JJ)633,632,633
632  DIF(II,JJ)=0.0
      GO TO 634
633  DIF(II,JJ)=(XLAS(II,I)*MOFLX(JJ,I)-XLAS(JJ,I)*MOFLX(II,I))
1  /(DG(II,JJ)*RHO(I)/MW(I))
634  SUMDIF(II,I)=DIF(II,JJ)+SUMDIF(II,I)
      IF(DIFDIF,50,1)GO TO 635
      SUMDIF(II,I)=SUMDIF(II,I)-MOFLX(II,I)/(OK(II,I)*RHO(I)/MW(I))
635  CONTINUE
      TEST1(I)=DELX1(I)/SUMDIF(1,I)
      TEST2(I)=DELX2(I)/SUMDIF(2,I)
      TEST3(I)=DELX3(I)/SUMDIF(3,I)
636  CONTINUE
C
C      CALCULATE PHYSICAL PROPERTIES
C
      DO 640 KK=1,KKK
      TLAS(I)=TLAS(I)/1.9

```

```

TBASE=TBASE/1.0
CPG(KK)=CPG1(KK)+CPG2(KK)*TLAS(I)+CPG3(KK)*TLAS(I)**2.0
1 +CPG4(KK)*TLAS(I)**3.0+CPG5(KK)/TLAS(I)**2.0
HG(KK)=CPG1(KK)*(TLAS(I)-TBASE)+CPG2(KK)/2.0*(TLAS(I)**2.0-TBASE**
1 2.0)+CPG3(KK)/3.0*(TLAS(I)**3.0-TBASE**3.0)+HGVAP0(KK)
2 +CPG4(KK)/4.0*(TLAS(I)**4.0-TBASE**4.0)-CPG5(KK)*
3 (1.0/TLAS(I)-1.0/TBASE)
TBASE=TBASE*1.0
TR=TLAS(I)/E(KK)
COLINV(KK)=1.0/(CIV1*(1.0+CIV2*ALOG(TR)))
TLAS(I)=TLAS(I)*1.0
MUG(KK)=2.6692E-5*(M(KK)*(TLAS(I)/1.0)**0.5/(SIG(KK)**2.0
1 *COLINV(KK))
2 =1.987
KG(KK)=(CPG(KK)+1.25*TR)/M(KK)*MUG(KK)
MUG(KK)=MUG(KK)*2.4191E02
KG(KK)=KG(KK)*2.4175E02
640 CONTINUE
II=0
MU(I)=0.0
CP(I)=0.0
KM(I)=0.0
HI(I)=J.0
DO 660 II=1,KKK
JJ=0
SUMXPH=0.0
DO 650 JJ=1,KKK
PHI(I,JJ)=(0.125)**0.5*(1.0+(M(IJ)/M(JJ))**(-0.5))*
1 (1.0+(MUG(IJ)/MUG(JJ))**1.5*(M(JJ)/M(IJ))**0.25)**2.0
XPHI(I,JJ)=XLAS(IJ,I)*PHI(IJ,JJ)
SUMXPH=XPHI(IJ,JJ)+SUMXPH
650 CONTINUE
XK=XLAS(II,I)*KG(II)/SUMXPH
XMU=XLAS(IJ,I)*MUG(IJ)/SUMXPH
XCPG=XLAS(II,I)*CPG(II)
XHG=XLAS(II,I)*HG(II)
XM(I)=XK+KM(I)
MU(I)=XMU+MU(I)
CP(I)=XCPG+CP(I)
HI(I)=XHG+HI(I)
HG(II)=HG(II)/M(II)
660 CONTINUE
CF(I)=CP(I)/MW(I)
HI(I)=HI(I)/MW(I)
PHOC(I)=PHOC1+PHOC2*TLAS(I)+PHOC3*TLAS(I)**2.0
CEC(I)=CEC1+CEC2*TLAS(I)+CEC3/TLAS(I)**2.0
HC(I)=CPC1*(TLAS(I)-TBASE)+CPC2*(TLAS(I)**2.0-TBASE**2.0)+
1 CEC3*(1.0/TLAS(I)-1.0/TBASE)+HCO
FACTK(I)=1.0-ETALAS(I)*EXP(-1.0/ETALAS(I))-(1.0-ETALAS(I))
1 *EXP(-1.0/(1.0-ETALAS(I)))
KP(I)=(TCP1+TCP2/TLAS(I)
EPS(I)=ESP
KRC(I)=0.693*EPS(I)*PART0*TLAS(I)**3.0/30.4*E12
KP(I)=(1.0-ETALAS(I))/(1.0/KP(I)+1.0/KPD(I))+ETALAS(I)*KRC(I)
KE(I)=(1.0-ETALAS(I))*KP(I)*EXP(-1.0/(1.0-ETALAS(I)))+ETALAS(I)
1 *(KM(I)+KP(I))*(EXP(-1.0/ETALAS(I))+FACTK(I)**2.0/ETALAS(I)
2 **2.0/(1.0-EXP(-1.0/ETALAS(I))))

```

```

      K(I)=KE(I)
C
C      SOLVE ENERGY EQUATION
C
      SUM1(I)=HG(1)*W1DOT(I)+HG(2)*W2DOT(I)+HG(3)*W3DOT(I)
      SUM2(I)=HG(1)*DELW1(I)+HG(2)*DELW2(I)+HG(3)*DELW3(I)
      SUM3(I)=HG(1)*FLUXJ1(I)+HG(2)*FLUXJ2(I)+HG(3)*FLUXJ3(I)
      IF(I.EQ.1) SUM4=HG(1)*N1E(I)+HG(2)*N2E(I)+HG(3)*N3E(I)
      IF(I.EQ.1) SUM4C=HG(1)*N1E(I)+HG(2)*N2E(I)+HG(3)*N3E(I)
      ERC=ETALAS(I)*RHO(I)*CP(I)+(1.0-ETA0)*PHOC*CPPC
      1 +(ETA0-ETALAS(I))*GPC(I)*RHOC(I)
      TMO(I)=K(I)/ESC*DELTAU/DELTA**2.0
      TDO(I)=(PHOC(I)*(HG(I)-H(I))+PLAS(I)/0.3676)*ETACTL(I)-
      1 ETALAS(I)*RHO(I)*SUM1(I)-PHO(I)*CP(I)*VLAS(I)*DELT(I)-
      2 PHO(I)*VLAS(I)*SUM2(I)-DELSUM(I)+K(I)/PAO(I)*DELT(I)+
      3 K(I)*LAPLT(I)*DELT(I)*DELK(I)+ETALAS(I)*PCOT(I)/ERC
      T(I)=TLAS(I)+DELTAU*TDO(I)
C
C      CALCULATE EQUILIBRIUM CONSTANT
C
      LOGKEQ(I)=KEQ1+KEQ2/(T(I)/1.9)
      KEQ(I)=EXP(LOGKEQ(I)*2.303)
C
C      DETERMINE WHETHER DEPOSITION HAS OCCURED
C
      DINDEX(I)=1.0/(XLAS(1,I)*XLAS(2,I)/XLAS(3,I)**3.0*PLAS(I))
      IF(1CT1(I)-1)669,670,670
669 IF(DINDEX(I)-KEQ(I))670,670,680
670 CONTINUE
      1CT1(I)=1
C
C      SOLVE SIMULTANEOUS EQUATIONS FOR MOLE FRACTIONS
C
      W1(I)=W1DOT(I)*DELTAU+W1LAS(I)
      X(1,I)=W1(I)/M1*MW(I)
      W3(I)=W3DOT(I)*DELTAU+W3LAS(I)
      X(3,I)=W3(I)/M3*MW(I)
      ARGX2=X(1,I)*X(3,I)*KEQ(I)/PLAS(I)
      IF(ARGX2.LT.0.0)GO TO 675
      X(2,I)=ARGX2**DUMM
      GO TO 676
675 X(2,I)=-ABS(ARGX2)**DUMM
676 DX=X(1,I)+X(2,I)+X(3,I)
      X(1,I)=X(1,I)/DX
      X(2,I)=X(2,I)/DX
      X(3,I)=X(3,I)/DX
      MW(I)=X(1,I)*M1+X(2,I)*M2+X(3,I)*M3
      W1(I)=X(1,I)*M1/MW(I)
      W2(I)=X(2,I)*M2/MW(I)
      W3(I)=X(3,I)*M3/MW(I)
      W=W1(I)+W2(I)+W3(I)
      W1(I)=W1(I)/W
      W2(I)=W2(I)/W
      W3(I)=W3(I)/W
C
C      CALCULATE THE DEPOSITION RATE
C      AND THE NEW POROSITY

```

```

C
W3CT=(W3(I)-W3LAS(I))/DELTAU
GEN3(I)=W3CT*ETALAS(I)*PHO(I)+W3(I)*(ETALAS(I)
1 *PHOCT(I)+PHC(I)*ETACTL(I)+OIVN3(I)
GEN4(I)=-ME3/M3*GEN3(I)
SUMGEN(I)=SUMGEL(I)+GEN4(I)
IF(SUMGEN(I)-0.0)677,677,673
677 GEN4(I)=-SUMGEL(I)
GEN3(I)=-M3/ME3*GEN4(I)
ICT1(I)=0
679 GEN2(I)=M2/ME2*(-3.0*ME2/M3*GEN3(I))
GEN1(I)=-GEN2(I)-GEN3(I)-GEN4(I)
ETA0CT(I)=-GEN4(I)/PHOC(I)
ETA(I)=DELTAU*ETA0CT(I)+ETALAS(I)
GO TO 685
680 CONTINUE
C
C      NO REACTION HAS OCCURED, CONTINUE
C
W1(I)=W1LAS(I)+W1DOT(I)*DELTAU
W2(I)=W2LAS(I)+W2DOT(I)*DELTAU
W3(I)=W3LAS(I)+W3DOT(I)*DELTAU
W=W1(I)+W2(I)+W3(I)
W1(I)=W1(I)/W
W2(I)=W2(I)/W
W3(I)=W3(I)/W
MW(I)=1.0/(W1(I)/M1+W2(I)/M2+W3(I)/M3)
X(1,I)=W1(I)*MW(I)/M1
X(2,I)=W2(I)*MW(I)/M2
X(3,I)=W3(I)*MW(I)/M3
OX=X(1,I)+X(2,I)+X(3,I)
X(1,I)=X(1,I)/OX
X(2,I)=X(2,I)/OX
X(3,I)=X(3,I)/OX
GEN1(I)=0.0
GEN2(I)=0.0
GEN3(I)=0.0
GEN4(I)=0.0
ETA0CT(I)=0.0
ETA(I)=ETALAS(I)
685 CONTINUE
C
C      CALCULATE THE FUNCTIONS FOR PRESSURE INTEGRATION
C
WBAR1=2.0*W1(I)/M1+W2(I)/M2+W3(I)/M3
F(I)=ETA(I)*MW(I)*RAD(I)*WBAR1/T(I)
700 CONTINUE
C
C***** ELEMENT 4 *****
C
C      SOLVE EQUATIONS FOR THE CORE INTERFACE
C
I=LCW
LCWP2=LCW+2
LCWF1=LCW+1
LCWM2=LCW-2
LCWM1=LCW-1

```

```

      ETALAS(I)=ETA0
C
C      CALCULATE SPACE DERIVATIVES
C
      DELW1(I)=(W1LAS(LCWP1)-W1LAS(I))/DELX2
      DELW2(I)=(W2LAS(LCWP1)-W2LAS(I))/DELX2
      DELW3(I)=(W3LAS(LCWP1)-W3LAS(I))/DELX2
      DELX1(I)=(XLAS(1,LCWP1)-XLAS(1,I))/DELX2
      DELX2(I)=(XLAS(2,LCWP1)-XLAS(2,I))/DELX2
      DELX3(I)=(XLAS(3,LCWP1)-XLAS(3,I))/DELX2
      DELRCV(I)=RHOLAS(LCWP1)*VLAS(LCWP1)/DELX2
      DELT(I)=(TLAS(LCWP1)-TLAS(LCH))*(DELX2/DELX2+
1 (TLAS(LCH)-TLAS(LCWP1))*DELX2/DELX2)/(DELX2+DELX2)
C
C      CALCULATE DENSITY AND VELOCITY
C
      R=0.7302
      RHO(I)=PLAS(I)*MW(I)/(R*TLAS(I))
      V(I)=(N1ELAS(I)+N2ELAS(I)+N3ELAS(I))/RHO(I)
C
C      CALCULATE FLUXES FROM OLD VALUES
C
      CALL DIFF
      DMOC1(I)=01M(I)*DELTAU/DELX2**2.0/ETALAS(I)
      DMOC2(I)=02M(I)*DELTAU/DELX2**2.0/ETALAS(I)
      DMOC3(I)=03M(I)*DELTAU/DELX2**2.0/ETALAS(I)
      MOFLX(1,I)=-RHO(I)*01M(I)/MW(I)*DELX1(I)+XLAS(1,I)*TOTMOF(I)
      MOFLX(2,I)=-RHO(I)*02M(I)/MW(I)*DELX2(I)+XLAS(2,I)*TOTMOF(I)
      MOFLX(3,I)=-RHO(I)*03M(I)/MW(I)*DELX3(I)+XLAS(3,I)*TOTMOF(I)
      TOTMOF(I)=MOFLX(1,I)+MOFLX(2,I)+MOFLX(3,I)
      N1E(I)=MOFLX(1,I)*M1
      N2E(I)=MOFLX(2,I)*M2
      N3E(I)=MOFLX(3,I)*M3
      FLUXJ1(I)=N1E(I)-W1LAS(I)*RHO(I)*V(I)
      FLUXJ2(I)=N2E(I)-W2LAS(I)*RHO(I)*V(I)
      FLUXJ3(I)=N3E(I)-W3LAS(I)*RHO(I)*V(I)
C
C      CHECK ACCURACY OF THE DIFFUSION EQUATION
C
      IF(ABS(TOTMOF(I))-0.01730,730,731)
730 TEST1(I)=1.0
      TEST2(I)=1.0
      TEST3(I)=1.0
      GO TO 736
731 CONTINUE
      DO 735 II=1,KKK
      SUMDIF(II,I)=0.0
      DO 734 JJ=1,KKK
      IF(II-JJ)733,732,733
732 DIF(II,JJ)=0.0
      GO TO 734
733 DIF(II,JJ)=(XLAS(II,I)*MOFLX(JJ,I)-XLAS(JJ,I)*MOFLX(II,I))
1 / (CG(II,JJ)*RHO(I)/MW(I))
734 SUMDIF(II,I)=DIF(II,JJ)+SUMDIF(II,I)
      IF(DIFOPT.EQ.1)GO TO 735
      SUMDIF(II,I)=SUMDIF(II,I)-MOFLX(II,I)/(CK(II,I)*RHO(I)/MW(I))
735 CONTINUE

```

```

TEST1(I)=DELX1(I)/SUMDIF(1,I)
TEST2(I)=DELX2(I)/SUMDIF(2,I)
TEST3(I)=DELX3(I)/SUMDIF(3,I)
775 CONTINUE
C
C SOLVE SPECIES I CONSERVATION EQUATIONS
C
RHCCOT(I)=(-RAC(LCWP1)/RAD(I)*RHO(LCWP1)*V(LCWP1)/DELPP
1 -(RHC(I)-RHOC(I))*DRPOT/DELPP-(RHO(I)-RHOC(I))*ETAOTL(I))
2 /(1.0+DELPPG/DELPP*(ETALAS(I)-1.0))
W1DOT(I)=(GEN1(I)*DELPP/DELPPG-W1LAS(I)*(ETALAS(I)+DELPP
1 /DELPPG-1.0)*RHODOT(I)-RHO(I)*W1LAS(I)*(ETAOTL(I)+DRPOT
2 /DELPP)-N1E(LCWP1)*RAD(LCWP1)/RAD(I)/DELRF0)
3 /(RHO(I)*(ETALAS(I)-1.0+DELPP/DELPPG))
W2DOT(I)=(GEN2(I)*DELPP/DELPPG-W2LAS(I)*(ETALAS(I)+DELPP
1 /DELPPG-1.0)*RHODOT(I)-RHO(I)*W2LAS(I)*(ETAOTL(I)+DRPOT
2 /DELPP)-N2E(LCWP1)*RAD(LCWP1)/RAD(I)/DELRF0)
3 /(RHO(I)*(ETALAS(I)-1.0+DELPP/DELPPG))
W3DOT(I)=(GEN3(I)*DELPP/DELPPG-W3LAS(I)*(ETALAS(I)+DELPP
1 /DELPPG-1.0)*RHODOT(I)-RHO(I)*W3LAS(I)*(ETAOTL(I)+DRPOT
2 /DELPP)-N3E(LCWP1)*RAD(LCWP1)/RAD(I)/DELRF0)
3 /(RHO(I)*(ETALAS(I)-1.0+DELPP/DELPPG))
C
C CALCULATE PHYSICAL PROPERTIES
C
RHOC(I)=RHOP0
RHCC(I)=RHOC1+RHOC2*TLAS(I)+RHOC3*TLAS(I)**2.0
CPC(I)=CPC1+CPC2*TLAS(I)+CPC3/TLAS(I)**2.0
HC(I)=CPC1*(TLAS(I)-TBASE)+CPC2*(TLAS(I)**2.0-TBASE**2.0)-
1 CPC3*(1.0/TLAS(I)-1.0/TBASE)+HCO
CPF(I)=CPF1+CPF2*TLAS(I)+CPF3/TLAS(I)**2.0
DO 7640 KK=1,KKK
TLAS(I)=TLAS(I)/1.9
TBASE=TBASE/1.9
CPF(KK)=CPF1(KK)+CPF2(KK)*TLAS(I)+CPF3(KK)/TLAS(I)**2.0
1 +CPF4(KK)*TLAS(I)**3.0+CPF5(KK)/TLAS(I)**2.0
HG(KK)=CPF1(KK)*(TLAS(I)-TBASE)+CPF2(KK)/2.0*(TLAS(I)**2.0-TBASE**
1 2.0)+CPF3(KK)/3.0*(TLAS(I)**3.0-TBASE**3.0)+HGVAP0(KK)
2 +CPF4(KK)/4.0*(TLAS(I)**4.0-TBASE**4.0)-CPF5(KK)*
3 (1.0/TLAS(I)-1.0/TBASE)
TBASE=TBASE*1.9
TP=TLAS(I)/Z(KK)
COLINV(KK)=1.0/(CIV1*(1.0+CIV2*ALOG(TP)))
TLAS(I)=TLAS(I)*1.9
MUG(KK)=2.6693E-5*(M(KK)*(TLAS(I)/1.9))**3.5/(SIG(KK)**2.0
1 *COLINV(KK))
P=1.987
KG(KK)=(CPF(KK)+1.25*P)/M(KK)*MUG(KK)
MUG(KK)=MUG(KK)*2.4191E02
KG(KK)=KG(KK)*2.4175E02
7640 CONTINUE
II=0
MU(I)=0.0
CP(I)=0.0
KM(I)=0.0
H(I)=0.0
DO 7660 II=1,KKK

```

```

JJ=0
SUMX=H=0.0
DO 7650 JJ=1,KKK
  PHI(JJ)=(0.125)**0.5*(1.0+(X(JJ)/H(JJ))**(-1.5))*
1 (1.0+(MUG(JJ)/HUG(JJ))**0.5*(M(JJ)/H(JJ))**0.25)**2.0
  XPHI(JJ)=XLAS(JJ,1)*PHI(JJ,JJ)
  SUMXPH=XPHI(JJ)+SUMXPH
7650 CONTINUE
  XK=XLAS(JJ,1)*KG(JJ)/SUMXPH
  XMU=XLAS(JJ,1)*MUG(JJ)/SUMXPH
  XCPG=XLAS(JJ,1)*CPG(JJ)
  XHG=XLAS(JJ,1)*HG(JJ)
  KM(JJ)=XK+KM(J)
  MU(JJ)=XMU+MU(J)
  CF(JJ)=XCPG+CF(J)
  H(JJ)=XHG+H(J)
  HG(JJ)=HG(JJ)/H(JJ)
7660 CONTINUE
  CP(JJ)=CP(JJ)/MU(JJ)
  H(JJ)=H(JJ)/MU(JJ)
  FACTK(JJ)=1.0-ETALAS(JJ)*EXP(-1.0/ETALAS(JJ))-(1.0-ETALAS(JJ))
1 *EXP(-1.0/(1.0-ETALAS(JJ)))
  KP(JJ)=TCP1+TCP2/TLAS(JJ)
  EPS(JJ)=ESP
  KRC(JJ)=0.693*EPS(JJ)*PARTO*TLAS(JJ)**7.0/30.36212
  KR(JJ)=(1.0-ETALAS(JJ))/(1.0/KP(JJ)+1.0/KRC(JJ)+ETALAS(JJ)*KRC(JJ)
  KE(JJ)=(1.0-ETALAS(JJ))*KP(JJ)*EXP(-1.0/(1.0-ETALAS(JJ))+ETALAS(JJ)
1 *(KM(JJ)+KP(JJ))*EXP(-1.0/ETALAS(JJ))+FACTK(JJ)**2.0/ETALAS(JJ)
2 **2.0/(1.0-EXP(-1.0/ETALAS(JJ)))
  K(JJ)=DELPP/RAD(LCW)/ALOG((RAD(LCW)+DELPP-DELPP0)/
1 RAD(LCW))/KM(JJ)+ALOG((RAD(LCW)+DELPP)/RAD(LCW)+
2 DELPP-DELPP0)/KE(JJ)
C
C SOLVE ENERGY EQUATION
C
  SUM1(JJ)=HUG(1)*W1DOT(JJ)+HG(2)*W2DOT(JJ)+HG(3)*W3DOT(JJ)*ETALAS(JJ)
1 *FHC(JJ)
  SUM2(JJ)=HG(1)*DELW1(JJ)+HG(2)*DELW2(JJ)+HG(3)*DELW3(JJ)*FHO(JJ)*
1 VLAS(JJ)
  SUM3(JJ)=HG(1)*FLUXJ1(JJ)+HG(2)*FLUXJ2(JJ)+
1 HG(3)*FLUXJ3(JJ)
  ARGRC=(H(JJ)*FHO(JJ)-PLAS(JJ)/0.3676)*(1.0+ETALAS(JJ))
1 -HC(JJ)*RHOC(JJ)+1.0/0.3676
  ARGH0=H(JJ)*ETALAS(JJ)*DELPP+DELPP-DELPP0
  ARGTA=(H(JJ)*FHO(JJ)-PLAS(JJ)/0.3676)*DELPP
1 -(HC(JJ)*RHOC(JJ)-1.0/0.3676)*DELPP
  ARGF=DELPP*(1.0+ETALAS(JJ))-DELPP0
  EPC=ETALAS(JJ)*FHO(JJ)*CF(JJ)*DELPP
1 *FHC(JJ)*CP(JJ)*(DELPP-DELPP0)+(1.0-ETALAS(JJ)*RHOF0)*CPP(JJ)*CFLOPC
2 *(ETALAS(JJ)*RHOC(JJ)*DELPP2*CPG(JJ)
3 *FHC(LCWP1)*CPC(LCWP1)*DELPP
  IMCC(JJ)=K(JJ)/EPC*DELTAU/DELPP**2.0
  T(JJ)=(TLAS(JJ)+DELTAU*(1-RAD(LCWP1)/RAD(JJ))*(SUM4C-K(LCWP1)
2 *TL(LCWP1)/DELPP)+RAD(LCWP1)/RAD(JJ)*K(LCWP1)*T(LCWP1)/DELPP
1 -ARGTA*ETASTL(JJ)-ARGRH0*RHODOT(JJ)-APCRP*DRPDOT+ARGP*PDOT)
3 /EPC/(1.0+DELTAU*(RAD(LCWP1)/RAD(JJ)*K(LCWP1)/DELPP
4 *RAD(LCWP1)/RAD(JJ)*K(LCWP1)/DELPP)/ERG)

```



```

C
C      CALCULATE THE EQUILIBRIUM CONSTANT AND THE
C      DEPOSITION INDEX
C
      LOGKEQ(I)=KEQ1+KEQ2/(T(I)/1.8)
      KEQ(I)=EXP(2.303*LOGKEQ(I))

C
C      CALCULATE THE NEW CONCENTRATIONS
C
      DINDEX(I)=1.0/(XLAS(1,I)*XLAS(3,I)/XLAS(2,I)**3.0*PLAS(I))
      IF(J.GT.1)GO TO 7740
      CUP=-3.0*XLAS(2,I)
      CUC=(9.0*(XLAS(1,I)+XLAS(3,I)-XLAS(1,I)*XLAS(3,I))
      1 +81.0*XLAS(2,I)**2.0*PLAS(I)/KEQ(I))/
      2 (27.0*PLAS(I)/KEQ(I)-1.0)
      CUD=27.0*(XLAS(1,I)*XLAS(3,I)-PLAS(I)/KEQ(I)*
      1 XLAS(2,I)**3.0)/(27.0*PLAS(I)/KEQ(I)-1.0)
      CUP=(3.0*CUC-CUD**2.0)/3.0
      CUD=(27.0*CUC-9.0*CUD**2.0+2.0*CUD**3.0)/27.0
      CUR=(CUD/3.0)**3.0+(CUC/2.0)**2.0
      CUR1=-CUR/2.0+CUR**0.5
      CUR2=-CUR/2.0-CUR**0.5
      IF(CUR1.LT.0.0)GO TO 7741
      CCA=CUR1**DUMM
      GO TO 7742
7741 CCA=-(ABS(CUR1))**DUMM
7742 IF(CUR2.LT.0.0)GO TO 7743
      CCR=CUR2**DUMM
      GO TO 7744
7743 CCR=-(ABS(CUR2))**DUMM
7744 CLAMB=CCA+CCR
      XLAMB=CLAMB-CUP/3.0
      X(1,I)=XLAS(1,I)+XLAMB/3.0
      X(2,I)=XLAS(2,I)-XLAMB
      X(3,I)=XLAS(3,I)+XLAMB/3.0
      GO TO 7750
7740 W1(I)=(W1LAS(I)+DELTAU/2.0*W1DOT(I)+DELTAU/2.0*(GEN1(I)
      1 *DELRF/DELRP0+RAD(LCWP1)/RAD(I)*(RHO(LCWP1)*
      2 CIP(LCWP1)/MW(LCWP1)*(DELRP/DELR*(X(1,LCWP1)-
      3 X(1,LCWP1))+DELR/DELRP*X(1,LCWP1))/(DELR+DELRP)
      4 +X(1,LCWP1)*TOTMOF(LCWP1))*M1/DELRP)/(RHO(I)*(ETALAS(I)
      5 +DELR/DELRP-1.0)))/(1.0+DELTAU/2.0*(RAD(LCWP1)
      6 /RAD(I)*RHO(LCWP1)*CIP(LCWP1)/MW(LCWP1)*DELR/DELRP
      7 /(DELR+DELRP)*MW(I)/DELRP+(ETALAS(I)+DELRP
      8 /DELRP-1.0)*RHODOT(I)+RHO(I)*(ETADTL(I)+CRPDOT
      9 /DELRP))/(RHO(I)*(ETALAS(I)+DELRP/DELRP-1.0)))
      X(1,I)=W1(I)/M1*MW(I)
      W3(I)=(W3LAS(I)+DELTAU/2.0*W3DOT(I)+DELTAU/2.0*(GEN3(I)
      1 *DELRF/DELRP0+RAD(LCWP1)/RAD(I)*(RHO(LCWP1)*
      2 GEN(LCWP1)/MW(LCWP1)*(DELRP/DELR*(X(3,LCWP1)-
      3 X(3,LCWP1))+DELR/DELRP*X(3,LCWP1))/(DELR+DELRP)
      4 +X(3,LCWP1)*TOTMOF(LCWP1))*M3/DELRP)/(RHO(I)*(ETALAS(I)
      5 +DELRP/DELRP-1.0)))/(1.0+DELTAU/2.0*(RAD(LCWP1)
      6 /RAD(I)*RHO(LCWP1)*GEN(LCWP1)/MW(LCWP1)*DELR/DELRP
      7 /(DELR+DELRP)*MW(I)/DELRP+(ETALAS(I)+DELRP
      8 /DELRP-1.0)*RHODOT(I)+RHO(I)*(ETADTL(I)+CRPDOT
      9 /DELRP))/(RHO(I)*(ETALAS(I)+DELRP/DELRP-1.0)))

```

```

X(3,I)=W3(I)/M3*MW(I)
APGX2=X(1,I)*X(3,I)*KEO(I)/PLAS(I)
IF (APGX2.LT.0.0) GO TO 7745
X(2,I)=APGX2**CUMM
GO TO 7750
7745 X(2,I)=-IABS(APGX2)**CUMM
7750 DX=X(1,I)+X(2,I)+X(3,I)
X(1,I)=X(1,I)/DX
X(2,I)=X(2,I)/DX
X(3,I)=X(3,I)/DX
IF (J.GT.1) GO TO 740
EQUIX(1)=X(1,I)
EQUIX(2)=X(2,I)
EQUIX(3)=X(3,I)
740 CONTINUE
MW(I)=X(1,I)*M1+X(2,I)*M2+X(3,I)*M3
W1(I)=X(1,I)*P1/MW(I)
W2(I)=X(2,I)*P2/MW(I)
W3(I)=X(3,I)*P3/MW(I)
W=W1(I)+W2(I)+W3(I)
W1(I)=W1(I)/W
W2(I)=W2(I)/W
W3(I)=W3(I)/W
C
C CALCULATE THE DEPOSITION RATE
C THE NEW POROSITY, AND DEPLETION OF THE COPE
C
W3OT=(W3(I)-W3LAS(I))/DELTAU
GEN2(I)=W3OT*ETALAS(I)*PHOLAS(I)+W3(I)*(ETALAS(I)
1 *PHOCOT(I)+PHOLAS(I)*ETADIL(I)+DELN3(I)
GEN4(I)=-W3/M3*GEN3(I)
GEN2(I)=M2/MF2*(-1.0*M2/M3*GEN3(I))
GEN1(I)=-GEN2(I)-GEN3(I)-GEN4(I)
ETADOT(I)=ETADOT(LCHW1)
ETA(I)=ETAILCHW1
OREQTE=DELPL*GEN4(I)/PHOC(I)-ETADOT(I)*DELPP
DELPP=DELPL+OREQTE*DELTAU
DELCH=DELPL-DELPP
RAD(I)=RAD(LCHW1)+DELOR
C
C CALCULATE THE FUNCTIONS FOR PRESSURE INTEGRATION
C
WPAR1=2.0*W1(I)/M1+W2(I)/M2+W3(I)/M3
F(I)=ETA(I)*MW(I)*RAD(I)*WPAR1/T(I)
C
C***** ELEMENT 5 *****
C
C SOLVE ENERGY EQUATION FOR SHELL MATERIAL
C
LEW1=LPW+1
750 DO 800 I=LPW,LS
CPS(I)=CPS1
RHOS(I)=RHOS1
KS(I)=KCS1
K(I)=KS(I)
ALPHAS(I)=KS(I)/(RHOS(I)*CPS(I))
800 TMOD(I)=ALPHAS(I)*DELTAU/DEL2**2.0

```

```

      DO 160 I=LPHF1,NRE
      IMINUS=I-1
      IPLUS=I+1
      IF (IMINUS-LPH) 105,105,106
105  DELS=DEL2
      DELX=DEL2S
      DPDS=DELX/DELS
      DSDP=DELS/DELX
      KLAS(LPH)=KSLPH
      GO TO 130
106  CONTINUE
      IF (I-NRE) 110,120,120
110  DELS=DEL2
      DELX=DEL2
      DPDS=1.0
      DSDP=1.0
      GO TO 130
120  DELS=DELSP
      DPDS=DELSP/DELS
      DSDP=DELS/DELSP
130  CONTINUE
      CELKS(I)=(IKLAS(IPLUS)-KLAS(I))*DPDS+(KLAS(I)-
1  KLAS(IMINUS))*DSDP/(DELS+DELX)
      DTL1=TLAS(I)-TLAS(IMINUS)
      DTL2=TLAS(IPLUS)-TLAS(I)
      DTL(I)=(DTL2*DPDS+DTL1*DSDP)/(DELX+DELS)
      LAPL(I)=2.0*(DTL2/DELS-DTL1/DELX)/(DELS+DELX)
      TROT(I)=ALPHAS(I)*(DELT(I)/RAO(I)+LAPL(I))+1.0/(RHOS(I)
1  *CPS(I))*DELKS(I)*DELT(I)
      IF (I-NRE) 140,150,150
140  T(I)=TLAS(I)+DELTAN*TROT(I)
      GO TO 160
150  T(I)=(TLAS(I)+DELTAN*TROT(I))/2.0+DELTAN/2.0
1  /(RHOS(I)*CPS(I))/(DELS+DELX)*((K(I)/RAO(I)
2  +DELKS(I))*(CPDS*T(IPLUS)-DSDP*T(IMINUS))+2.0*K(I)
3  *(IIEIUS)/DELS+T(I,INUS)/DELX))/2.0
4  +DELTAN/2.0/(DELS+DELX)/(RHOS(I)*CPS(I))*((K(I)/RAO(I)
5  +DELKS(I))*(CPDS-DSDP)+2.0*K(I)*(1.0/DELS+1.0/DELX)))
160  CONTINUE
C
C***** ELEMENT 6 *****
C
C   SOLVE THE EQUATIONS FOR THE SHELL INTERFACE
C
      I=LPH
      LPHF2=LPH+2
      LPHF1=LPH+1
      LPHM2=LPH-2
      LPHM1=LPH-1
      TALAS(I)=ETA0
C
C   CALCULATE SPACE DERIVATIVES
C
      DELW1(I)=-(W1LAS(LPHM1)-W1LAS(I))/DEL2S
      DELW2(I)=-(W2LAS(LPHM1)-W2LAS(I))/DEL2S
      DELW3(I)=-(W3LAS(LPHM1)-W3LAS(I))/DEL2S
      DELX1(I)=-(XLAS(1,LPHM1)-XLAS(1,I))/DEL2S

```

```

DEFLX2(I) = -(XLAS(2,LPWM1) - XLAS(2,I)) / DELPR
DEFLX3(I) = -(XLAS(3,LPWM1) - XLAS(3,I)) / DELPR
DELT(I) = ((TLAS(LPW1) - TLAS(LPW)) * DELPR / DELPS
1 * (TLAS(LPW) - TLAS(LPWM1)) * DELRS / DELPR) / (DELRS + DELPR)
C
C   CALCULATE DENSITY AND VELOCITY
C
R = 0.7302
RHO(I) = PLAS(I) * MW(I) / (R * TLAS(I))
V(I) = (N1ELAS(I) + N2ELAS(I) + N3ELAS(I)) / RHO(I)
C
C   CALCULATE FLUXES FROM OLD VALUES
C
CALL DIFF
OMCO1(I) = O1M(I) * DELTAU / DELPR ** 2.0 / ETALAS(I)
OMCO2(I) = O2M(I) * DELTAU / DELPR ** 2.0 / ETALAS(I)
OMCO3(I) = O3M(I) * DELTAU / DELPR ** 2.0 / ETALAS(I)
MOFLX(1,I) = -RHO(I) * O1M(I) / MW(I) * DELX1(I) + XLAS(1,I) * TOTMOF(I)
MOFLX(2,I) = -RHO(I) * O2M(I) / MW(I) * DELX2(I) + XLAS(2,I) * TOTMOF(I)
MOFLX(3,I) = -RHO(I) * O3M(I) / MW(I) * DELX3(I) + XLAS(3,I) * TOTMOF(I)
TOTMOF(I) = MOFLX(1,I) + MOFLX(2,I) + MOFLX(3,I)
N1E(I) = MOFLX(1,I) * M1
N2E(I) = MOFLX(2,I) * M2
N3E(I) = MOFLX(3,I) * M3
FLUXJ1(I) = N1E(I) - W1LAS(I) * RHO(I) * V(I)
FLUXJ2(I) = N2E(I) - W2LAS(I) * RHO(I) * V(I)
FLUXJ3(I) = N3E(I) - W3LAS(I) * RHO(I) * V(I)
C
C   CHECK ACCURACY OF THE DIFFUSION EQUATION
C
IF(ABS(TOTMOF(I)) - 0.0) .GT. 1.E-6
861 TEST1(I) = 1.0
TEST2(I) = 1.0
TEST3(I) = 1.0
GO TO 867
862 CONTINUE
DO 865 II = 1, KKK
SUMOIF(II,I) = 0.0
DO 865 JJ = 1, KKK
IF(II - JJ) .GT. 1.E-6
863 OIF(II,JJ) = 0.0
GO TO 865
864 OIF(II,JJ) = (XLAS(II,I) * MOFLX(JJ,I) - XLAS(JJ,I) * MOFLX(II,I))
1 / (O2(I,II) * RHO(I) / MW(I))
865 SUMOIF(II,I) = OIF(II,JJ) + SUMOIF(II,I)
IF(DISOPT.CO.1) GO TO 866
SUMOIF(II,I) = SUMOIF(II,I) - MOFLX(II,I) / (OK(II,I) * RHO(I) / MW(I))
866 CONTINUE
TEST1(I) = DELX1(I) / SUMOIF(1,I)
TEST2(I) = DELX2(I) / SUMOIF(2,I)
TEST3(I) = DELX3(I) / SUMOIF(3,I)
867 CONTINUE
C
C   SOLVE SPECIES I CONSERVATION EQUATIONS
C
OMCO1(I) = 1.0 / ETALAS(I) * (RAD(LPWM1) / RAD(I) * RHO(LPWM1)
1 * V(LPWM1) / DELPR - (RHO(I) - RHO(I)) * ETADTL(I) + (ETALAS(I)

```

```

2 *RHO(I)=RHO(I)*(1.0-ETA)+ETALAS(I))/DELF*OPRDOT)
WIDOT(I)=1.0/(ETALAS(I)*RHO(I))*(GEN1(I)-ETALAS(I)
1 *WILAS(I)*RHOCOT(I)+N1ELAS(LPM1)*RAC(LPM1)/RAC(I)/DELF
2 -WILAS(I)*RHO(I)*ETADTL(I)-RHO(I)*ETALAS(I)*WILAS(I)
3 *CFRCOT/DELF
W2DOT(I)=1.0/(ETALAS(I)*RHO(I))*(GEN2(I)-ETALAS(I)
1 *W2LAS(I)*RHOCOT(I)+N2ELAS(LPM1)*RAC(LPM1)/RAC(I)/DELF
2 -W2LAS(I)*RHO(I)*ETADTL(I)-RHO(I)*ETALAS(I)*W2LAS(I)
3 *CFRCOT/DELF
W3DOT(I)=1.0/(ETALAS(I)*RHO(I))*(GEN3(I)-ETALAS(I)
1 *W3LAS(I)*RHOCOT(I)+N3ELAS(LPM1)*RAC(LPM1)/RAC(I)/DELF
2 -W3LAS(I)*RHO(I)*ETADTL(I)-RHO(I)*ETALAS(I)*W3LAS(I)
3 *CFRCOT/DELF
C
C      CALCULATE PHYSICAL PROPERTIES
C
CPF(I)=CPF1+CPF2*TLAS(I)+CPF3/TLAS(I)**2.0
CPC(I)=CPC1+CPC2*TLAS(I)+CPC3/TLAS(I)**2.0
HC(I)=CPC1*(TLAS(I)-TBASE)+CPC2*(TLAS(I)**2.0-TBASE**2.0)+
1 CPC3*(1.0/TLAS(I)-1.0/TBASE)+HCO
HS(LPM1)=CPS1*(T(LPM1)-TBASE)+CPS2*
1 (T(LPM1)**2.0-TBASE**2.0)-
2 CPS3*(1.0/T(LPM1)-1.0/TBASE)+HS0
RHO(I)=RHOC1+RHOC2*TLAS(I)+RHOC3*TLAS(I)**2.0
RHO(I)=RHOC1
DO 8640 KK=1,KKK
TLAS(I)=TLAS(I)/1.9
TBASE=TBASE/1.9
CPG(KK)=CPG1(KK)+CPG2(KK)*TLAS(I)+CPG3(KK)*TLAS(I)**2.0
1 +CPG4(KK)*TLAS(I)**3.0+CPG5(KK)/TLAS(I)**2.0
HG(KK)=CPG1(KK)*(TLAS(I)-TBASE)+CPG2(KK)/2.0*(TLAS(I)**2.0-TBASE**
1 2.0)+CPG3(KK)/3.0*(TLAS(I)**3.0-TBASE**3.0)+HGVAP0(KK)
2 +CPG4(KK)/4.0*(TLAS(I)**4.0-TBASE**4.0)-CPG5(KK)*
3 (1.0/TLAS(I)-1.0/TBASE)
TBASE=TBASE*1.9
TP=TLAS(I)/E(KK)
COLINV(KK)=1.0/(CIV1*(1.0+CIV2*ALOG(TP)))
TLAS(I)=TLAS(I)*1.9
MUG(KK)=2.6693E-5*(M(KK)*(TLAS(I)/1.9))**0.5/(SIG(KK)**2.0)
1 *COLINV(KK)
P=1.987
KG(KK)=(CPG(KK)+1.25*R)/M(KK)*MUG(KK)
MUG(KK)=MUG(KK)*2.4191E02
KG(KK)=KG(KK)*2.4175E02
8640 CONTINUE
IT=C
MU(I)=0.0
CP(I)=0.0
KM(I)=0.0
H(I)=0.0
DO 8650 II=1,KKK
JJ=1
SINXPH=0.0
DO 8650 JJ=1,KKK
PHI(II,JJ)=(0.125)**J.5*(1.0+(H(II)/H(JJ))**(-0.5))*
1 (1.0+(MUG(II)/MUG(JJ))**0.5*(H(JJ)/H(II))**0.25)**2.0
XPHI(JJ)=XLAS(JJ,I)*PHI(II,JJ)

```

```

SUMXPH=XPHI(JJ)+SUMXPH
#65# CONTINUE
XK=XLAS(II,I)*KG(II)/SUMXPH
XMU=XLAS(II,I)*MUG(II)/SUMXCH
XCPG=XLAS(II,I)*CPG(II)
XHG=XLAS(II,I)*HG(II)
KM(II)=XK+KM(I)
MU(II)=XMU+MU(I)
CP(II)=XCPG+CP(I)
H(II)=XHG+H(I)
HG(II)=HG(II)/M(II)
#66# CONTINUE
CP(II)=CP(II)/MH(II)
H(II)=H(II)/MH(II)
FACTK(II)=1.0-ETALAS(II)*EXP(-1.0/ETALAS(II))-(1.0-ETALAS(II))
1 *EXP(-1.0/(1.0-ETALAS(II)))
KP(II)=TCP1+TCP2/TLAS(II)
EPS(II)=ESP
KRG(II)=0.697*EPS(II)*PART0*TLAS(II)**3.0/30.44E12
KR(II)=(1.0-ETALAS(II))/(1.0/KR(II)+1.0/KRG(II)+ETALAS(II)*KPC(II)
KE(II)=(1.0-ETALAS(II))*KP(II)*EXP(-1.0/(1.0-ETALAS(II)))+ETALAS(II)
1 *(KM(II)*KR(II))*(EXP(-1.0/ETALAS(II))+FACTK(II)**2.0/ETALAS(II)
2 **2.0/(1.0-EXP(-1.0/ETALAS(II))))
K(II)=KE(II)
C
C SOLVE ENERGY EQUATION
C
SUM1(II)=(HG(II)*W1DOT(II)+HG(2)*W2DOT(II)+HG(3)*W3DOT(II))*ETALAS(II)
1 *FHC(II)
SUM2(II)=(HG(II)*DELW1(II)+HG(2)*DELW2(II)+HG(3)*DELW3(II))*PHO(II)*
1 VLAS(II)
SUM3(II)=HG(II)*FLUXJ1(II)+HG(2)*FLUXJ2(II)+HG(3)*FLUXJ3(II)
ARGPR=ETALAS(II)*(RHO(II)*H(II)-PLAS(II)/0.7676)
1 -FHC(II)*HG(II)+1.0/0.7676
ARGPJ=ETALAS(II)*H(II)*DELPR
ARGEIA=DELPR*(H(II)*PHO(II)-O(II)/0.7675)
1 -DELPR*(HG(II)*RHO(II)-1.0/0.7676)
ARGCP=ETALAS(II)*DELPR
ERC=ETALAS(II)*HG(II)*CP(II)*DELPR+(1.0-ETA0)*
1 DELPR*CFP(II)*RHOP(II)+DELRS0*PHOS(LPW1)*CPS(LPW1)+
2 (ETA0-ETALAS(II))*PHOC(II)*CPC(II)*DELPR+
3 (DELPR-DELPR0)*CPC(II)*RHOC(II)
TGO(II)=K(II)/EPC*DELTAU/DELPR**2.0
T(II)=(TLAS(II)+DELTAU*(RAD(LPWM1)/RAD(II))*(SUM4S+
1 K(LPWM1)*T(LPWM1)/DELPR0)+RAD(LPW1)/RAD(II)*K(LPW1)
2 *T(LPWM1)/0.7675-ARGETA*ETA0TL(II)-ARGFHC*RHO0DOT(II)
3 -ARGCFP*CFP0DOT+ARGCP*P0DOT)/ERC/(1.0+DELTAU*(RAD(LPWM1)/RAD(II)
4 *K(LPWM1)/DELPR0)+RAD(LPW1)/RAD(II)*K(LPW1)/DELRS0)/EPC)
C
C CALCULATE THE EQUILIBRIUM CONSTANT AND THE
C DEPOSITION INDEX
C
LOGKEQ(II)=KEQ1+KEQ2/(T(II)/1.8)
KEQ(II)=EXP(LOGKEQ(II)*2.303)
C
C DETERMINE IF DEPOSITION HAS OCCURED
C

```

```

P=0.7352
QINDEX(I)=1.0/(XLAS(1,I)*XLAS(3,I)/XLAS(2,I)**3.0*PLAS(I))
IF(ICT1(I)-1)869,870,870
*69 IF(QINDEX(I)-KEQ(I))870,870,875
870 CONTINUE
ICT1(I)=1
C
C      SOLVE SIMULTANEOUS EQUATIONS FOR MOLE FRACTIONS
C      AND CALCULATE THE NEW COMPOSITION
C
W1(I)=(WILAS(I)+DELTAU/2.0*W1DOT(I)+DELTAU/2.0*(GEN1(I)
1 +PAC(LPM1)/RAD(I)*M1/DELPR*(RHO(LPM1)*Z1M(LPM1)
2 /MH(LPM1)*(X(1,LPM1)*DELPR/DELPR+(X(1,LPM2)-
3 X(1,LPM1))*DELPR/DELPR)/(DELPR+DELPR)*X(1,LPM1)
4 *TCTMCF(LPM1)))/(ETALAS(I)*RHO(I))/(1.0+DELTAU
5 /2.0*(PAC(LPM1)/RAD(I)*PHO(LPM1)*Z1M(LPM1)/
6 MH(LPM1)*DELPR/DELPR/(DELPR+DELPR)*M1(I)/DELPR+
7 RHO(I)*(ETADTL(I)+ETALAS(I)*DEROOT/DELPR)+
8 ETALAS(I)*RHOCOT(I))/(ETALAS(I)*RHO(I))
X(1,I)=W1(I)*MW(I)/M1
W2(I)=(WILAS(I)+DELTAU/2.0*W2DOT(I)+DELTAU/2.0*(GEN3(I)
1 +PAC(LPM1)/RAD(I)*M3/DELPR*(RHO(LPM1)*Z3M(LPM1)
2 /MH(LPM1)*(X(3,LPM1)*DELPR/DELPR+(X(3,LPM2)-
3 X(3,LPM1))*DELPR/DELPR)/(DELPR+DELPR)*X(3,LPM1)
4 *TCTMCF(LPM1)))/(ETALAS(I)*RHO(I))/(1.0+DELTAU
5 /2.0*(PAC(LPM1)/RAD(I)*PHO(LPM1)*Z3M(LPM1)/
6 MH(LPM1)*DELPR/DELPR/(DELPR+DELPR)*M3(I)/DELPR+
7 RHO(I)*(ETADTL(I)+ETALAS(I)*DEROOT/DELPR)+
8 ETALAS(I)*RHOCOT(I))/(ETALAS(I)*RHO(I))
X(3,I)=W2(I)/M3*MH(I)
ARGX2=X(1,I)*X(3,I)*KEQ(I)/PLAS(I)
IF(ARGX2.LT.0.0)GO TO 872
X(2,I)=ARGX2**DUMM
GO TO 877
872 X(2,I)=-(LOG(ARGX2))**DUMM
873 DX=X(1,I)+X(2,I)+X(3,I)
X(1,I)=X(1,I)/DX
X(2,I)=X(2,I)/DX
X(3,I)=X(3,I)/DX
MH(I)=X(1,I)*M1+X(2,I)*M2+X(3,I)*M3
W1(I)=X(1,I)*M1/MH(I)
W2(I)=X(2,I)*M2/MH(I)
W3(I)=X(3,I)*M3/MH(I)
W=W1(I)+W2(I)+W3(I)
W1(I)=W1(I)/W
W2(I)=W2(I)/W
W3(I)=W3(I)/W
WCTE=(W3(I)-W3LAS(I))/DELTAU
GEN3(I)=WCTE*ETALAS(I)*RHO(I)+W3(I)*(ETALAS(I)
1 +RHOCOT(I)+RHO(I)*ETADTL(I)+DELN3E(I)
GEN4(I)=-M3/M3*GEN3(I)
SUMGEN(I)=SUMGEL(I)+GEN4(I)
IF(SUMGEN(I)-0.0)8874,8874,8875
8874 GEN4(I)=-SUMGEL(I)
GEN3(I)=-M*/M3*GEN4(I)
ICT1(I)=0
8875 GEN2(I)=M2/M2*(-3.0*M2/M3*GEN3(I))

```

```

GEN1(I)=-GEN2(I)-GEN3(I)-GEN4(I)
ETA(I)=ETA(LCW*1)
ETA00T(I)=0.0
GO TO 880
875 CONTINUE
C
C      NO REACTION HAS OCCURED. CONTINUE
C
W1(I)=W1LAS(I)+W100T(I)*DELTAU
W2(I)=W2LAS(I)+W200T(I)*DELTAU
W3(I)=W3LAS(I)+W300T(I)*DELTAU
W=W1(I)+W2(I)+W3(I)
M1(I)=W1(I)/W
M2(I)=W2(I)/W
M3(I)=W3(I)/W
MW(I)=1.0/(M1(I)/M1+W2(I)/M2+W3(I)/M3)
X(1,I)=W1(I)*MW(I)/M1
X(2,I)=W2(I)*MW(I)/M2
X(3,I)=W3(I)*MW(I)/M3
DX=X(1,I)+X(2,I)+X(3,I)
X(1,I)=X(1,I)/DX
X(2,I)=X(2,I)/DX
X(3,I)=X(3,I)/DX
GEN1(I)=0.0
GEN2(I)=0.0
GEN3(I)=0.0
GEN4(I)=0.0
ETA00T(I)=0.0
ETA(I)=ETALAS(I)
880 CONTINUE
C
C      CALCULATE CHANGE IN WALL THICK. DUE TO DEPOSIT.
C
DEPRDT=(-(DELPR0*GEN4(I)+FHOC(I)*DELPR*ETA00T(I))/
1 (FHOC(I)*(ETA(I)+1.0-ETA0))
DELP=DELPR+DEPRDT*DELTAU
RAD(I)=RAD(LCW*1)+DELP
C
C      CALCULATE THE FUNCTIONS FOR PRESSURE INTEGRATION
C
WPAR1=2.0*W1(I)/M1+W2(I)/M2+W3(I)/M3
F(I)=ETA(I)*MW(I)*RAD(I)*WPAR1/T(I)
C
C      CALCULATE THE QUASI-STEADY PRESSURE
C
S0=6.0/PAPIO/30.94504
DO 891 I=LCW,LPW
KAPPA(I)=ETA(I)**3.0/(2.5*(1.0/ETA(I))**2.0*S0**2.0
1 *(1.0-ETA(I))**2.0)
DELP(I)=-MU(I)/KAPPA(I)*V(I)/(144.0*
1 72.17*3600**2.0)/14.7
891 CONTINUE
SUM=0.0
DO 897 I=LCW,LPW,2
I1=I+1
I2=I+2
IF(I-LCW)6444,6884,6885

```



```

6886 RINC=DELRF+DELR
GO TO 6886
6887 RINC=2.0*DELR
6888 CONTINUE
SUM=SUM+RINC/5.0*(F(I)+F(I2)+4.0*F(I3))
IF(I2-L0)6887,6893,6893
6887 CONTINUE
6889 SUM=SUM+(F(LP)+F(LPW))/2.0*DELR
6889 CONTINUE
R=0.7302
DO 6890 I=L0W,LPW
P(I)=CONTH*R/(2.0*PI*SUM)
6890 CONTINUE
POOT=(P(LPW)-PLAS(LPW))/(DELTAH*0.3576)
C
C CALCULATE DEPOSITION RATE, COATING DEPOSITED,
C COFE DEPLETED, AND HEAT FLUX ALL AT THE WALL
C
FLUX=-K(LPW)*DELT(LPW)
RHOVW=GEN4(LPW)
COFE1=(DELCRL-DELCR)*12.0*1000.0*1.0506
COFEDF=(DELCF0-DELCR)*12.0*1000.0
COAT1=(DELPRL-DELP2)*12.0*1000.0*1.0506
COATIH=(DELPED-DELP2)*12.0*1000.0
C
C CALCULATE DATA FOR THE ARNOLD SOLUTION
C
DO 882 I=L0W,L0W
DO 882 II=1,KKK
CAEX(II,I)=(X(II,I)-XINIT(II))/(EGUXX(II)-XINIT(II))
882 97(II,I)=(9AD(II)-9AD(L0W))/(ABS(2.0*DM(II,I)*TIME2))**0.5
882 CONTINUE
C
C ESTABLISH OLD PROPERTIES
C
KSLPW=KS(L0W)
DO 885 I=L0W,L0W
N1ELAS(I)=N1E(I)
N2ELAS(I)=N2E(I)
N3ELAS(I)=N3E(I)
PLAS(I)=P(I)
ETALAS(I)=ETA(I)
RHOLAS(I)=RHO(I)
W1LAS(I)=W1(I)
W2LAS(I)=W2(I)
W3LAS(I)=W3(I)
SUML3(I)=SUM3(I)
XLAS(1,I)=X(1,I)
XLAS(2,I)=X(2,I)
XLAS(3,I)=X(3,I)
VLAS(I)=V(I)
DELCRL=DELCR
DELCRL=DELCR
DELPRL=DELP2
ETADTL(II)=ETACOT(I)
SUMGEL(I)=SUMGEN(I)
885 CONTINUE

```

```

      DO 890 I=1,LS
      KLAS(I)=K(I)
      TLAS(I)=T(I)
890  CONTINUE
C
C      DATA PRINTOUT ROUTINE
C
      DO 900 I=1,LS
      IF(I.EQ.LCW)GO TO 900
      IF(I.EQ.LFW)GO TO 900
      IF(TM0(I).GT.0.5)WRITE(6,92)TM0(I),J,I
      IF(CM001(I).GT.0.5)WRITE(6,96)CM001(I),J,I
      IF(CM002(I).GT.0.5)WRITE(6,96)CM002(I),J,I
      IF(CM003(I).GT.0.5)WRITE(6,96)CM003(I),J,I
900  CONTINUE
      IF(J-JERINT) 1000,912,1000
912  OUTIME=3600.0*TIME2
      OUTP=9(LCW)
      WRITE(6,92)OUTIME,OUTP,FLUX,RHOVH,COATTH,COAT1,
      1 CORCOS,CORF1
      TCOI(1)=(T(1)-TLAS(1))/DELTAU
      TCOI(LS)=(TSURE-TLAS(LS))/DELTAU
      DIST=0.0
      WRITE(6,90)
      DO 950 I=1,LS
      DEGE=T(I)-459.6
      IF(I-LS)915,916,916
915  OUTC=12.2*PAC(I)
      GO TO 918
916  OUTC=RADIUS*12.0
919  IF(I-LCW)920,920,920
920  IF(I-LFW)930,930,940
930  OUTVR=V(I)/3600
      WRITE(6,91)I,OUTD,DEGE,K(I),RH0(I),C0(I),OUTVR,STA(I),CPLP(I)
      GO TO 960
940  WRITE(6,92)I,OUTD,DEGE,K(I),RH0S(I),CPS(I)
      GO TO 960
950  WRITE(6,92)I,OUTD,DEGE,K(I),RHOC(I),CPC(I)
960  CONTINUE
      WRITE(6,99)
      DO 990 I=LFW,LFW
980  WRITE(6,95)I,C1M(I),O2M(I),O3M(I),MOFLX(1,I),MOFLX(2,I),
      1 MOFLX(3,I),TOTMOF(I),GEN4(I)
      WRITE(6,99)
      DO 990 I=LFW,LFW
990  WRITE(6,97)I,X(1,I),X(2,I),X(3,I),TEST1(I),TEST2(I),TEST3(I)
      1 ,KEC(I),OTINDEX(I)
      WRITE(6,71)
      DO 995 I=LFW,LFW
995  WRITE(6,72)I,CAPX(1,I),PZ(1,I),CAPX(2,I),PZ(2,I)
      1 ,CAPX(3,I),PZ(3,I)
996  JPRINT=J+JPRINT
1000 TIME=TIME2
      WRITE(6,59)
      GO TO 110
2000 STOP
      END

```

SUBROUTINE DIFF

```

SUBROUTINE DIFF
C
C ALGORITHM FOR BINARY DIFFUSIVITY CALCULATION
C
COMMON I, KKK, J, LCN, LP, DIFOPT
COMMON TOTMOF(50), RHOP(50)
COMMON MBAP(10,10), PLAS(50), SIGSQ(10,10), M(10), MW(50)
COMMON RHO(50), MOFLX(10,50), FOVEPK(10,10), TLAS(50)
COMMON XLAS(10,50), DM(10,50), D1M(50), D2M(50), D3M(50), ETALAS(50)
COMMON DK(10,50), DG(11,10), COLIND(10,10), DIF(10,10), SUMDIF(10,50)
COMMON MP, POPEP, CIO1, CIO2, DFLT(50), RAD(50)
COMMON DTLPP, CFLPP0, DELPP, DELPP0
REAL MOFLX, MBAP, M, MP, MW
DATA PI/3.14159/
DO 620 II=1, KKK
R=8.314607
TLAS(I)=TLAS(I)/1.8
DK(II,I)=0.6675-0.8*POPEP*(8.0*P*TLAS(I)/M(II)/PI)**0.5
DK(II,I)=DK(II,I)*3.875
TLAS(I)=TLAS(I)*1.8
JJ=0
605 DO 611 JJ=1, KKK
IF (II-JJ) 610, 609, 608
60* DG(II, JJ)=DG(JJ, II)
GO TO 611
609 DG(II, JJ)=0.0
GO TO 611
610 CONTINUE
TLAS(I)=TLAS(I)/1.8
IP=TLAS(I)/FOVEPK(II, JJ)
COLIND(II, JJ)=1.0/(CIO1*(1.0+CIO2*ALOG(IP)))
DG(II, JJ)=1.95832-13*(TLAS(II)**3.0*MBAP(II, JJ)**.5/(PLAS(I)*
1 SIGSQ(II, JJ)*COLIND(II, JJ)))
TLAS(I)=TLAS(I)*1.8
DG(II, JJ)=DG(II, JJ)*1.975*ETALAS(II)**2.0
IF (DIFOPT, 1, 2) DG(II, JJ)=DG(1, 2)
IF (DIFOPT, 2, 2) DG(II, JJ)=DG(1, 2)
611 CONTINUE
620 CONTINUE
IF (ABS(TOTMOF(I))-0.0) 636, 636, 621
521 DO 622 II=1, KKK
622 SUMDIF(II, I)=0.0
DO 635 II=1, KKK
DO 634 JJ=1, KKK
IF (II-JJ) 631, 630, 631
630 DIF(II, JJ)=0.0
GO TO 634
631 DIF(II, JJ)=(XLAS(JJ, I)*MOFLX(II, I)-XLAS(II, I)*MOFLX(JJ, I))/
1 DG(II, JJ)
634 SUMDIF(II, I)=SUMDIF(II, I)+DIF(II, JJ)
IF (DIFOPT-1) 6634, 6635, 6634
6634 DM(II, I)=(MOFLX(II, I)-XLAS(II, I)*TOTMOF(I))/(SUMDIF(II, I)+
1 MOFLX(II, I)/DK(II, I))
GO TO 635
6635 DM(II, I)=(MOFLX(II, I)-XLAS(II, I)*TOTMOF(I))/SUMDIF(II, I)
635 CONTINUE
IF (I-LCN) 6636, 6636, 641

```

```

6636 DO 6637 II=1,KKK
      DGM=(MOFLX(II,I)-XLAS(II,I)*TOTMCF(I))/SUMCIF(II,I)
      DM(II,I)=DELRP/PAD(LCW)/(ALOG((PAD(LCW)+DELRP-DELRP0)
1 /PAD(LCW))/CGM*ALOG((PAD(LCW)+DELRP)/(PAD(LCW)+
2 DELRP-DELRP0))/DM(II,I)
6637 CONTINUE
      GO TO 641
636 DO 700 II=1,KKK
700 SUMDIF(II,I)=0.0
      DO 640 II=1,KKK
      DO 639 JJ=1,KKK
      IF(II-JJ)638,637,638
637 DIF(II,JJ)=0.0
      GO TO 639
638 DIF(II,JJ)=XLAS(JJ,I)/DG(II,JJ)
639 SUMCIF(II,I)=CIF(II,JJ)+SUMCIF(II,I)
640 DM(II,I)=(1.0-XLAS(II,I))/SUMDIF(II,I)
641 CONTINUE
      DO 642 II=1,KKK
642 IF(ABS(DM(II,I)).LT.1.0E-36)DM(II,I)=1.0E-36
      D1M(I)=DM(1,I)
      D2M(I)=DM(2,I)
      D3M(I)=DM(3,I)
      RETURN
      END

```

APPENDIX XII

PROPERTIES FOR GAS PHASE SPECIES

Species	CONSTANTS FOR THE HEAT CAPACITY EQUATION					Reference
	A	$B \times (10^2)$	$C \times (10)$	$D \times (10^9)$	$E \times (10^{-4})$	
H ₂	6.952	-0.04576	0.09563	-0.2079	0	0 73
HCl	7.244	-0.1820	0.3170	-1.036	0	-22.063 73
HSCl ₃	21.514	0.2325	0	0	-29.4	-123.7

VALUES FOR THE CRITICAL CONSTANTS

Species	V_c (cc/mole)	T_{c_i} (°K)	$(e/k)_i$ (°K)	σ_i (Å°)
H ₂	64.5	33.26	25.61	3.372
HCl	86.9	324.56	249.91	3.725
HS·Cl ₃	254.0	495.0	381.0	6.33

COEFFICIENTS FOR THE EQUILIBRIUM CONSTANT

Species	A	$-B(10^{-4})$	Range	Correlation Coefficient
HS·Cl ₃	6.856.75	0.99496	200-1500 °K	

APPENDIX XIII

PROPERTIES FOR SOLID SPECIES

VALUES FOR THE THERMAL CONDUCTIVITY AND DENSITY

<u>Species</u>	<u>A(BTU/ft hr°K)</u>	<u>B(BTU/ft hr°K²)</u>	<u>(#m/ft³)</u>	<u>($\frac{in}{in°C}$)</u>
Si	84.6125	0	145.314	2.33
Al ₂ O ₃	-1.35239	1.1498E4	248.432	2.61
Al ₂ O ₃ (80%)	-1.23226	6.1728E3	198.746	-

APPENDIX XIV

CALCULATION OF THE AVERAGE PRESSURE

For the problem chosen for this thesis, the pressure of the system is assumed to be independent of position within the porous medium. However, the pressure will change with time because solid silicon is either deposited or depleted within a closed container. For the reaction system chosen, the quantity of the element hydrogen will remain constant for all time. With this fact, the value for the pressure at any time can be calculated as follows.

In an incremental volume of porous medium, ϵdV , the amount of elemental hydrogen, dX , is calculated from the following equation.

$$p \bar{\omega}_H \epsilon dV = dX \quad (\text{A13-1})$$

where $dV = 2\pi L_0 r dr$ (A13-2)

and L_0 is the length of the cylinder.

The term $\bar{\omega}_H$ can be calculated from the following equation:

$$\bar{\omega}_H = \frac{W_{HCl}}{M_{HCl}} + W_{H_2} + \frac{W_{HSiCl_3}}{M_{HSiCl_3}} \quad (\text{A13-3})$$

Inserting the ideal gas law and the last two equations into equation A13-1 gives:

$$\epsilon \frac{PM_w}{RT} \left(\frac{W_{HCl}}{M_{HCl}} + W_{H_2} + \frac{W_{HSiCl_3}}{M_{HSiCl_3}} \right) \pi r L_0 dr = dX \quad (\text{A13-4})$$

If the pressure is assumed to be independent of position, the total amount of elemental hydrogen can be obtained by integrating equation A13-4 over the limits of the radii bounding the porous medium as follows:

$$X = \bar{P} \frac{2\pi L_0}{R} \int_{R_c}^{R_p} \frac{\epsilon M_w}{T} \left(\frac{W_{HCl}}{M_{HCl}} + W_{H_2} + \frac{W_{H_2Cl_2}}{M_{H_2Cl_2}} \right) r dr \quad (A-13-5)$$

where \bar{P} is the average pressure at time t .

In the problem at hand, all quantities within the integral are constant with respect to position so $\frac{X}{L_0}$ can be obtained as follows:

$$\frac{X}{L_0} = \frac{\epsilon_0 P_0 M_w}{R T_0} \bar{\omega}_0 \pi (R_p^2 - R_c^2) \quad (A-13-6)$$

Equation A13-5 can be rearranged to calculate the average pressure at any time.

$$\bar{P} = \frac{X}{L_0} \frac{R}{2\pi} \int_{R_c}^{R_p} \frac{\epsilon M_w}{T} \left(\frac{W_{HCl}}{M_{HCl}} + W_{H_2} + \frac{W_{H_2Cl_2}}{M_{H_2Cl_2}} \right) r dr \quad (A-13-7)$$

LITERATURE CITED

1. Gorton, C. W. and A. C. Merritt, "A Survey of the Literature and Industry Involved with High Temperature Oxidation Resistant Surface and Diffusion Coating," unpublished report for Project THEMIS contract F44620-68-C-0008, August 1969.
2. Dickinson, C. W., et al., "Protective Coatings for Tungsten," Journal of Metals, 787 (1963).
3. Powell, C. F., et al., Vapor Deposition, John Wiley and Sons, New York, N. Y., 1965.
4. Biedler, E. A., "The Formation of Molybdenum Disilicide Coatings on Molybdenum," J. Electrochem. Soc. 98(1), 21 (1965).
5. Shephard, W. H., "Vapor Phase Deposition and Etching of Silicon," J. Electrochem. Soc. 112 (10), 988 (1965).
6. Sangster, R. C., et al., "Growth of Silicon Crystals by a Vapor Phase Pyrolytic Deposition Method," J. Electrochem. Soc. 104 (5), 319 (1957).
7. Bylander, E. G., "Kinetics of Silicon Crystal Growth from SiCl_4 Deposition," J. Electrochem. Soc. 109 (12), 1171 (1962).
8. Goodman, M. F., Fabrication and Evaluation of Silicon Epitaxial Films, APC TG-731, September 1965.
9. Steinmaier, W., "Thermodynamical Approach to the Growth Rate of Epitaxial Silicon from SiCl_4 ," Philips Res. Rep. 18, 75 (1963).
10. Theuerer, H. C., "Epitaxial Silicon Films by Hydrogen Reduction of SiCl_4 ," J. Electrochem. Soc. 108 (7), 649 (1961).
11. Kesler, G. H., "Factors Affecting the Rate of Deposition of Metals in Thermal Dissociation Processes," Trans. Met. Soc. of AIME 218, 199 (1960).
12. Carlton, H. E., and Oxley, J. H., "Forced and Natural Convective Mass Transfer in Multicomponent Gaseous Mixtures," J. AIChE 13(3), 571 (1967).
13. Krier, C. A., "Fundamental Considerations in CVD of Diffusion Coatings," Chemical Vapor Deposition, AD281-887, June 1962.
14. Withers, J. C., "Methods for Applying Coatings," High Temperature Inorganic Coatings, J. Huminik ed., Reinhold Pub. Corp., New York, N.Y., 1963.
15. Samuel, R. C., and N. A. Lockington, "Protection of Metallic Surfaces by Chromium Diffusion," Metal Treatment 18, 354 (1951).

16. Kelly, F. C., "Chromizing," Trans. Amer. Electrochem. Soc. 43, 351 (1923).
17. Marshall, L. H., "Formation of Chromium Alloy Coatings," U.S. Pat. 1,853,369, 1932.
18. Klopp, N. D., et al., Development of Protective Coatings for Tantalum Based Alloys, ASD-TR-61-676, March 1962.
19. Aves, W. C. and G. M. Ecord, "Advances in Coating Deposition Techniques for Refractory Metal Structures," Met. Soc. Conf. 30, 663 (1967).
20. Hollowell, J. B., et al., Coatings for Tantalum Based Alloys, ASD-TDR-63-232, April 1963.
21. Chao, D. J., et al., Development of a Cementation Coating Process for High Temperature Protection of Molybdenum, MC-TDR-64-55, March 1964.
22. Aves, W. C. and Bourland, G. W., Investigation and Development of Techniques for the Utility of the Pack Cementation Process for Columbium and Molybdenum Alloys, Rept.-2-53052142-2147 1, 1967.
23. Sama, L. and B. Reznik, "Sn-Al-Mo Oxidation Protection for Tantalum Aerospace Parts," Electrochem. Technol. 6 (3), 113 (1968).
24. Samuel, R. C., "A Survey of Factors Controlling Metallic Diffusion from the Gas Phase," Murex Review 1 (18), 501 (1958).
25. Dioguardo, P. R., et al., "Scaleup of Pack Cementation Coatings," Met. Soc. Conf. 30, 651 (1967).
26. Carman, P. C., Flow Through Porous Media, Acad. Press, New York, N.Y., 1956.
27. Muskat, M., The Flow of Homogeneous Fluids Through Porous Media, McGraw Hill Book Co., New York, N.Y., 1937.
28. Scheidegger, A. G., The Physics of Flow through Porous Media, The MacMillan Co., London, England, 1960.
29. Bird, R. B., et al., Transport Phenomena, J. Wiley and Sons, New York, N. Y., 1960.
30. Brinkman, H. C., "A Calculation of Viscous Forces Exerted by a Flowing Fluid on a Dense Swarm of Particles," Appl. Sci. Res. A1, 27 (1947).

31. Slattery, J. C., Momentum, Energy, and Mass Transfer in Continua, McGraw Hill Book Co., New York, N. Y., 1972.
32. Blake, F. C., "The Resistance of Packing to Fluid Flow," Trans. AICHE 14, 45 (1922).
33. Kozeny, J., Akad. Wiss. Wien. Abt. IIa (136), 271 (1927).
34. Dupuit, AJEJ, "Etudes Theoriques et Pratiques sur le Mouvement des aux," as described in reference 26.
35. Wylie, M. R., and W. D. Rose, "Some Theoretical Considerations Related to the Quantitative Evaluation of the Physical Characteristics of Reservoir Rock from Electrical Log Data," Trans. Am. Inst. Min. Eng. 189, 105 (1950).
36. Masamune, S. and J. M. Smith, "Transient Mass Transfer in a Fixed Bed," I&EC Fundam. 3 (2), 179 (1964).
37. Evans, R. B., et al., "Gaseous Diffusion in Porous Media at Uniform Pressure," J. Chem. Phys. 35(6), 2076 (1961).
38. Bosanquet, C. H., British TA Rept. BR-507 (1944) as reported by Phys. Rev. 73, 762 (1948).
39. Epstein, P. S., "On the Resistance Experienced by Spheres in their Motion through Gases," Phys. Rev. 23, 710 (1924).
40. Schmitt, K. H., Z. Naturforsch 14a, 870 (1957) as reported in reference 37.
41. Rothfield, L. B., "Gaseous Counterdiffusion in Porous Pellets," J. AICHE 9(1), 19 (1963).
42. Scott, D. S. and F. A. C. Dullian, "Diffusion of Ideal Gases in Capillaries and Porous Solids," J. AICHE 8 (1), 113 (1962).
43. Youngquist, G. R., "Diffusion and Flow of Gases in Porous Solids," Ind. and Eng. Chem. 62 (8), 52 (1970).
44. Pollard, W. G. and R. D. Present, "On Gaseous Self Diffusion in Long Capillary Tubes," Phys. Rev. 73, 762 (1948).
45. Wakao, N. and Smith, J. M., "Diffusion in Catalyst Pellets," Chem. Eng. Sci. 17, 825 (1962).
46. Masamune, S. and J. M. Smith, "Pore Diffusion in Silver Catalysts," J. AICHE 8(3), 217 (1962).
47. Rao, M. R. and J. M. Smith, "Diffusion Resistance in Al_2O_3 and SiO_2 Catalysts," J. AICHE 9(4), 485 (1963).

48. Johnson, M. F. L. and W. E. Stewart, "Pore Structure and Gaseous Diffusion in Solid Catalysts," J. Catal. **4**, 248 (1965).
49. Brown, L. F., et al., "Prediction of the Diffusion Rates in Porous Materials at Different Pressures," J. Catal. **14**(3), 220 (1969).
50. Rao, M. R. and J. M. Smith, "Diffusion and Reaction in Porous Glass," J. AIChE **10**(3), 293 (1964).
51. Masamune, S. and J. M. Smith, "Absorption Rate Studies; Interaction of Diffusion and Surface Processes," J. AIChE **11**(1), 4 (1965).
52. Masamune, S. and J. M. Smith, "Absorption Rate Studies, Significance of Pore Diffusion," J. AIChE **10**(2), 246 (1964).
53. Wakao, N. and J. M. Smith, "Diffusion and Reaction in Porous Catalysts," Ind. and Eng. Fundam. **3**(2), 123 (1964).
54. Smith, J. M., "Kinetics of Absorption," Advan. Chem. Ser. **79**, 8 (1967).
55. Scott, D. S., "Gas Diffusion with Chemical Reaction in Porous Solids," Can. J. Chem. Eng. **T1C33**, 173 (1962).
56. Kunii, D. and J. M. Smith, "Heat Transfer Characteristics of Porous Rocks," J. AIChE **6**(1), 63 (1960).
57. Yagii, S. and D. Kunii, "Studies on Effective Thermal Conductivity in Packed Beds," J. AIChE **3** (3), 373 (1957).
58. Huang, J. H. and J. M. Smith, "Heat Transfer in Porous Media With a Known Pore Structure," Chem. Eng. Data **8**(3), 437 (1963).
59. Masamune, S. and J. M. Smith, "Thermal Conductivity of Porous Catalyst Pellets," Chem. Eng. Data **8**(1), 54 (1963).
60. Schotte, W., "Thermal Conductivity of Packed Beds," J. AIChE **6**(1), 63 (1960).
61. Hutt, J. R., and J. W. Berg, "Thermal and Electrical Conductivities of Sandstone Rocks and Ocean Sediments," Geophysics **33**(3), 489 (1968).
62. Newby, R. A., R. R. Rothfus, and K. Li, "The Effective Conductivity of Randomly Dispersed Heterogeneous Systems," Paper No. 42A presented at the 65th Annual Meeting of the AIChE, New York, November 26-30, 1972.
63. Huang, J. H., and J. M. Smith, "Diffusion and Heat Transfer in Process Alundum," I. & E. C. Fundam. **2**, 189 (1963).

64. Kunii, D. and J. M. Smith, "Heat Transfer Characteristics of Porous Rocks: II. Thermal Conductivities of Unconsolidated Particles with Flowing Fluids," J. AICHE 7(1), 29 (1961).
65. Willhite, G. P., D. Kunii, and J. M. Smith, "Heat Transfer in Beds of Fine Particles," J. AICHE 8(3), 340 (1962).
66. Mischke, R. A., and J. M. Smith, "Thermal Conductivity of Alumina Catalyst Pellets," Ind. and Eng. Chem. Fundam. 1(4), 228 (1962).
67. Huang, J. H., "Effective Thermal Conductivity of Porous Rocks," J. Geophysical Res. 76(26), 6420 (1971).
68. Lever, R. F., "The Equilibrium Behavior of the Silicon-Hydrogen-Chlorine System," IBM Journal, 460 (1964).
69. Harper, J. J. and T. J. Lewis, Thermodynamics of the Chlorine-Silicon Hydrogen System, Technical Memorandum No. 6/M/66, June 1966.
70. Mickley, H. S., et al., Applied Mathematics in Chemical Engineering, McGraw Hill Book Co., Inc., New York, N. Y., 1957.
71. O'Brien, G. G., et al., "A Study of the Numerical Solution of Partial Differential Equations," J. Math. Phys. 29, 223 (1951).
72. Basset, H. C., et al., High-Temperature Complex Permittivity Measurements on Reentry Vehicle Antenna Window Materials, Tech Rept. No. AFWL-TR-71-189, April, 1972.
73. Hougan, O. A., et al., Chemical Process Principals - Part II, John Wiley and Sons, New York, N.Y. (1956).
74. Curtis, C. F. and J. O. Hirschfelder, "Transport Properties of Multicomponent Gas Mixtures," J. Chem. Phys. 17 (6), 550 (1949).
75. Wilke, C. R., "A Viscosity Equation for Gas Mixtures," J. Chem. Phys. 18 (4), 517 (1950).
76. Hirschfelder, J. O., et al., The Molecular Theory of Gases and Liquids, J. Wiley and Sons, New York, N. Y., p. 584 (1954).
77. Camacho, T. F., "Transport Processes in the Combustion of Carbon," PhD Dissertation, Georgia Institute of Technology (1973).
78. Mason, E. A. and S. C. Saxena, "Approximate Formula for the Thermal Conductivity of Gas Mixtures," The Physics of Fluids 1 (5), 361 (1958).
79. Mason, E. A. and L. Monchick, "Transport Properties of Polar Gases," J. Chem. Phys. 35 (5), 1676 (1961).

80. Arnold, J. H., "Studies in Diffusion," I&EC 22(10), 1091 (1930).
81. Gilliland, E. R., "Diffusion Coefficients in Gaseous Systems," I&EC 26 (6), 681 (1934).
82. Hirschfelder, J. O., et al., "Viscosity and Other Physical Properties of Gases and Gas Mixtures," Trans. ASME 71 (11), 921 (1949).
83. Andrussow, L., "Uber die Diffusion in Gassen I," Z Elektrochem 54 (7), 566 (1950).
84. Wilke, C. R., and C. V. Lee, "Estimation of Diffusion Coefficients for Gases and Vapors," I&EC 47 (6), 1253 (1955).
85. Slattery, J. C. and R. B. Bird, "Calculations of the Diffusion Coefficients of Dilute Gases and of the Self Diffusion Coefficients of Dense Gases," J. AIChE 4 (2), 137 (1958).
86. Orthmer, D. G. and H. T. Chen, "Correlating Diffusion Coefficients in Binary Gas Systems," I&EC Process Design Develop. 1 (4), 249 (1962).
87. Chen, N. H., and D. F. Orthmer, "New Generalized Equation for Gas Diffusion Coefficients," Chem. Eng. Data 7 (1), 37 (1962).
88. Fuller, E. N., et al., "A New Method for Prediction of Binary Gas-Phase Diffusion Coefficients," I&EC 58 (5), 19 (1966).
89. Kelley, K. K., "Contributions to the Data on Theoretical Metallurgy," US Bur of Mines Bull. 371 (1934)
90. Furukawa, G. T., et al., "Thermal Properties of Aluminum Oxide from 0-1200 K," J. Res. USNBS Sect. A Phys. and Chem. 57A (2), 67 (1956).
91. Clements, J. F., "The Specific Heat of Some Refractory Materials," Trans. Brit. Cer. Soc. 61, 452 (1962).
92. Jakob, Max, Heat Trans. Vol. I, John Wiley and Sons, New York, N.Y., 1957.
93. Stull, D. R. and H. Prophet, JANAF Thermochemical Tables, NSRDS-NBS 37, 1971.

VITA

Allen Charles Merritt was born October 19, 1945 in Fort Collins, Colorado. The author attended the United States Military Academy and the Georgia Institute of Technology from which he received a Bachelor of Chemical Engineering degree in 1967.

The author was employed by the Proctor and Gamble Company as a summer engineer for two summers, served as a Lieutenant in the Air Defense Artillery of the United States Army, and was then employed as an Assistant Research Engineer with the Engineering Experiment Station. During this period the Master of Science in Chemical Engineering was completed at the Georgia Institute of Technology in 1969. The author has served as Manager of Technical Services for Gold Kist Incorporated since 1972.